Spring 1981

DIFFUSION CONTROLLED VINYL POLYMERIZATION

SUNG KUK SOH

SOH, SUNG KUK

DIFFUSION CONTROLLED VINYL POLYMERIZATION

University of New Hampshire PH.D. 1981

DIFFUSION CONTROLLED VINYL POLYMERIZATION

BY

Soh, Sung Kuk
B.S., Seoul National University, 1973
M.S., Seoul National University, 1976

DISSERTATION

Submitted to the University of New Hampshire
in Partial Fulfillment of
the Requirements for the Degree of

Doctor of Philosophy
in
Engineering
(Transport Phenomena)

May, 1981

This thesis has been examined and approved.

Donald C. Sundberg

Dissertation director, Donald C. Sundberg
Assistant Professor of Chemical Engineering

Gail D. Ulrich

Gail D. Ulrich
Associate Professor of Chemical Engineering

Stephen S-T. Fan

Stephen S. T. Fan
Professor of Chemical Engineering

Paul R. Jones

Paul R. Jones
Professor of Chemistry

Frank L. Pilar

Frank L. Pilar
Professor of Chemistry

May, 1981

Date

ACKNOWLEDGEMENTS

The author wishes to express his deep gratitude to Dr. D.C. Sundberg for his endless enthusiasm for this thesis and his time and effort.

He is also thankful to the Department of Chemical Engineering and especially to Dr. Stephen S. T. Fan for the continued financial support during his years in the University of New Hampshire.

His gratitude is also extended to CURF for the partial funding of this thesis.

TABLE OF CONTENTS

LIST OF TABLES

LIST OF FIGURES

ABSTRACT

DIFFUSION CONTROLLED VINYL POLYMERIZATION

by

Soh, Sung Kuk

University of New Hampshire, May 1981

It is well known that the polymerization rate and the molecular weight distribution of vinyl polymers can change markedly during the course of polymerization and that these changes are due to the influence of self-diffusion upon the termination reaction. This phenomenon is commonly referred to as the gel effect and in order to explain the polymerization behavior after the onset of the gel effect, the chain length dependence of the termination reaction should be considered.

A new method of handling polymerization kinetics with the chain length dependence termination reaction is proposed, which is largely independent of the form of the chain length dependency and is capable of dealing with both disproportionation and recombination modes of termination with chain transfer reaction to monomer.

The vinyl polymerization kinetics is modelled for each of the four distinct phases which show different polymerization kinetics-physical property interactions.

During Phase I, no interaction is significant and the polymerization kinetics conforms to the conventional kinetics and the molecular weight

distribution to the Schulz-Flory most probable distribution. During the Phase II, the termination reaction is controlled by the translational diffusion of the macroradicals. The polymerization kinetics begin to deviate from the conventional kinetics and the termination reaction rate constant shows chain length dependence and conversion dependence. The chain length dependence is modelled with the chain entanglement concept and the conversion dependence with the free volume theory.

During the Phase III, the gel effect disappears due to the change of the controlling mechanism of termination from translation diffusion to the excess chain mobility of the chain ends coupled with the propagation reaction. The resulting termination rate constant lacks chain length dependency and is named as the residual termination.

During the Phase IV, the propagation reaction and other elementary reactions become diffusion controlled, further slowing down the polymerization rate. A method of estimating the diffusion controlled propagation reaction is proposed.

These models, with the aid of general method of polymerization kinetics, were integrated to simulate the vinyl polymerization systems over the whole range of conversion.

Methyl methacrylate, ethyl acrylate, n-propyl acrylate, vinyl acetate, ethyl methacrylate, and styrene polymerization data are analyzed with the integrated model which has only one adjustable parameter and excellent agreements are observed.

Chapter 1

INTRODUCTION

1.1. OVERVIEW OF POLYMERIZATION KINETICS

Vinyl polymerization refers to the free radical addition polymerization of monomers with a vinyl functional group which forms a carbon-carbon chain upon polymerization. Vinyl polymerization can be performed in bulk, solution, suspension or in emulsion processes. Among the four methods of polymerization, bulk polymerization is the simplest as it does not contain components which do not react, as in solution polymerization, or a separate phase as in suspension and emulsion polymerizations. In this regard, the understanding of bulk polymerization is essential to the elucidation of the others.

This thesis is devoted to the explanation of bulk vinyl polymerization and will serve as a starting point for the detailed understanding of solution, suspension and emulsion polymerization of vinyl monomers.

The elementary reactions which constitute the overal free radical polymerization reaction are as follows:

initiation: $I_2 \longrightarrow 2I$

propagation: $R_i\cdot + M \longrightarrow R_{i+1}\cdot$

termination: $R_i\cdot + R_j\cdot \longrightarrow P_{i+j}$ (recombination)

$R_i\cdot + R_j\cdot \longrightarrow P_i + P_j$ (disproportionation)

chain transfer: $R_i\cdot + M \longrightarrow P_i + R_1\cdot$ (to monomer)

$R_i\cdot + S \longrightarrow P_i + R_1\cdot$ (to chain transfer agent)

These reactions remain unchanged even though the reaction rate constants

of the individual reactions may change with the progress of reaction

The description of the reaction of low molecular weight substances is usually complete with an expression for the reaction rate, which is equivalent to specifying dx/dt, the time rate of change of the fractional conversion in the mathematical sense. Unlike reactions of low molecular weight substances, the quantitative description of vinyl polymerization or any other polymerization is very complicated because no synthetic high polymers are chemically pure substances in the strict sense but are mixtures of various components differing in their chain lengths. Thus the description of a polymerization reaction necessitates the consideration of the polydispersity of the chain length distribution in addition to the description of the polymerization rate, or dx/dt.

The polydispersity of linear polymers is defined by a molecular weight distribution function ($F(M_i)$ written in terms of the molecular weight M_i of each components. It is well known that specifying the moments of the distribution function ($F(M_i)$ is mathematically equivalent to specifying the distribution function itself (1). Traditionally, the ratios of the moments are widely used and known as the various average molecular weights and are related to the distribution function as follows (2).

1) The number average molecular weight

$$\overline{M}_n = 1 / \left(\sum_i F(M_i)/M_i \right) = \sum_i N_i M_i / \sum_i N_i \qquad (1.1)$$

where N_i is the number of species i in the sample.

2) The weight average molecular weight

$$\overline{M}_w = \sum_i M_i F(M_i) = \sum_i N_i M_i^2 / \sum_i N_i M_i \qquad (1.2)$$

3) The z-average molecular weight

$$M_z = \sum M_i^2 F(M_i) \Big/ \sum M_i F(M_i) = \sum N_i M_i^3 \Big/ \sum N_i M_i^2 \qquad (1.3)$$

4) The z+i-average molecular weight

$$M_{z+i} = \sum M_i^{2+i} F(M_i) \Big/ \sum M_i^{1+i} F(M_i) = \sum N_i M_i^{3+1} \Big/ \sum N_i M_i^{2+i} \qquad (1.4)$$

where i=1,2,...,etc..

5) The viscosity average molecular weight

$$M_v = \left[\sum M_i^a F(M_i) \right]^{1/a} = \left[\sum N_i M_i^{a+1} \Big/ \sum N_i M_i \right]^{1/a} \qquad (1.5)$$

where a is a constant determined by viscosity measurements for standard polymer samples of narrow molecular weight distribution.

Considering that the reaction conditions will change with changing conversion, it is only possible to predict the instantaneous values of these average molecular weights theoretically, while the experimentally observed values are the cumulative values over the conversion range of the polymerization. The appearance of the bar is used to denote the cumulative average, and the lack of it refers to the instantaneous values henceforth. The relationship between the instantaneous and the cumulative averages are derived in the Appendix A. One computational aspect of this work will be to develop a set of models to obtain the expressions for dx/dt and M_l^is, where the first subscript refers to the kind or the order of the average, or i=n,w,z,etc..

1.2 DESCRIPTION OF VINYL POLYMERIZATION

Phase 1-Conventional Kinetics

Reading a textbook of polymerization usually gives the false impression that the understanding of vinyl polymerization kinetics is almost complete and the prediction of the polymerization behavior is at hand. This impression is substantiated with the availability of the

computer when the analytical solution is not available, and with the values of the elementary reaction rate constants easily found in a handbook or measureable by various experimental techniques.

Unfortunately this is the case only when the elementary reaction rate constants have no chain length dependence. This lack of chain length dependency is one of the critical assumptions of the conventional polymerization kinetics. The resulting molecular weight distribution conforms to the well-known Schulz-Flory most probable distribution where the number molecular weight distribution is identical to eq'n 2.29 and 2.30 with Z=1 and f(y)=1. Details of analyzing the molecular weight distribution will be presented in Chapter 2.

Phase II-The Gel Effect

However, conventional kinetics often fails to describe vinyl polymerization behavior after a critical conversion level which can sometimes be as low as a few % conversion. This departure from conventional kinetics is usually known as the "gel effect".

Phase III-The Plateau Region

At a still higher conversion level, approximately 50% or higher, most of the "gel effect", namely the autoacceleration of the polymerization rate and the ever-widening of the molecular weight distribution, begin to disappear. In the author's opinion, there has not previously been a satisfactory explanation of this observed phenomenon. It is partly due to the fact that most previous studies have been preoccupied with the accelerating phase of the gel effect. This work is the first to offer an explanation of the Phase III and is based on the concept of the excess chain end mobility.

Phase IV-The Final Stage Polymerization

From above 85% conversion, many other factors may become important because the reaction medium has transformed into solid or semi-solid state, so that the elementary reactions which can readily occur in the liquid phase may begin to be severely limited in the solid state. Although it is beyond the scope of this thesis to investigate the polymerization kinetics in the solid state, considerable discussions including the diffusion controlled propagation reaction will be given.

1.3 PROBLEM STATEMENT

The discussion given so far clearly indicates that the modelling of vinyl polymerization over the whole range of conversion cannot be successful with one simplistic theory of the gel effect or any other single phenomenon. It is because most vinyl polymerization systems go through a different state whose physical characteristics change progressively from ordinary liquid and finally to solid plastic material. These states roughly correspond to the Phase I-IV of polymerization behavior. Typically this conversion is accompanied by 10^{15} order of magnitude change in the viscosity of the medium. The objective of this thesis is to develop a set of theoretical methodologies and physical models which as a collection can explain the vinyl polymerization behavior over the whole conversion range. However, it should be emphasized that these theories are independent from each other and the success or the failure of one theory or model does not necessarily discredit other models proposed for the other phases of polymerization. As the reaction kinetics in the low viscosity liquid phases are considered to be adequately described by the well developed

conventional kinetics, this work is naturally concentrated on Phase II-IV of polymerization, which form the subject matter of Chapter 2,3, and 4, respectively.

1.4 APPROACH TO THE PROBLEM

As already pointed out, typical vinyl polymerization behavior goes through four stages of polymerization, which are named "Phase I", "Phase II", "Phase III", "Phase IV". Phase I is the phase where the well-known conventional kinetics can be applied and is not studied further in this thesis.

Phase II is characterized by the "gel effect" and is the result of decreased termination rate constant. The diffusion controlled termination reaction rate constant will inevitably show chain length dependence which is manifested in the broadening of the molecular weight distribution. Chapter 2 is devoted to the Phase II. As it is not generally recognized that the "gel effect" implies the chain length dependence, the first treatment of Phase II will be the discussion about the possibility of the chain length dependence. The chain length dependent polymerization kinetics have not been previously studied in sufficient depth, so a large portion of Chapter 2 is devoted to the development of such kinetics with arbitrary chain length dependence. This general approach is followed by the development of a model for the specific dependence, which is based on the free volume theory and the chain entanglement concepts. These are commonly used to describe the mobility of macromolecular chains.

Phase III is characterized by the disappearance of the once remp-ant gel effect. This is considered to be the result of reaching the

limit of the translational diffusion controlled termination mechanism and the gradual shift toward a new mechanism of termination. The resulting termination rate constant eventually reaches a plateau value. The word "plateau" is used in the sense that the rate of decrease of the termination rate constant with the increasing conversion slows down considerably. The computational method of dealing with such an additional contribution in Chapter 3.

Phase IV is complicated by the beginning of the solid-like behavior where all the previous assumptions of the liquid state radical polymerization may begin to fail. In Chapter 4, some discussion of this final stage polymerization is given. Also from Chapter 2, the free volume theory and the chain entanglement coupling were used throughout to describe the mobility of a polymer chain. As little information is available for the free volume parameters of the polymerization systems of interest, a data treatment method which can extract the necessary information from the viscosity measurements of polymer solutions is developed and used to determine the parameters.

The results of the modelling of Chapter 2-4 are tested for a variety of existing experimental data for methyl methacrylate, ethyl acrylate, n-propyl acrylate, vinyl acetate, ethyl methacrylate, and styrene in Chapter 5. This gives the final test of the proposed set of theories.

Chapter 2

CHAIN LENGTH DEPENDENT TERMINATION

2.1 INTRODUCTION

The analysis of many vinyl polymerizations is complicated by the influence of the physical properties of the reacting system upon the kinetic parameters which control the polymerization behavior. One example is the "gel effect" which refers to the autoacceleration of the polymerization rate due to the decrease in the termination rate constant. The authors view of vinyl polymerization of monomer soluble in its own polymer consists of four phases of distinctive polymerization behavior. Depending on the monomer used or reaction conditions, one or more of the four phases may be absent. They are schematically shown in Fig. 2.1 and 2.2, which display time-conversion and molecular weight-conversion data for methyl methacrylate polymerization at 90^{o}C (3). At low conversions, the polymerization rate is described by conventional kinetics (4), the cumulative molecular weight averages do not change appreciably, and the molecular weight distribution conforms to the "Schulz-Flory most probable distribution" (5) (Phase I). After a certain conversion which appears to be independent of initiator level at the same polymerization temperature, the well known "gel effect" is observed (Phase II). At still higher conversions, the gel effect appears to stop. The polymerization rate is very fast, but the

cumulative molecular weight averages (except the number average molecular weight) level off or begin decreasing slightly (Phase III). Eventually the deceleration becomes profound and when the polymerization temperature is lower than the glass transition temperature of the polymer formed, a limiting conversion is reached beyond which the reaction does not proceed further.(6) (Phase IV).

In this Chapter, it will be established that deviation from "conventional kinetics" during Phase II is fundamentally related to the physical property-kinetics interaction of the reaction medium which leads to diffusion controlled termination reaction. A unified and comprehensive method of analyzing such complicated kinetics will be presented.

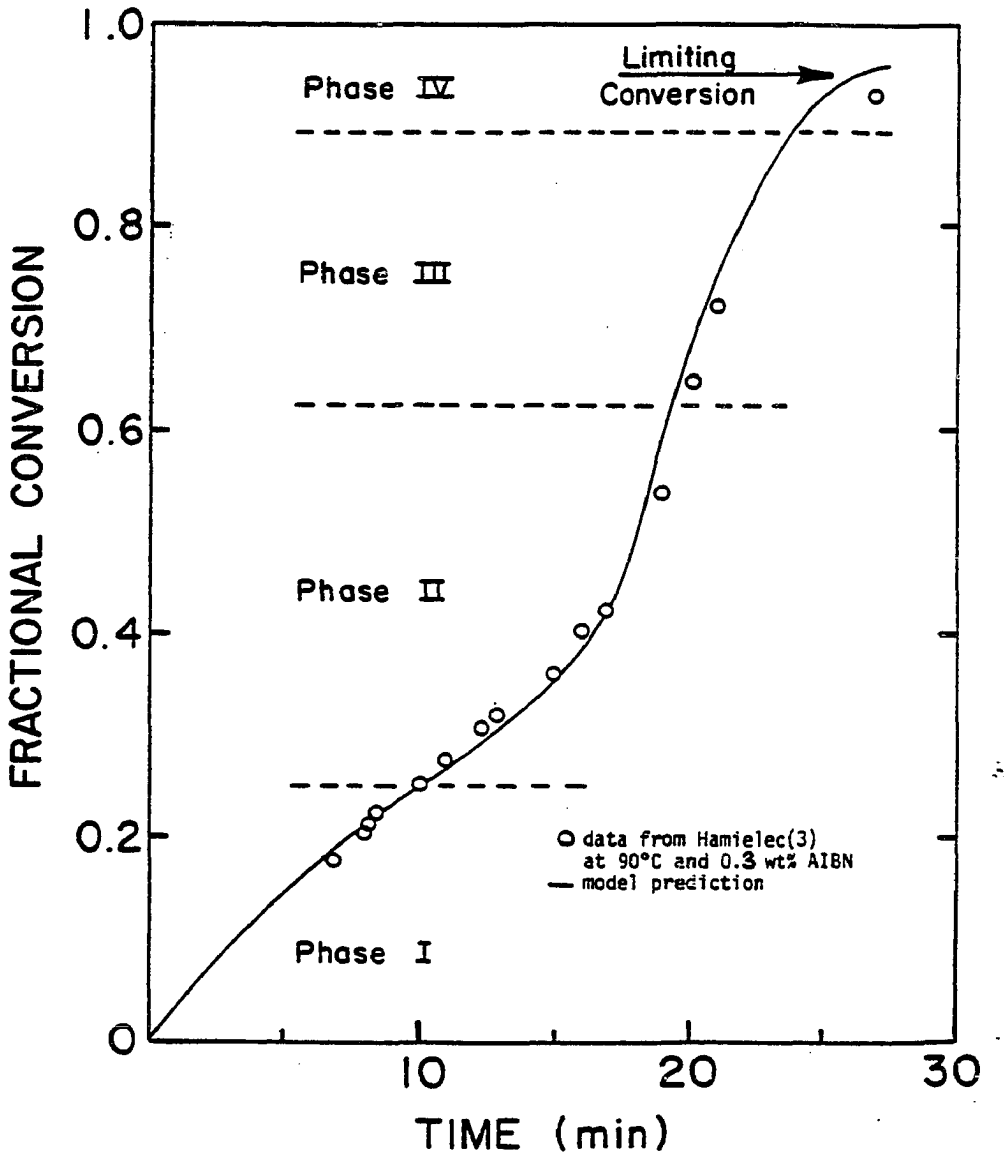

Fig. 2.1 Conversion Profile for Methyl methacrylate Polymerization

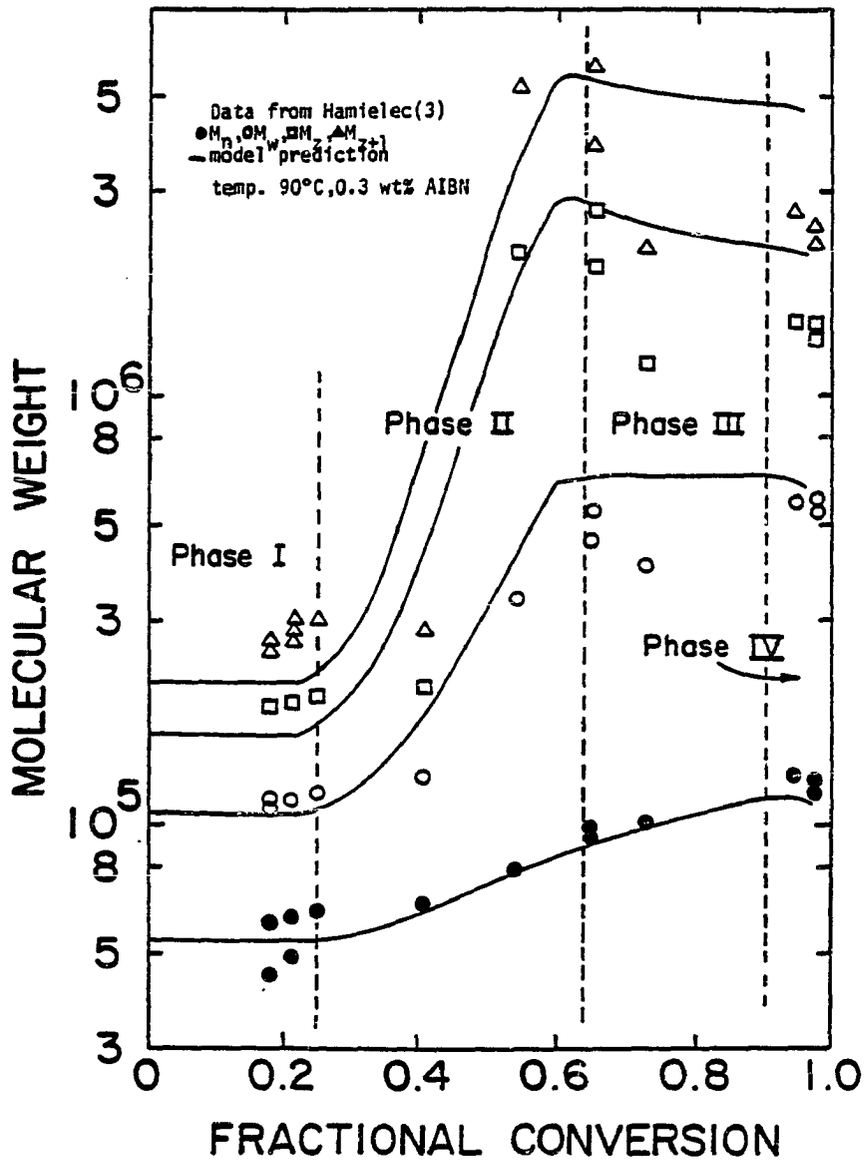

Fig. 2.2 Molecular Weight Development for MMA polymerization

2.2 BACKGROUND

Although there has been evidence that the termination reaction is influenced by the viscosity of the reaction medium from zero conversion (7), and the termination rate constant may not remain constant even at the very low conversion range (8), conventional kinetics are actually quite suitable in this region. Conventional kinetics are fully described by the two parameters, R_p and ν, which are related to the parameters of elementary reactions as

$$R_p = k_p[M]\ (R_i/k_t)^{1/2} \qquad (2.1)$$

$$\nu = k_p[M]/(R_i k_t)^{1/2} \qquad (2.2)$$

R_p determines the polymerization rate and the kinetic chain length ν determines the instantaneous molecular weight distribution, which can be integrated over the conversion range to yield the cumulative molecular weight development which can be observed experimentally. The instantaneous molecular weight averages are determined as multiples of the kinetic chain length ν as shown in Table 2.1. The values of the multiplication constants are characteristic of "the Schulz-Flory most probabl distribution" (9).

Equations 2.1 and 2.2 and the molecular weight distribution of Table 2.1 are valid beyond Phase I as long as there is no chain length dependence of termination rate constant k_t. If chain length dependence is imposed upon the termination rate constant, the analysis becomes quite complicated, but North (4) has elegantly shown that equation 2.1

Table 2.1

Instantaneous Molecular Weight Averages

Molecular Weights	Mode of Termination	
	Disproportionation	Recombination*
M_n	ν	2ν
M_w	2ν	3ν
M_z	3ν	4ν
M_{z+i}	$(3+i)\nu$	$(4+i)\nu$

*without chain transfer

and 2.2 are still valid if k_t is replaced by a proper average $\bar{k}_t$. It should be noted at this point that North's analysis implies that $\bar{k}_t$ is dependent upon the actual size distribution of macroradicals, and the kinetic chain length ν in equation 2.2 can only be used to calculate the number average instantaneous molecular weight M_n of Table 2.1 Higher molecular weight averages can be determined only after a specific form of size distribution function of macroradicals is specified.

These two important points have been generally overlooked and correlation between $\bar{k}_t$ and conversion, or equivalently, free volume, has been sought by various investigators(6,10-13) assuming the molecular weight distribution beyond Phase I still conforms to that of the Schulz-Flory most probable distribution characterizable by the multiplication constants of Table2.1. If one considers the fact that the termination reaction is diffusion controlled, and that the diffusivity of macroradicals is dependent upon chain length (14), such approaches are seen to be theoretically unsound. However, it is extremely difficult to prove chain length dependence experimentally. The difficulties

mainly in the fact that evaluation of the instantaneous molecular weight distribution requires numerical differentiation of experimental data and that it is impossible to generate monodisperse macroradicals for measurements of termination rate. It should also be noted that the number average molecular weight can be determined from the polymerization rate data alone by the relationship between equation 2.1 and 2.2 so that no information about chain length dependence can possibly be obtained from number average molecular weight data. It is no wonder that all previous works (6,10-13) which assumed no chain length dependence fit number average molecular weight data very well with adjustable constants obtained from polymerization rate data, while failing to fit weight average and higher average molecular weight data.

O'Driscoll (15) proposed a chain length dependent termination rate constant which may be rewritten as in equation 2.3.

$$k_{ti} = k_{to} - (k_{to}-k_{te})u(i-i_c) \qquad (2.3)$$

where $u(i-i_c)$ is the unit step function and $k_{tij} = \sqrt{k_{ti}k_{tj}}$. Ito (16) considered an exponential form,

$$k_{tij} = k_{to}(ij)^{-\lambda} \qquad (2.4)$$

O'Driscoll and Ito had considerable success for Phase II, with adjustable constants k_{te}, i_c, and λ, respectively, but the general method of treating chain length dependent polymerizations was left unsolved in their works.

Later in this Chapter a new form of chain length dependence will be proposed as,

$$k_{tij} = k_{tvf}\,[f(i)+f(j,\_/2 \qquad (2.5)$$

$$f(i) = 1.0, \qquad i \leq x_c$$

where $$f(i) = (i/x_c)^{-2.4}, \qquad i > x_c$$

The advantages of the new distribution function f(i) are; 1) it is derived from a theoretical model which will be presented, and not an "assumed" form as equations 2.3 or 2.4, 2) the constant x_c is a physical constant of the polymer whose tabulation is readily available (14), and is not an adjustable constant, 3) remarkable success is obtained for a variety of polymers (methyl methacrylate, ethyl acrylate, and styrene for example) which could not previously be explained with a single model. However, it should be emphasized that the theory of chain length dependent termination presented in the following section does not require a specific form of f(i), and is equally valid for arbitrary chain length dependence, including the conventional kinetics.

2.3 THEORY OF CHAIN LENGTH DEPENDENT TERMINATION

In this section the implications of the chain length dependence of k_t will be investigated with special emphasis upon molecular weight development. This description will be quite general, leaving the specification of a functional form of chain length dependence to a later section of this Chapter.

Termination Rate Constant

Consider a termination rate constant k_{tij} for macroradicals of size i and j. The rate of termination of radicals of length i, designated r_i, will be described by

$$r_i = \sum_{j=1}^{\infty} k_{tij} [R\cdot]_i [R\cdot]_j + k_{tii} [R\cdot]_i^2 \qquad (2.6)$$

Furthermore, in terms of mole fractions of radicals (X_i) of chain length i, defined as

$$X_i \equiv [R\cdot]_i / \sum_{i=1}^{\infty} [R\cdot]_i \equiv [R\cdot]_i / [R\cdot] \qquad (2.7)$$

equation 2.6 can be rewritten as

$$r_i = [R\cdot]^2 \{ \sum_{j=1}^{\infty} k_{tij} X_i X_j + k_{tii} X_i^2 \}. \qquad (2.8)$$

The total termination rate, R_t is given by

$$R_t = \sum_{i=1}^{\infty} r_i = [R\cdot]^2 \{ \sum_{i=1}^{\infty} \sum_{j=1}^{\infty} k_{tij} X_i X_j + \sum_{i=1}^{\infty} k_{tii} X_i^2 \} \qquad (2.9)$$

It is reasonable to assume that k_{tij} is the arithematical average of k_{tii} and k_{tjj}, or

$$k_{tij} = 1/2(k_{tii} + k_{tjj}) \tag{2.10}$$

This assumption is closely related to the generally accepted assumption of the additivity of the mutual diffusivity (21),

$$D_{A,B} = D_A + D_B \tag{2.11}$$

Note that equation 2.10 and equation 2.5 are equivalent with the definition $k_{tii} = k_{tvf}\, f(i)$, where k_{tvf} is a constant. With equation 2.10, equation 2.9 can be further simplified using the relationship $\sum_{i=1} X = 1.0$ and neglecting the small contribution of the X_i^2 term,

$$R_t = [R\cdot]^2 \sum_{i=1}^{\infty} k_{tii} X_i \tag{2.12}$$

As the average termination rate constant $\bar{k}_t$ which is suitable for equation 2.1 and 2.2 should predict the total termination rate,

$$R_t = \bar{k}_t\, [R\cdot]^2 \tag{2.13}$$

$\bar{k}_t$ is then related to the individual constant k_{tii} as

$$\bar{k}_t = \sum_{i=1}^{\infty} k_{tii} X_i \tag{2.14}$$

If one defines a probability P(i) such that it represents the probability that a primary radical survives to become a macroradical of chain length i, X_i can be expressed as

$$X_i = P(i) / \sum_{i=1}^{\infty} P(i) \tag{2.15}$$

Combining equations 2.14, 2.5, and 2.15,

$$\bar{k}_t = k_{tvf} \sum_{i=1}^{\infty} f(i)P(i) / \sum_{i=1}^{\infty} P(i) \tag{2.16}$$

Dealing with discrete summations as in equation 2.16 makes computations tedious, and the approximation to a continuous variable is a routine practice. Choosing an arbitrary reference chain length x_c which is large enough to make $1/x_c \cong 0$, the relative chain length y is defined as

$$y = i/x_c \tag{2.17}$$

Then the ratio $Z \equiv \bar{k}_t/k_{tvf}$ can be determined from equation 2.16 as

$$Z = \bar{k}_t/k_{tvf} = \int_0^\infty f(y)P(y)dy / \int_0^\infty P(y)dy \tag{2.18}$$

Although it is intended to leave f(y) unspecified at this point, P(y) does need further identification. The probability that a radical survives termination and chain transfer at any single growth step is given by the ratio of propagation to (propagation + termination + transfer) rates,

$$p(i) = k_p[M]/\{k_p[M] + 1/2(k_{ii}+\bar{k}_t)[R\cdot] + k_{tr,M}[M] + k_{tr,S}[S]\}$$

Using the pseudo-steady state conditon ($R_i=R_t$), and equations 2.5, 2.13 and 2.18,

$$1/p(i) = 1+\gamma f(i)/(2x_c\sqrt{Z}) + \gamma\sqrt{Z}/2x_c + \beta/x_c \tag{2.19}$$

where

$$\gamma = x_c(R_i k_{tvf})^{1/2}/(k_p[M]) \tag{2.20}$$

$$\beta = C_M x_c + C_S x_c[S]/[M] \tag{2.21}$$

Note that the kinetic chain length ν of equation 2.2 is related to γ as

$$\nu = x_c/(\gamma\sqrt{Z}) \tag{2.22}$$

The probability that a polymer radical survives a series of steps (P(i)) is the multiple of the individual probabilities, p(i), or

$$P(i) = \prod_{i=1}^{i} p(i) \qquad (2.23)$$

It is a mathematical identity that

$$\prod_{i=1}^{i} p(i) = \exp\left[\sum_{i=1}^{i} \ln p(i)\right] \qquad (2.24)$$

and from equation 2.19

$$\ln p(i) = -\ln 1/p(i) = -\ln\{1+\gamma f(i)/(2x_c\sqrt{Z}) + (1/x_c)(\gamma\sqrt{Z}/2+\beta)\} \qquad (2.25)$$

Since termination and transfer are rare events compared to propagation, the last two terms in equation 2.25 are very small compared to unity (i.e. $p(i) \cong 1.0$). Thus the logarithm term can be expanded in the form of a Taylor series as

$$\ln p(i) \cong -\{\gamma f(i)/(2x_c\sqrt{Z}) + (1/x_c)(\gamma\sqrt{Z}/2 + \beta)\}$$

Combining this expression with equation 2.24 and transforming to the continuous variable y,

$$P(y) = \exp\{-(\beta+\gamma\sqrt{Z}/2)y - \gamma/(2\sqrt{Z})\int_0^y f(y)dy\} \qquad (2.26)$$

At this point the general description of the termination rate constant is complete and is embodied in equations 2.18, 2.20, 2.21 and 2.26.

Molecular Weight Development

The probability of formation of dead polymer chains of length i is denoted as $N_d(i)$ and $N_r(i)$ where the subscript d and r refer to disproportionation and recombination, respectively.

$$N_d(i) = (C_M+C_S[S]/[M])[R\cdot]X_i + [R\cdot]^2 \sum_{j=1}^{\infty} k_{tij}X_iX_j /k_p[M] \qquad (2.27)$$

$$N_r(i) = (C_M+C_S[S]/[M])[R\cdot]X_i + [R\cdot]^2 \sum_{j=1}^{i-1} k_{tjk}X_jX_k /k_p[M] \qquad (2.28)$$

with k = i-j and where the first term represents the contribution from chain transfer and the right term that from termination. In terms of the continuous variable y, using the relationships developed previously, equations 2.27and 2.28 becomes

$$x_cN_d(y) = [\beta + \gamma\{Z+f(y)\}/2\sqrt{Z}]P(y) \qquad (2.29)$$

$$x_cN_r(y) = \beta P(y) + \gamma(\beta+\gamma\sqrt{Z})/(\sqrt{Z}) \int_0^{y/2} 1/2[f(t)+f(y-t)]P(t)P(y-t)dt \qquad (2.30)$$

To generate a series of molecular weight averages from equations 2.29 and 2.30, it is necessary to define the ith moments of N(y), P(y), and f(y)P(y) as

$$N_i^m \equiv \int_0^{\infty} y^iN_m(y)dy \qquad (2.31)$$

$$P_i \equiv \int_0^{\infty} y^iP(y)dy \qquad (2.32)$$

$$F_i \equiv \int_0^{\infty} y^if(y)P(y)dy \qquad (2.33)$$

where m can be d or r. Equation 2.29 and 2.30 can be substituted into equation 2.31 to give, as shown in detail in the Appendix B,

$$x_cN_i^d = (\beta+\gamma\sqrt{Z}/2)\ P_i + (\gamma/2\sqrt{Z})\ F_i \qquad (2.34)$$

$$x_cN_i^r = \beta P_i + (\gamma/2\sqrt{Z})\ (\beta+\gamma\sqrt{Z}) \sum_{j=0}^{i} \binom{i}{j} F_jP_{ij} \qquad (2.35)$$

where $\binom{i}{j} = i!/(j!(i-j)!)$

With some algebra, F_i of equation 2.33 can be expressed by P_i (Appendix B).

$$F_i = (2\sqrt{Z}/\gamma)\ \{iP_{i-1} - (\beta + \gamma\sqrt{Z}/2)P_i\}, \qquad (i \geq 1)$$

$$F_0 = Z/(\beta+\gamma\sqrt{Z}) \qquad (2.36)$$

Equations 2.34-36 show that only P_i need be evaluated for any particular distribution function f(y) to evaluate N_m^i, which is necessary to evaluate molecular weight averages. It should also be noted that the two dimensionless parameters β and γ uniquely determine the polymerization rate and the molecular weight distribution given a specific form of f(y).

Previous discussions predict that the number average molecular weight should not be dependent upon the form of the distribution function f(y) as long as it gives the same average termination rate constant, or equivalently, the same value of Z. This is indeed the case and integration performed in the Appendix C is rewritten as follows;

$$y_n^d = x_n^d/x_c = N_1^d/N_0^d = 1/(\beta + \gamma\sqrt{Z}) \qquad (2.37)$$

$$y_n^r = x_n^r/x_c = N_1^r/N_0^r = 1/(\beta + \gamma\sqrt{Z}/2) \qquad (2.38)$$

It should be noted that equations 2.37 and 2.38 are identical to the more familiar form via equations 2.24 - 2.26.

$$1/x_n^d = C_M + C_S[S]/[M] + 1/\nu \qquad (2.39)$$

$$1/x_n^r = C_M + C_S[S]/[M] + 1/2\nu \qquad (2.40)$$

As the number average molecular weight is the same for different distribution functions if they yield same average termination rate constant, it is advantageous to define the molecular weight indices, ℓ_i's, as the

ratio of ith order molecular weight average to the number average molecular weight M_n,

$$\ell_i = M_i/M_n \tag{2.41}$$

For termination by disproportionation, the indices (ℓ_i^d's) are readily expressed in terms of the moments P_i's, but for the case of recombination with chain transfer to monomer, it is much simpler to express the ℓ_i^r's in terms of ℓ_i^d's. These expressions are given in Table 2.2.It should be noted that the indices are identical to the multiplication constants of Table 2.1 if Z=1, as expected. Details of derivations are given in the Appendix D. The expressions in Table 2.2 show that in order to evaluate molecular weight developments in any mode of termination, only the indices for disproportionation are necessary.

The results of the theoretical investigations of this section may be summarized as follows. Given any distribution function f(y) which characterizes the chain length dependence of the termination rate constant, there are only two dimensionless parameters, β and γ, which determine the polymerization rate and molecular weight distribution. The indices of polymerization rate (Z) and molecular weight distribtuion (ℓ_w,ℓ_z,ℓ_{z+1}) can be plotted in the form of master curves once the form of f(y) is specified. These curves will be shown at the end of the next section which discusses f(y).

Table 2.2

Indices of the Molecular Weight Distribution

Molecular Weight Index	Mode of Termination	
	Disproportionation	Recombination
$\ell_w \equiv M_w/M_n$	$2(\beta+\gamma\sqrt{Z})^2 P_1$	$f_1 f_2 \ell_w^d$
$\ell_z \equiv M_z/M_n$	$3/2(\beta+\gamma\sqrt{Z})P_2/P_1$	$3(f_1/f_2)(2\ell_z^d+\ell_w^d/2-f_1\ell_w^d\ell_z^d)$
$\ell_{z+1} \equiv M_{z+1}/M_n$	$4/3(\beta+\gamma\sqrt{Z})P_3/P_2$	$4f_1\ell_z^d(f_2\ell_{z+1}^d+\ell_w^d[1-(\ell_w^d+\ell_z^d)/2])/$ $\ell_z^d(2-f_1\ell_w^d+\ell_w^d/2)$
$\ell_{z+i} \equiv M_{z+i}/M_n$	$(\frac{i+3}{i+2})(\beta+\gamma\sqrt{Z})P_{2+i}/P_{1+i}$	

$$f_1 \equiv N_o^r = (\beta+\gamma\sqrt{Z}/2)/(\beta+\gamma\sqrt{Z}) = M_n^r/M_n^d$$

$$f_2 \equiv 2 - f_1\ell_w^d/2$$

2.4 DISTRIBUTION FUNCTION FROM ENTANGLEMENT THEORY

The results of the previous section are valid for any form of the distribution function f(y). Conceptually f(y) can be determined from the actual molecular weight distribution obtained from experimental data. However, this inversion problem would require extremely accurate differential GPC chromatograms. Even if errorless chromatograms are available, the inversion will require very cumbersome numerical calculations. The approach taken in this investigation is to propose a reasonable form of the distribution function consistent with the present theories of polymer physics and compare its predictions with experimental data.

A theoretical expression of the translational diffusion controlled termination rate constant can be developed by visualizing the polymer chain as a sphere of equivalent radius R_{hi} with diffusivity D_i in the reaction medium. Several models have already been developed for the equivalent case for small molecules (21) and can be applied here. Although the proportionality constant may differ among different models, the following proportionality is common for all major models.

$$k_{tii} \propto R_{hi} D_i \tag{2.42}$$

The diffusivity D_i may be described in terms of the friction coefficient ζ_i by the Stokes-Einstein equation (14).

$$D_i = kT/\zeta_i \tag{2.43}$$

For the case of a dilute solution corresponding to the low conversion range, the friction coefficient is proportional to the hydrodynamic equivalent radius R_{hi} (17),

$$\zeta_i = 6\pi\eta_o R_{hi} \qquad (2.44)$$

R_{hi} is proportional to chain length i for the freely draining chain and to root-mean-square radius of gyration for the impenetrable coil (17). In either case, the collision radius R_{hi} of equation **2.42** should be equal or proportional to the hydrodynamic radius R_{hi} of equation **2.44.**

$$k_{tii} \propto kT/\eta_o \qquad (2.45)$$

and is a constant at a given temperature. This is because equation **2.42** is based on the visualization of translational diffusion as that of a sphere. It may easily be identified as the molecule itself for small molecules, but it will be logical to identify it as the hydrodynamic equivalent radius of the polymer as it is the closest visualization of the translating spherical body.

Equation **2.45** shows the termination rate controlled by translational diffusion at low concentration is inversely proportional to the solvent viscosity η_o. It should be noted that one of the "evidences" presented by North and Reed (8) to propose that the termination rate is segmental diffusion controlled at low conversion is the inverse proportionality of the termination rate to the solvent viscosity. Equation **2.45** raises the question of whether there is segmental-to-translational transition of the controlling mechanism at low concentrations.

The diffusivity at moderate to high polymer concentration ranges is generally treated by free volume theory (18). The Doolittle equation

for the shift factor a_c for the monomeric friction coefficient ζ_1 is the usual starting point of free volume correlations (14).

$$\ln a_c = \ln \zeta_1/\zeta_1^* = B(1/v_f - 1/v_f^*) \qquad (2.46)$$

where * denotes an arbitrary reference point. Fujita's approach is to assume B=1 and define the fractional free volume v_f accordingly (18). Recently, Vrentas and Duda (19) proposed a refined theory of the diffusion in polymer-solvent systems. Fujita's theory and Vrentas and Duda's are equivalent for monomer-polymer pairs. More detailed investigation on this subject will be **presented in Chapter 4.** It will suffice here to note that both theories reduce to equation **2.48** for the diffusivity of macromolecules if the polymer chains are in the state of entanglement, a condition which is satisfied when equation **2.47** holds.

$$\begin{aligned} \overline{M}_w &\geqq x_c M_o \\ &= (x_{co})M_o/(1-\phi_M) \end{aligned} \qquad (2.47)$$

$$D_i = (A/(iQ_e))\exp(-B/v_f) \qquad (2.48)$$

where Q_e is given by Bueche (20) as

$$Q_e = (1+Mo/8Me)\{1+a(Mo/2Me)^{3/2}\sum_{n=1}^{\infty} S^n(2n-1)^{3/2}[1-\exp(-a[2n-1]^{3/2}]\}$$

$$\text{where } a = (\rho N_{Av}/3)(\langle R^2\rangle/Mo)^{3/2}(2Me)^{1/2} \qquad (2.49)$$

Due to the complexity of equation **2.49**, the author decided to avoid using it, but instead to use the entanglement coupling factor determined experimentally (14). In this case Q_e is given as

$$Q_e = \begin{cases} 1 & i \leqq x_c \\ (i/x_c)^{+2.4} & i > x_c \end{cases} \qquad (2.50)$$

It may be noticed that the function Q_e is identical to the function f(y) proposed in equation 2.5. It is not a coincidence but a result of the following derivation.

Equations 2.48 and 2.50 give an expression for the diffusivity of macroradicals, but an estimation of the collison radius R_{hi} in equation 2.44 requires more inspection. From the previous discussion, the collision diameter was assumed to be proportional to the hydrodynamic equivalent diameter, who's proportionality to chain length i ranges from $i^{1/2}$ to i depending upon the flexibility of chain. By the word flexible it is meant the ease of assuming more chain configurations within the time scale of translational movement. At the conversion range where free volume theory is applicable, the chain-chain interaction visualized by entanglement should have increased by orders of magnitude compared to the dilute concentration range. Based on the shift factor a_c, this means that the movement of a whole chain (translation) becomes slower and slower relative to the movements of individual segments, which results in new chain configurations. Thus in the time scale of translational diffusion, the chain will become more flexible, approaching the behavior of freely draining chain. Therefore it was decided that the collision radius R_{hi} is proportional to i. Combing this idea with equations 2.42 and 2.48 leads to

$$k_{tii} \propto (A/Q_e)\exp(-B/v_f)$$

or that

$$k_{tii} = (k_t^*/Q_e)\exp(-B/v_f) \qquad (2.51)$$

where k_t^* is some constant. Comparing this with equation 2.5 ($k_{tii} = k_{tvf}\, f(i)$) yields,

$$k_{tvf} = k_t^* \exp(-B/v_f) \tag{2.52}$$

$$f(i) = Q_e^{-1} = \begin{cases} 1 & i \leq x_c \\ (i/x_c)^{-2.4} & i > x_c \end{cases} \tag{2.53}$$

It is now evident that the proportionality constant k_{tvf} is proportional to the shift factor, a_c, of equation **2.46**.

Because the mechanism of the transition from Phase I into the translation diffusion controlled Phase II is not certain, it was approximated that the transition is abrupt at a critical free volume v_{fc}. It is further assumed that k_{tvf} at v_{fc} is equal to k_{to}, the termination rate constant of Phase I. Then equation **2.52** becomes

$$k_{tvf} = k_{to}^* \exp\left(B(1/v_{fc} - 1/v_f)\right) \quad \text{for } (v_f < v_{fc}) \tag{2.54}$$

The conclusion of this description of the termination rate constant is that it may be written as a chain length independent factor, k_{tvf}, which is related to the free volume, and a chain length factor, Q_e, which describes the degree of chain entanglements. Utilizing equations **2.53** and **2.54**, the termination rate constant k_{tii} is completely specified. The value of k_{to}^* is determined by the requirement that $\bar{k}_t$ is continuous at $v_f = v_{fc}$.

$$\bar{k}_t\Big|_{v_{fc}} = k_{to}^* Z = k_{to} \tag{2.55}$$

It is now possible to develop a set of master curves which describe the indices of polymerization rate (Z) and the molecular weight distribution ($\ell_w, \ell_z, \ell_{z+1}$). The chain length distribution function f(i) is cast into the continuous variable form f(y) as

$$f(y) = \begin{cases} 1 & y \leq 1 \\ y^{-2.4} & y > 1 \end{cases} \qquad (2.56)$$

and used eq'n 2.26 to calculate P(y). Details of these procedures will be discussed in the next section. The resultant master curves for Z, 1^d_w, 1^d_z, and 1^d_{z+1} in terms of β and γ are shown in Figs. 2.3-2.6.

For the case when the condition of eq'n 2.47 is not met, there can be no chain length dependence as the entanglement coupling factor Q_e equals 1, yielding

$$f(y) = 1 \qquad \text{(all } y\text{)} \qquad (2.57)$$

In this case the polymerization becomes "pseudo-conventional", which means that the value of the effective terminationrate constant k_t changes with conversion (due to the decreasing free volume) while the instantaneous molecular weight distribution becomes to that of the Schulz-Flory most probable distribution. Such cases are often observed in styrene polymerization in the middle conversion range.

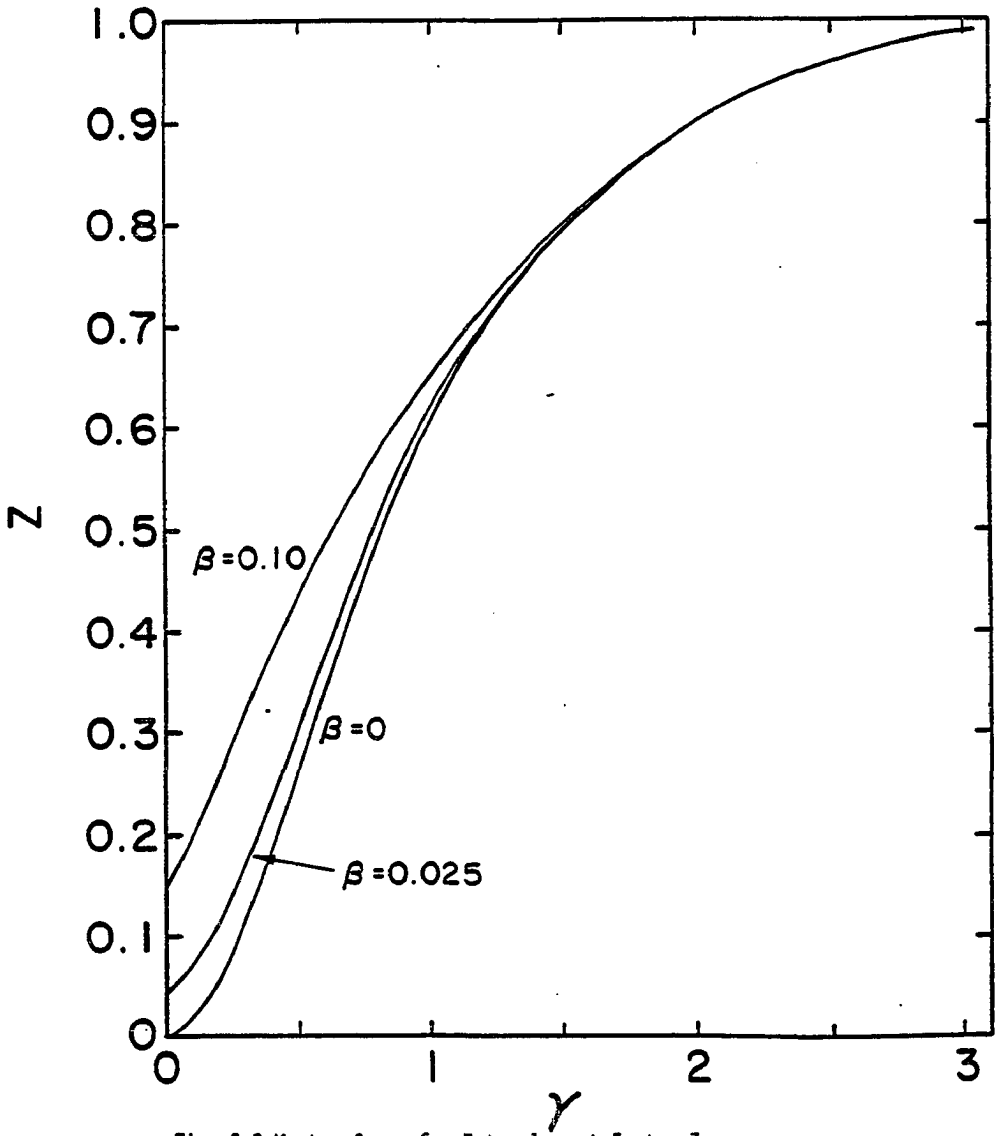

Fig. 2.3 Master Curve for Entanglement Factor Z

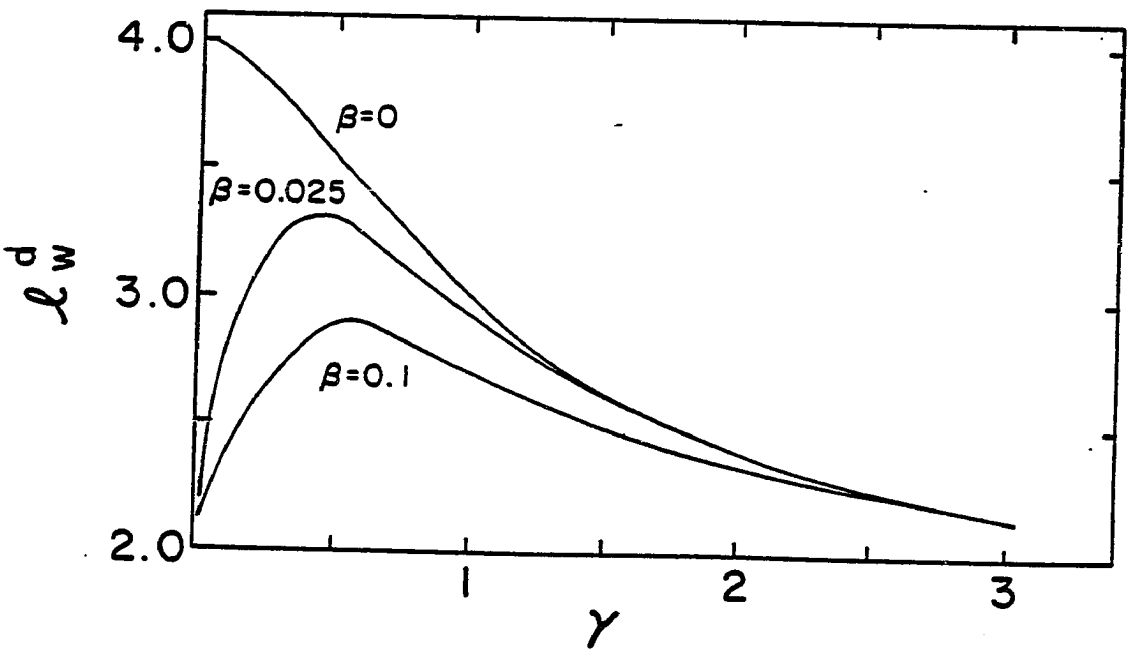

Fig. 2.4 Master Curve for l_w^d

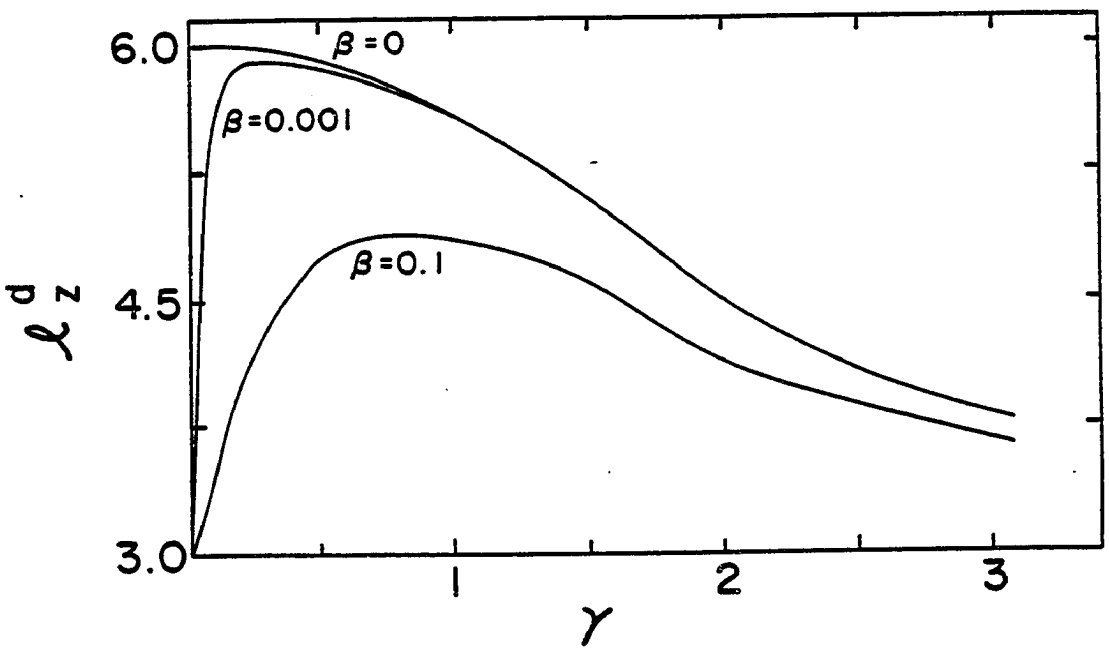

Fig. 2.5 Master Curve for l_z^d

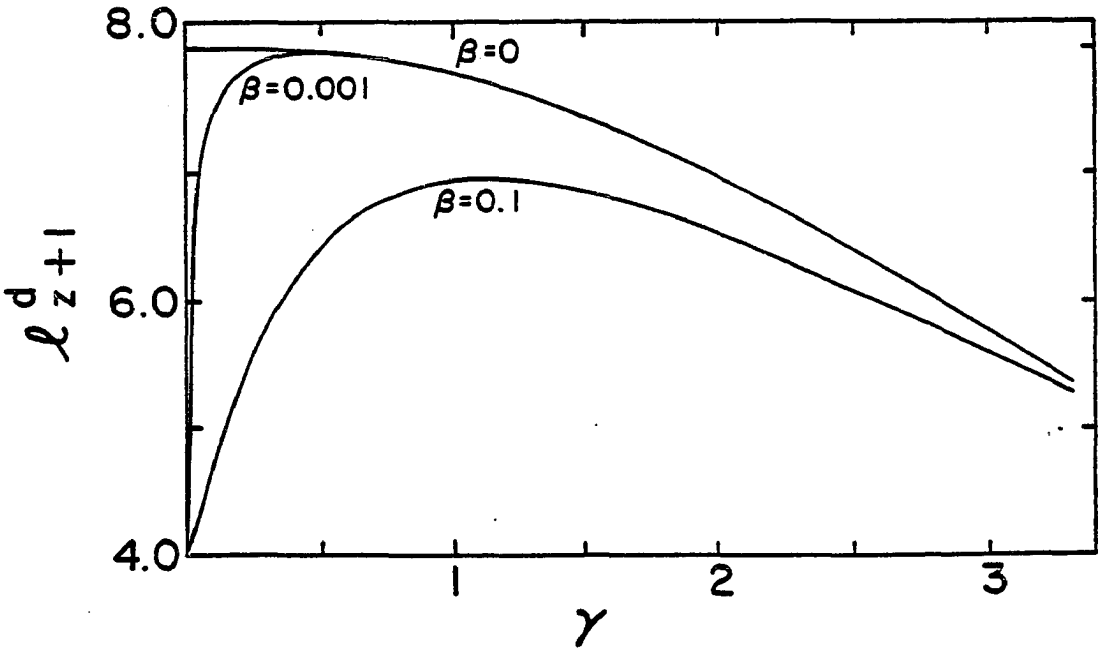

Fig. 2.6 Master Curve for l^d_{z+1}

2.5 RESULTS AND DISCUSSION

It was shown in 2.3 that the molecular weight indices l_i's and the entanglement factor Z are determined with the two dimensionless parameters β and γ. Using the chain length dependence function $f(y)$ proposed in 2.4, it is now possible to calculate these indices and will result in the master charts already shown in Figs. 2.3-2.6.

ENTANGLEMENT FACTOR Z

The entanglement factor Z is to be evaluated first as the expressions for other indices contain Z, so they can not be evaluated before Z is. For arbitrary values of β and γ, Z should be found from the following integral equation 2.58.

$$Z = \frac{\int_0^\infty f(y)P(Z, \beta, \gamma, y)dy}{\int_0^\infty P(Z, \beta, \gamma, y)dy} \qquad (2.58)$$

Substitution of eq'n 2.26 gives the more specific form.

$$Z = \frac{\int_0^\infty f(y)\exp[-(\beta + \frac{\gamma\sqrt{Z}}{2})y - \gamma\sqrt{Z}\int_0^y f(y)dy]dy}{\int_0^\infty \exp[-(\beta + \frac{\gamma\sqrt{Z}}{2})y - \frac{\gamma}{2\sqrt{Z}}\int_0^y f(y)dy]dy} \qquad (2.59')$$

Using the eq'n 2.56, $f(y)$ and $\int f(y)dy$ can be evaluated as

$$f(y) = \begin{cases} 1 & y \leq 1 \\ y^{-2.4} & y > 1 \end{cases} \qquad (2.60)$$

and

$$\int_0^\infty f(y)dy = y \qquad y \leq 1$$

$$= \frac{2.4-y^{-1.4}}{1.4} \qquad y > 1 \qquad (2.61)$$

Now eq'n 2.61 can be integrated numerically and was done by the CSMP program CSMP.DIS (or CSMP.FOR) shown in the Appendix E. In this program, with the given values of β and γ, a trial value of Z is substituted in eq'n 2.59, and is integrated from 0 to the value given by the TIMER statement. The value of the recalculated Z is printed as a function of the integration limit FINTIM.

$$Z(\text{FINTIM}) = \frac{\int_0^{\text{FINTIM}} f(y)P(Z,\beta,\gamma,y)dy}{\int_0^{\text{FINTIM}} P(Z,\beta,\gamma,y)dy} \qquad (2.62)$$

The convergence of Z(FINTIM) with increasing FINTIM is readily checked in the print-out. The procedure is repeated until the trial value of Z is equal to the Z(FINTIM) as FINTIM approaches infinity. Fig. 2.3 shows the result of such calculations, where Z value is plotted as a function of β and γ as parameters. The range $0 \leq \beta \leq 0.1$ is sufficient for most purposes. It can be observed in Fig. 2.3 that until γ becomes very small ($\gamma < 1$), the effect of the chain transfer to monomer, determined by β, is negligible. It should also be noted that it requires $\gamma > 3$ to assume $Z = 1$. This means that the effect of chain entanglement coupling is significant even when the kinetic chain length is smaller than the chain length required for entanglement, or even when most radicals terminate before they grow to a sufficient length for entanglement coupling, the small fraction which grow very long play very significant role in determining the polymerization behavior of the system.

MOLECULAR WEIGHT INDICES

Once the Z chart is prepared, the calculation of the molecular weight indices are straightforward using the relationships given in Table 2.3. The calculations were done by the same CSMP program CSMP.DIS as P_i is readily calculated from the definition.

$$P_i \cong \int_0^{FINTIM_i} y^i P(y)dy \qquad (i=1,2,3) \qquad (2.6)$$

Again the convergence of the integral to P_i is checked by the print-out as a function of FINTIM.

Figs. 2.4-2.6 shows the results of the computations for λ_i^d (i=w, z, and z+1). The values can be as much as twice the value expected from the Schulz-Flory most probable distribution.

As chain transfer to monomer is a chain length independent reaction which forces the distribution closer to the Schulz-Flory most probable distribution, the deviation from the Schulz-Flory distribution decreases as β increases. It can also be observed that the increased γ value produces less deviation. For $\gamma<1$, the deviation becomes very profound.

INTERPOLATION TECHNIQUE

For computer modelling of vinyl polymerizations, it is more convenient to have an interpolation function for the entanglement factor Z and the molecular weight indices λ_i^d's. This was done by using IMSL subroutine IQHSCU which computes the bicubic spline coefficients from a given set of data points. The values of Z, λ_w^d, λ_z^d, and λ_{z+1}^d

calculated for the ten γ values ranging from 0 to 10 for the β values of 0, 0.01, and 0.1 using the previously mentioned CSMP.DIS program were used to obtain the ten interpolation constants in the CONST.FOR program shown in the Appendix E. These 40 spline coefficients were stored in the data file CONST.DAT. These data were read when necessary by calling the subroutine COEFF.FOR also found in the Appendix E.

The indices Z, 1_w^d, 1_z^d, 1_{z+1}^d for any γ value with β=0, β=0.001, or β=0.1 are computed in a subroutine AUX.FOR. When the γ value lies within 0 to 10, the indices are interpolated with the spline coefficients stored in the CONST.DAT file. For γ values of greater than 10, it was set equal to the values for the conventional kinetics, which are; Z = 1, 1_w^d = 2, 1_z^d = 3, and 1_{z+1}^d = 4.

For arbitrary values of β and γ which may be required by the main program or the other subroutines, the calculation of the indices are performed by the subroutine CALCU.FOR, which in turn calls the subroutine AUX.FOR. When the β value lies between 0 and 0.001 or between 0.001 and 0.1, the indices are linearly interpolated between the values calculated by AUX.FOR. When the β value is greater than 10, the indices are approximated to equal to the conventional kinetics values. When the β value lies between 0.1 and 10, the indices arelinearly interpolated between the values for β=0.1 and β=10.

RECOMBINATION MODE

For the same values of β and γ, the mode of termination has no

effect on Z value and the molecular weight indices can be calculated from the indices for the disproportionation mode of termination by the relationships given in Table 2.3. This computation is done by the subroutine SBRKPL.FOR, which calls the subroutine CALCU for the values of Z and l_i^d's and calculates the corresponding l_i^r's if the mode of termination is recombination. The mode of termination is supplied as the first argument of SBRKPL.

2.6 CONCLUDING REMARKS

The translational diffusion-termination reaction interaction is completely described once the function f(y) is specified. When the condition of eq'n 2.47 is met, for any form of f(y) only two dimensionless parameters, β and γ, determine all of the observable features of a polymerization reaction (rate and molecular weight distribution). A realistic form of f(y) has been proposed which is based on the entanglement theory, and the master charts for the rate and molecular distribution have been proposed. This offers a complete description of events during Phase II, or the "gel effect", of vinyl polymerizations.

Chapter 3

RESIDUAL TERMINATION

3.1 INTRODUCTION

In Chapter 2, it was proposed that many vinyl polymerizations consist of four distinctive phases which have different physical property - kinetic interactions. Phase I can be described by conventional kinetics as the termination reaction is generally thought to be controlled by segmental diffusion. The resulting termination rate constant is chain length independent, which enables the molecular weight distribution of Phase I to conform to the Schultz-Flory most probably distribution. In Phase II, which is commonly described by the phrase "gel effect", the termination reaction becomes controlled by translational diffusion which is inherently chain length dependent. Phase II was the subject of Chapter 2 where a new theoretical model of chain length dependent termination reactions was proposed and the subsequent kinetics and molecular weight distributions were presented. These were seen to be different from conventional kinetics and the Schultz-Flory most probably distribution of Phase I. The characteristic of the molecular weight development was the profound broadening of the molecular weight distribution, which makes higher order molecular weight averages increase at a much faster rate than the lower order molecular weight averages such as $\overline{M}_n$. This is

shown dramatically in Fig. 3.1.

In Phase III, the polymerization rate stops increasing and the higher molecular weight averages level off or begin decreasing while the number average molecular weight continues to increase as shown in Fig. 3.1. This apparent disappearance of the "gel effect" and the narrowing of the molecular weight distribution strongly suggests the existence of a mechanism by which the translational diffusion controlled termination mechanism is changed. This has not generally been recognized and O'Driscoll [15] and Hamielec [13] have proposed different models which in effect limit the oolymerization rate. Their models will be critically reviewed in the following section 3.2. This Chapter will deal with the chain end mobility controlled termination mechanism which the author believes to be dominant in Phase III and which is believed to be responsible for the disappearance of the gel effect.

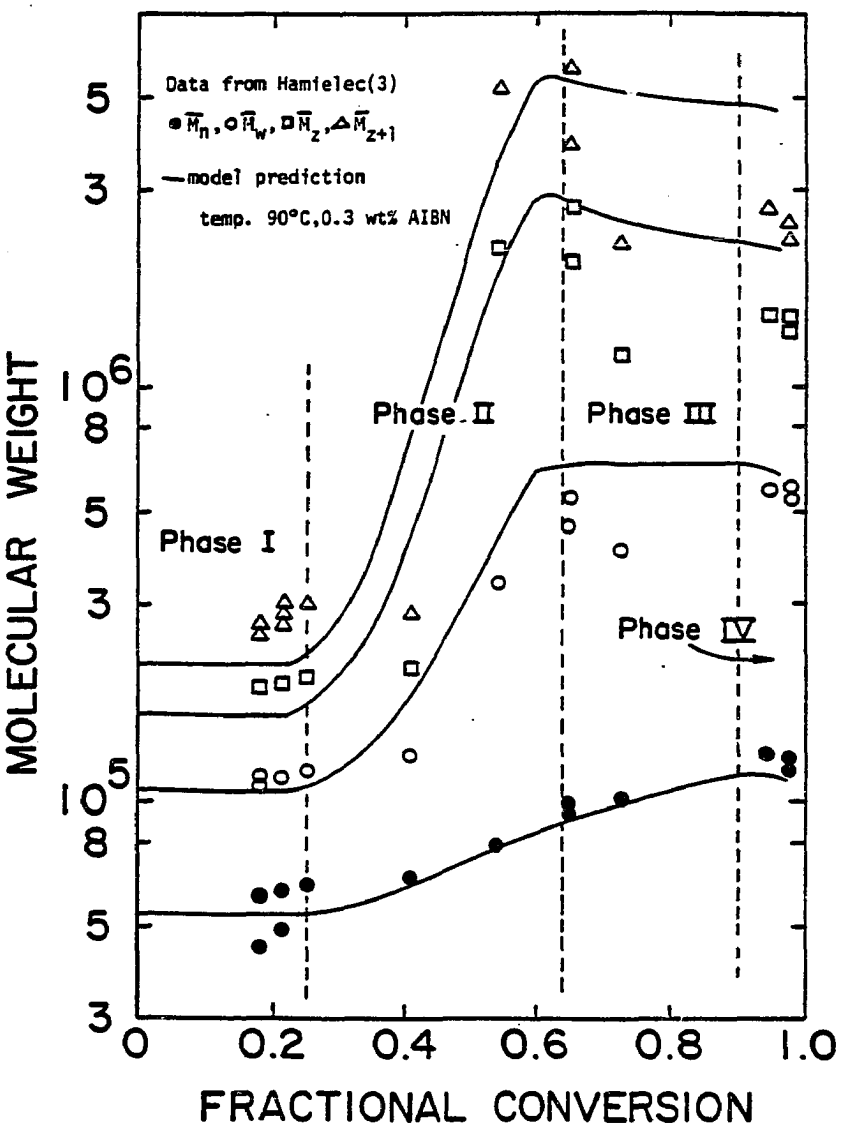

Fig. 3.1 Molecular Weight Development for MMA polymerization

3.2 REVIEW OF EXISTING THEORIES

It has already been mentioned that O'Driscoll and Hamielec have theories which in effect limit the gel effect. It is the purpose of this section to show that the existing theories should not be considered to be the general mechanism controlling Phase III. It should be mentioned here that the evolution of the theory presented here owes heavily to O'Driscoll's and Hamielec's theories.

Cardenas and O'Driscoll(15) have presented a model which describes the effective termination rate constant at any conversion as a value which lies between the conventional value k_{to} and a limiting value for entangled polymer, k_{te}. This is equivalent to assuming a step function for the chain length dependent termination rate constant, which is perhaps the simplest way of introducing chain length dependence into the polymerization kinetics. The rate constant k_{te} is limiting in the sense that when all polymer chains are long enough to be entangled, the effective rate constant is k_{te}. In their work they have described this rate constant as

$$k_{te} = k_{to}\, \alpha_o^2\, K_c/(\phi_p x_n^{\beta'}) \qquad (3.1)$$

which states that the termination rate constant for entangled molecules is inversely proportional to the entanglement density. Here, K_c and α_o were taken to be adjustable parameters. The termination rate constant k_{tc} between the entangled chain and the unentangled chain was assumed to be

$$k_{tc} = \sqrt{k_{to} k_{te}} \qquad (3.2)$$

This is in direct contrast to the assumption used in **Chapter 2, which in this case would be;**

$$k_{tc} = \frac{1}{2}(k_{to} + k_{te}) \qquad (3.3)$$

While equation **3.3** is directly related to the assumption of the additivity of the mutual diffusion constants as discussed in **Chapter 2,the** author was not able to find a theoretical basis for equation **3.2**, used by Cardenas and O'Driscoll. Moreover, equation **3.2** predicts zero termination rate when the entangled radicals are completely immobilized ($k_{te} = 0$). This is clearly not acceptable, as immobilized radicals can certainly react with mobile radicals as long as the entire system is not completely frozen. One of the bases of introducing equation **3.3** was the consideration that the value of the termination rate constant is determined by the mobility of the chain. It is well known that the chain mobility is determined by two factors, the entanglement and the free volume effect (**14**). Equation **3.2** assumes the termination rate constant, which is affected by the chain mobility, is somehow dependent only upon the entanglement density and not dependent upon the changing free volume. This assumption is difficult to accept. Even if one does accept equation **3.1** and equation **3.2** without question, there is still no reason to believe that the termination rate constant for entangled chains should be inversely proportional to the entanglement density. It should be mentioned that it is known that the mobility of an entangled chain at a given conversion level is proportional to -3.4th power of the entanglement density (**14**). This would require (according to O'Driscoll) that k_{te} is proportional to + 3.4th power of the chain mobility, which is difficult to accept without justification. However, contributions made

by O'Driscoll's model should be appreciated as the first serious attempt to introduce the chain length dependence into the modelling of polymerization kinetics. It is interesting to note that even the relatively simplistic model of O'Driscoll's does show a widening molecular weight distribution in Phase II and a narrowing distribution during Phase III.

More recently Marten and Hamielec(13) presented an interpretation of translational diffusion controlled termination reactions in terms of the free volume theory. Their model was not chain length dependent but assumed that the average effect of chain entanglements upon $\bar{k}_t$ could be described through the weight average molecular weight as

$$\bar{k}_t \propto (\bar{M}_w)^{-m}\exp(-A/v_f) \qquad (3.4)$$

The values of m and A were treated as adjustable constants to be determined by fitting experimental conversion-time data. They assumed that the distribution of molecular weights conformed to the Schulz-Flory most probable distribution throughout the reaction. It is inconsistent in the author's opinion that $\bar{k}_t$ is assumed to depend upon the molecular weight as in equation **3.4** while the molecular weight distribution is assumed to conform to the Schulz-Flory most probable distribution. More pertinent to the present discussion is the fact that these authors proposed that the apparent deceleration in the reaction rate at higher conversions was entirely due to a rapid decrease in the propagation rate constant which eventually overtakes the decrease in $\bar{k}_t$ and ends the gel effect. This interpretation gives rise to an exponential increase in the concentration of macroradicals which has no bound, with its rate of increase only limited by the dissociation rate of the initiator. This

does not appear to be plausible as the macroradical concentration at high conversion computed in this fashion is usually orders of magnitude larger than those that have been observed experimentally (22).

The constants in Hamielec's model are determined by fitting the conversion-time data very closely. As shown in Chapter 2 of this thesis, this necessarily means that the number average molecular weight data should be well described also. As pointed out in Chapter 2, it is only the higher molecular weight averages which have any dependence upon the functional form of the chain length dependence. In this area Hamielec's model generally predicts values too low with differences often in excess of 100% for weight average molecular weight. Moreover, his model does not show any narrowing of the distribution evident in the data of Fig. 3.1. Using this model there is no way for the higher molecular weight averages to level off or decrease while allowing the number average molecular weight to continue to rise.

Perhaps the most important criticism of Hamielec's model is that if the limitation of the gel effect (i.e. the appearance of deceleration) is due to the decrease of k_p caused by diffusional restrictions of the monomer at low free volumes, there should be little such behavior when the polymerization temperature is well above the glass transition temperature of the polymer. Patra's data(23) for ethyl and n-propyl acrylate polymerizations at 59 and 83°C above the respective glass points clearly show the disappearance of the gel effect at about 50-60% conversion level. (These data will be discussed in detail in Chapter 5). Thus there appears to be the need for an alternate explanation of these phenomena.

The above considerations led the present author to the conclusion that the polymerization behavior during both Phase II and Phase

III should only be a result of changes in the chain length dependent termination rate constant. We postulate that a point is reached at which the termination rate constant stops decreasing as rapidly as it had been before, and then stays constant or decreases at a less rapid rate. This is based upon the fact that the notion of a $\bar{k}_t$ value approaching zero is not plausible as it is clear that termination reactions can still take place even when the polymer radical chain is completely immobile. Under this condition the very end of the chain will continue to translate in space with every propagation step and will eventually lead to termination (24). The detailed discussion of this chain end mobility and its general effect upon the behavior of the overall termination rate constant will be described in the following sections.

The above comments lead to the concept that the overall termination behavior is made up of a chain length dependent (translational diffusion) portion and a propagation step dependent portion. The latter is not related to chain length. Considering that these dual mechanisms operate simultaneously, the overall termination rate constant should be expressed as

$$k_t(y) = (k_t)_{tr} + k_{tp} \qquad (3.5)$$

The polymerization behavior during Phase III can be understood as the period when the relative significance of the two terms of equation 3.5 changes from one extreme ($(k_t)_{tr} >> k_{tp}$) to the other ($(k_t)_{tr} << k_{tp}$).

3.3 GENERAL TREATMENT OF RESIDUAL TERMINATION RATE

The general theory for the chain length dependent termination was presented in Chapter 2 where it was shown that the kinetics and molecular weight development are completely determined by the two dimensionless parameters, β and γ, and the dimensionless distribution function $f(y)$. When the chain length dependence is governed only by the translational diffusion of macroradicals, it is expected that the value of $f(y)$ will approach zero as chain length increases without bound, or

$$\lim_{y\to\infty} f(y) = 0 \qquad (3.6)$$

This is because the translational diffusion controlled termination rate constant can be expressed by equation 3.7, which was proposed in Chap.2.

$$(k_t)_{tr} \propto R_h(y)D(y) \qquad (3.7)$$

The condition of equation 3.6 is obtained when the decrease of the diffusivity $D(y)$ is faster than the increase of the hydrodynamic radius $R_h(y)$ with increasing dimensionless chain length y. The particular functional form derived from entanglement theory shows -3.4th power exponent of $D(y)$ while $R_h(y)$ shows at most a 1st power exponent and satisfies the condition for equation 3.6. However, it has been stated earlier in this Chapter that this limiting behavior is an insufficient description for Phase III of the reaction and that a residual termination rate must be considered. This residual rate is related to the propagation reaction and the overall termination rate constant should be expressed as equation 3.5. The purpose of this section

is to set forth a general way of using equation 3.5 to follow the events during Phase III leaving the specific description of the residual rate constant, k_{tp}, to a later section of this Chapter.

In Chapter 2, eq'n 2.55, it was shown that

$$(k_t)_{tr} = k_{tvf}\, f(y) \tag{3.8}$$

and thus using equation 3.5,

$$k_t(y) = k_{tvf}\, f(y) + k_{tp} \tag{3.9}$$

It is convenient to express $k_t(y)$ in the manner of equation 3.8 by defining

$$k_t(y) \equiv k^\circ_{tvf} f^\circ(y) \tag{3.10}$$

where the superscripts refer to the conditions of Phase III. Noting that k°_{tvf} is the chain length independent contribution to $k_t(y)$, it can be described as

$$k^\circ_{tvf} = k_{tvf} + k_{tp} \tag{3.11}$$

which gives rise to a simple ratio, W, describing the transition from total chain length dependence to no chain length dependence,

$$W \equiv k_{tvf}/k^\circ_{tvf} = k_{tvf}/(k_{tvf} + k_{tp}) \tag{3.12}$$

Here it is clear that when $k_{tvf} >> k_{tp}$, W = 1 and there is total chain length dependence, but when $k_{tvf} << k_{tp}$, $W \cong 0$ and there is no chain length dependence. Equations 3.11 and 3.12 give rise to the following description of $f^\circ(y)$,

$$f^\circ(y) = Wf(y) + 1-W \tag{3.13}$$

Utilizing equation 3.4 to describe the limit at very high chain length,

$$\lim_{y\to\infty} f^\circ(y) = 1-W \qquad (3.14)$$

Following the approach taken in Chapter 2, the average termination rate constant for all polymer radicals terminating at any moment in Phase III, $\bar{k}_t^\circ$, can be described as

$$\bar{k}_t^\circ = k_{tvf}^\circ Z^\circ = (k_{tvf}+k_{tp})Z^\circ \qquad (3.15)$$

The polymerization behavior of Phase III should also be described by two dimensionless parameters β° and γ° (related to β and γ of Phase II) as long as they have the following relationships,

$$\beta^\circ = x_c(C_M+C_S[S]/[M]) = \beta \qquad (3.16)$$

$$\gamma^\circ = x_c (R_i k_{tvf}^\circ)^{1/2}/k_p[M] = \gamma/W^{1/2} \qquad (3.17)$$

Likewise the probability distribution function $P^\circ(y)$ for Phase III should be of the same form as that of Phase II, or

$$P^\circ(y) = \exp\{-(\beta^\circ+\gamma^\circ\sqrt{Z^\circ}/2)y - [\gamma^\circ/(2\sqrt{Z^\circ})]\int_0^y f^\circ(y)dy\} \qquad (3.18)$$

Using equation 3.11, equation 3.18 can be rearranged as

$$P^\circ(y) = \exp\{-[\beta^\circ+\gamma^\circ\sqrt{Z^\circ}/2 + \gamma^\circ(1-W)/(2\sqrt{Z^\circ})]y-[\gamma^\circ W/(2\sqrt{Z^\circ})]\int_0^y f(y)dy\} \qquad (3.19)$$

Equation 3.19 shows that $P^\circ(y)$ is identical to a hypothetical system controlled only by translational diffusion, $P'(y)$, provided that the parameters γ' and β' of the hypothetical system satisfy the following identities,

$$P'(y) = \exp\{-(\beta'+\gamma'\sqrt{Z'}/2)y - [\gamma'/(2\sqrt{Z'})]\int_0^y f(y)dy\} \quad (3.20)$$

$$\gamma' = \gamma^\circ W\sqrt{Z'}/\sqrt{Z^\circ} \quad (3.21)$$

$$\beta' = \beta^\circ+\gamma^\circ\sqrt{Z^\circ}/2+\gamma^\circ(1-W)/(2\sqrt{Z^\circ}) - \gamma^\circ WZ'/(2\sqrt{Z^\circ}) \quad (3.22)$$

where the entanglement factor Z' for the hypothetical system is defined as

$$Z' = \int_0^\infty f(y)P'(y)dy/\int_0^\infty P'(y)dy \quad (3.23)$$

In an analogous fashion, the Z° necessary for the complete definition of equations 3.16 and 3.17 is

$$Z^\circ = \int_0^\infty f^\circ(y)P^\circ(y)dy/\int_0^\infty P^\circ(y)dy$$

$$= 1 - W + W\int_0^\infty f(y)P^\circ(y)dy/\int_0^\infty P^\circ(y)dy \quad (3.24)$$

Since $P^\circ(y) = P'(y)$ when equations 3.21 and 3.22 are satisfied,

$$Z^\circ = 1 - W + WZ' \quad (3.25)$$

The molecular weight distribution indices, ℓ_i, of the real and hypothetical systems are identical due to the equivalency of $P^\circ(y)$ and $P'(y)$. Thus the master charts for Z, and the ℓ_i's of Chapter 2 can be used to determine the kinetics and molecular weight distribution of Phase III with the use of equations 3.21, 3.22, and 3.25. This requires a trial and error solution which involves guessing a value for Z° at the W of interest, computing Z', γ' and β' from equations 3.25, 3.21, and 3.22, and then reading the value of Z' from the master chart provided in Part I of this series. The procedure is repeated until the Z' computed equation 3.25 is equal to that obtained from the master chart.

The results of the theoretical development of this section may be summarized as follows. Given any residual termination rate constant k_{tp} which is not dependent upon chain length, there are three dimensionless parameters, W, γ° and β°, which determine the polymerization rate and molecular weight distribution in Phase III. The indices of polymerization rate (Z°) and molecular weight distribution (ℓ_i's) can be obtained from the master curves of **Chap.2** given a knowledge of f(y) and k_{tp}. It should be noted here that as W approaches zero, all the relations for Phase III reduce to the psuedo-conventional case with the Schulz-Flory most probable molecular weight distribution, as is expected since the termination reaction is then no longer chain length dependent. The only parameter left undefined is k_{tp}. It can only be estimated with a specific theory for the residual termination rate constant and will be the subject of the next section **3.5.**

3.4 THEORY OF EXCESS CHAIN END MOBILITY

Gardon(24) was the first to realize that termination can take place even when the movements of all chain segments are completely frozen. His lattice model presents the theoretical lower limit of the termination rate constant. However, the actual termination rate constant should be larger by orders of magnitude than his values due to the relative ease of movements of chain ends. The concept of the freely dangling chain end, first introduced by Flory(25) to explain rubber elasticity, will be employed extensively in the theoretical development that follows.

Consider a chain whose end is active in polymerization. One wants to derive an expression for the termination rate when the active radical as a whole is not capable of translational movement, but its chain end is free to move in the relatively restricted region which is visualized as the sphere of radius (σ) with the node of an entanglement at the center. Considering that the movement of each chain segment contributes to the movement of the center of gravity resulting in translation, the overall chain needs infinite chain length for the dangling movement of a chain end to be negligible for translation. However, this conditon can be closely approximated when σ is small compared to the overall chain length. The active center will sweep the sphere defined by σ constantly so that any radical which may penetrate this sphere will terminate nearly instantly. The probability of radical initiation in this sphere is too small for significant contribution as the total volume occupied by the termination spheres formed by the dangling active

chain ends should be only a very small fraction of the total volume of the system. However, as the radical will continue to propagate, the sphere of termination will travel in the reaction medium resulting in significant termination rate.

Utilizing this concept of the sphere of termination reactions, the appropriate rate constant may be given by the "volume-swept-out" model as shown by Allen and Patrick (21),

$$k_{tp} = 6D_{AB}\pi\sigma^2 N_{Av}/(1000\bar{\ell}) \qquad (3.26)$$

where $\pi\sigma^2$ is the collision cross-section, $\bar{\ell}$ is the average jump length of the sphere of termination per propagation step, and the mutual diffusivity D_{AB} can be defined as

$$D_{AB} = \phi\bar{\ell}^2/6 \qquad (3.27)$$

where ϕ is the jump frequency of the molecule. Although equation 3.26 is developed for small molecules, it can be applied to the present problem by visualizing the movement of the dangling chain end as a traveling sphere. For this case the appropriate jump frequency is that of the propagation reaction (i.e. $\phi = k_p[M]$, $sec.^{-1}$), the jump distance $\bar{\ell}$ is the average root-mean-square displacement of the center of the sphere due to the propagation, and the radius of the sphere is related to the distance from the node of an entanglement to the chain end. Coupling equations 3.24 and 3.25 yields

$$k_{tp} = \pi\sigma^2\bar{\ell}\, N_{Av}k_p[M]/1000 \qquad (3.28)$$

The quantities that require further description are $\bar{\ell}$ and σ.

The author envisioned the center of the travelling sphere to be the node of the entanglement and that the average number of monomer units in

a dangling chain, j_c, is equal to the entanglement spacing. The entanglement spacing for pure polymers are tabulated(14), but considering the reaction medium is a monomer-polymer solution, it was decided to use one half of the degree of polymerization for entanglement measured from solution viscosity measurements, x_c.

$$j_c = x_c/2 = x_{co}/(2\phi_p) \tag{3.29}$$

Generally x_{co} is about twice the entanglement spacing of pure polymers measured by other methods. This was discussed on p. 408 of reference 14. The author thought the data obtained from solution viscosity may better represent the reaction condition than data from pure polymer. If one assumes that the length between the node of the entanglement and the active chain end is kept constant, one propagation step will move the active chain end by the quantity a, the average root-mean-square end-to-end distance per square root of the number of monomer units in the chain. Ferry (14) (p. 362) has tabulated values of a for various polymers. Since a is measured experimentally, it takes into account restricted bond rotations. The movement of the chain end by a distance a will lead to the movement of the node by the distance $(a/j_c^{1/2})$. This is shown in detail in the Appendix F.

From this discussion it can be seen that

$$\bar{\ell} = a/j_c^{1/2} \tag{3.30}$$

Now the termination rate constant can be written as

$$k_{tp} = \pi\sigma^2 a N_{Av} k_p [M]/(1000 j_c^{1/2}) \tag{3.31}$$

The only unknown remaining in equation 3.31 is the radius of

termination, σ. This can be estimated as follows. Consider a single radical chain end which is placed in a system having a uniform radical concentration profile $[R\cdot]$. The origin of the coordinate system will be the node of the last entanglement for the macroradical of interest and the dangling chain end will be distributed about that center. The manner in which the chain end is distributed may be estimated by a Gaussian randon flight distribution function as given by Flory **(25)**,

$$W(r) = \left(\frac{3}{2\pi\langle R^2\rangle}\right)^{3/2} \exp\left(-\frac{3r^2}{2\langle R^2\rangle}\right) \qquad (3.32)$$

where $W(r)$ is the probability (per unit volume) of finding the chain end at a position r from the node. $\langle R^2\rangle$ is the mean square node-to-chain end displacement and may be written as

$$\langle R^2\rangle = j_c a^2 \qquad (3.33)$$

Equation **3.32** predicts that the most likely position for the chain end is at the node itself. Since we are dealing with a single radical, its local concentration, $[R\cdot]_{local}$, must be proportional to $W(r)$. The proportionality constant may be determined by noting that when all possible chain end positions are considered (i.e. r between zero and infinity) we still must have only a single radical in that space. Thus

$$1 \text{ (radical)} = \left(\frac{N_{Av}}{1000}\right) \int_0^\infty [R\cdot]_{local} dV$$

$$= \left(\frac{N_{Av}}{1000}\right) \int_0^\infty C\, W(r)\, 4\pi r^2 dr$$

Solving for C,

$$C = 1000/\left(N_{Av} \int_0^\infty W(r)\, 4\pi r^2 dr\right) = 1000/N_{Av}$$

since the integral term is equal to unity. Now the local concentration

can be written as

$$[R\cdot]_{local} = C\,W(r) = 1000\,W(r)/N_{Av} \qquad (3.34)$$

This concentration distribution is shown in Fig. 3. 2a with the uniform concentration distribution, [R·], superimposed. The author chose to define σ as the point at which these two distributions intersect. This is reasonable since the macroradicals making up [R·] do not readily diffuse during this portion of the reaction, and when the motion of the chain end under consideration is very fast, the local radical concentration of the chain end will completely wipe out the uniform radical concentration by termination within the sphere of radius σ. This interpretation is somewhat analogous to the Smoluchowski model for diffusion controlled reactions(21). This allows us to define σ through $W(\sigma)$ at the point where $[R\cdot]_{local} = [R\cdot]$, or

$$[R\cdot] = 1000W(\sigma)/N_{Av} \qquad (3.35)$$

Utilizing equations 3.32 and 3.33 to solve for σ via equation 3.35,

$$\sigma = (1/\rho)[\ln(1000\rho^3/(N_{Av}[R\cdot]\pi^{3/2}))]^{1/2} \qquad (3.36)$$

where $$\rho^2 = 3/(2j_c a^2) \qquad (3.37)$$

The combination of equations 3.31, 3.36 and 3.37 complete the theoretical development of the residual termination rate constant, k_{tp}. However it must be mentioned that this expression of k_{tp} may be an over-estimate of the real value because of the manner in which σ has been described. Consequently it has been necessary to introduce an efficiency factor, f_t, into equation 3.37 as follows:

$$k_{tp} = f_t \pi \sigma^2 \alpha N_{Av} k_p [M]/(1000 j_c^{1/2}) \qquad (3.38)$$

As with any efficiency factor, f_t may have values between zero and unity. The need for f_t comes about because two of the assumptions used in the development for σ may not always be realized in the real situation. The first is that the motion of the chain end is fast enough to completely sweep out the volume described within σ between each propagation step, and the second is that the diffusion of external macroradicals into the termination sphere described by σ is negligible. If either assumption is not met, the result is an actual value of σ smaller than that given by equation 3.36. It is shown in Appendix G that the difficulties associated with the first assumption only influence σ towards the end of Phase III and during Phase IV, while those associated with the second assumption only influence the early part of Phase III. The manner in which f_t was computed for comparisons to experimental data is detailed in Appendix G. It should be noted that f_t is not an adjustable parameter, but is calculated continuously from the knowledge of β, γ, and $f(y)$. This is shown in equation (G-1) in the Appendix.

It is instructive to show in graphical form the significant effect that the residual termination rate constant has on the overall termination rate constant, $\bar{k}_t$. This is shown in Fig. 3.3 which describes the value of $\bar{k}_t$ as a function of conversion for the methyl methacrylate polymerization described in Fig. 3. 1. Here it is clearly shown that the effect of k_{tp} is to prevent $\bar{k}_t$ from decreasing without bound, instead forming somewhat of a plateau in the curve during Phase III. When compared with the $\bar{k}_t$ values computed without regard to the residual termination reaction mechanism, it is apparent that k_{tp} places a limit on the extent of the gel

effect. This will be clearly seen in molecular weight development as a leveling off or decrease in $\bar{M}_w$ (and higher averages) during Phase III. The effect of k_{tp} will also restrict the increase of the free radical concentration, [R·], to keep its maximum value within reason.

It is readily apparent from Fig3.3 that at conversion levels above 65-70% (for this particular set of reaction conditions) k_{tp} completely controls the value of $\bar{k}_t$ ($(k_t)_{tr}$ being more than an order of magnitude lower). From equation 3.38 it is seen that k_{tp} will continually decrease with conversion (via the monomer concentration) during Phase III and should decrease even more rapidly during Phase IV due to decreases in k_p (see Part III of this series). The residual chain end behavior during Phase IV may be significantly more complex than presented by equation 3.38, as chain transfer to monomer and/or polymer reactions should provide additional mobility of the chain end. Primary radical termination and diffusion controlled initiator dissociation reactions may also become significant during Phase IV. It is thought that these combined effects will probably cause $\bar{k}_t$ to decrease even less rapidly during Phase IV than shown in Fig.3.3. Although these effects have not been quantified in this thesis, such consideration will certainly result in better explanations of experimental data in the very high conversion range.

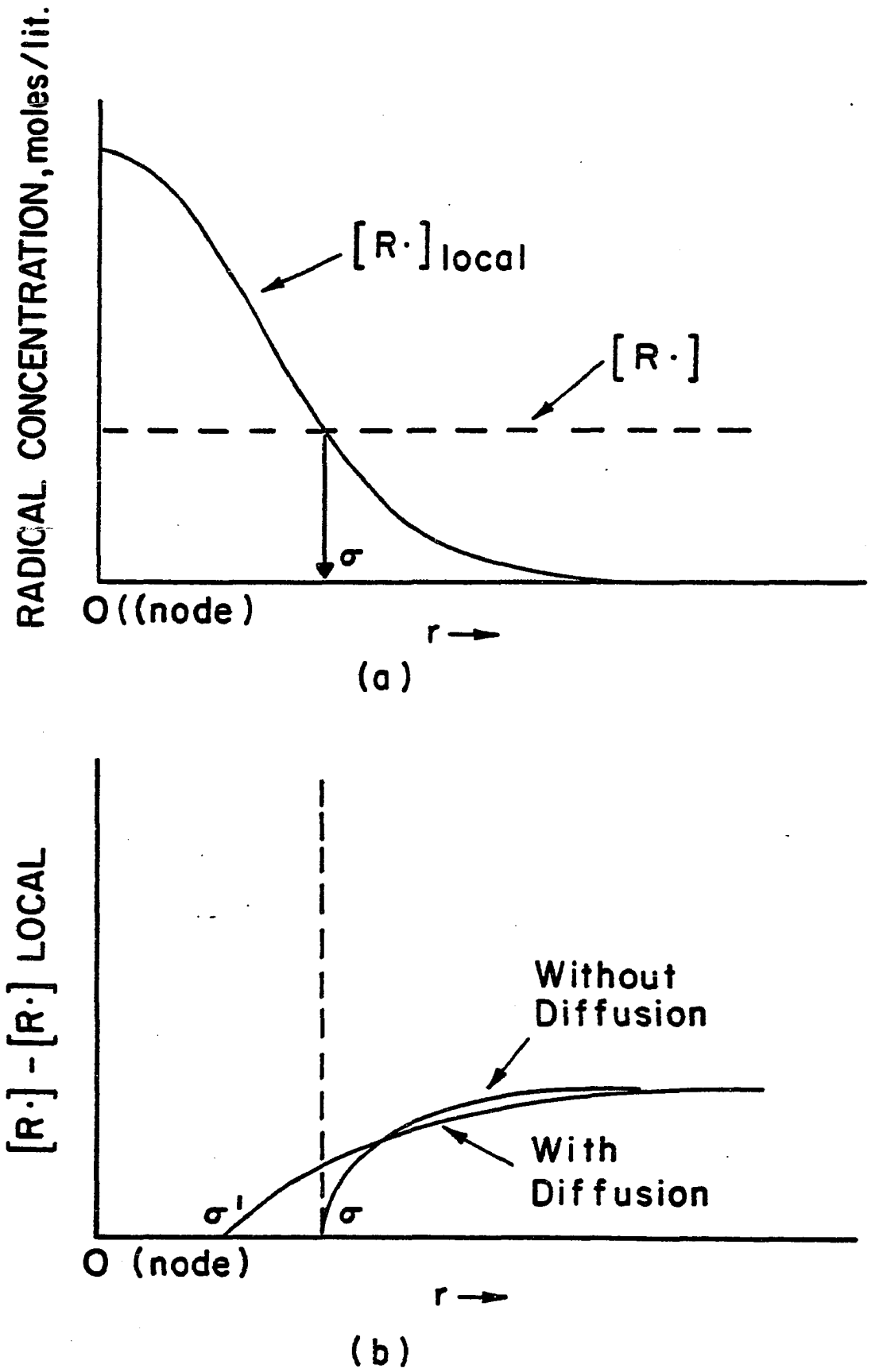

Fig. 3.2 Radius of Termination

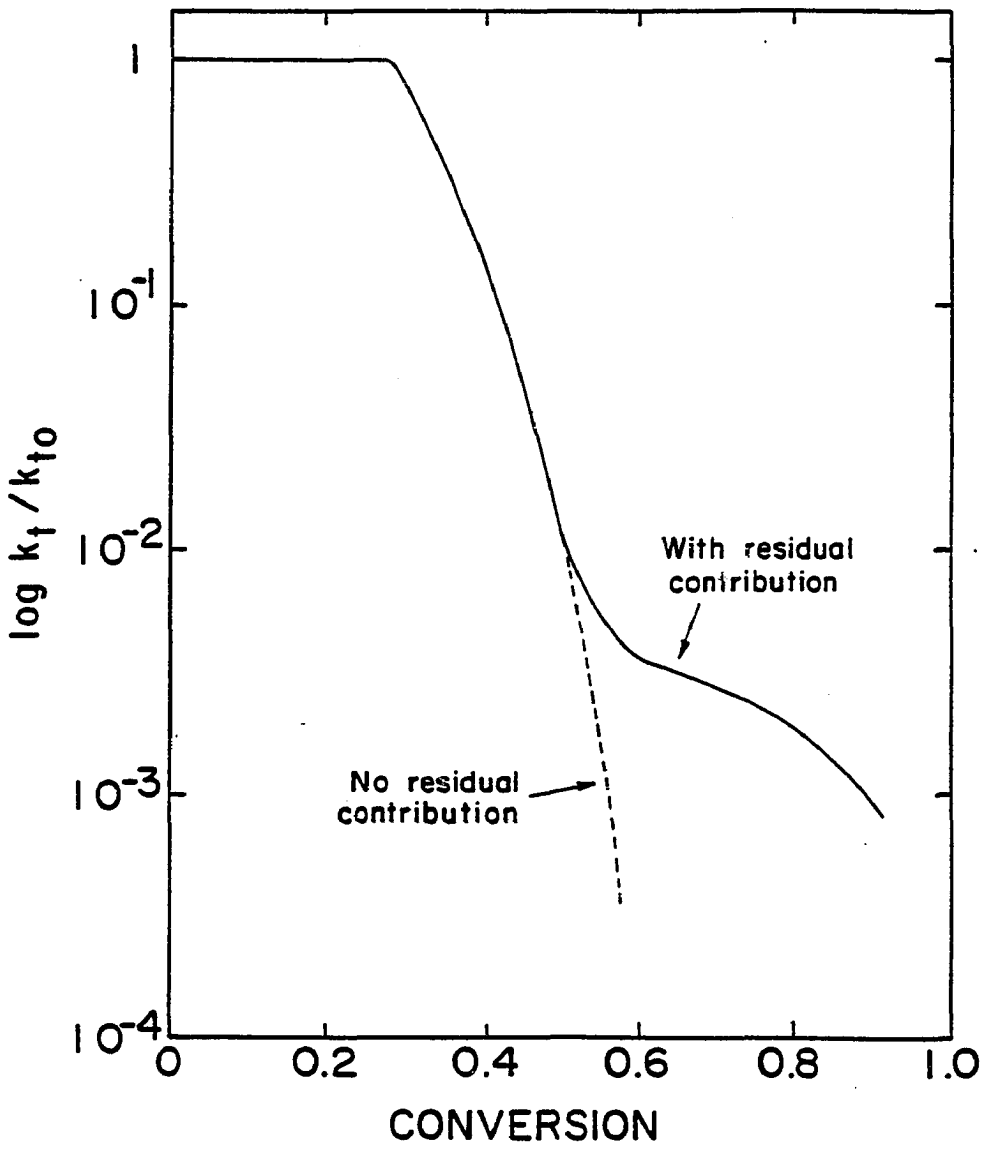

Fig. 3.3 Effect of Residual Contribution

3.5 RESULTS AND DISCUSSION

The entanglement factor Z and the molecular weight indices l_i's are determined by the three dimensionless parameters β, γ, and W. This makes the graphical representation of the master charts comparable to those of Chapter 2 impractical. However, because of the relationships presented in 3.3, the numerical computations can be done easily via the hypothetical system. This is done by the subroutine SBRKPL.FOR, which uses the last value of Z as the first trial value. The Z' value of the hypothetical system is calculated by eq'n 3.25, and the β' and γ' values by eq'n 3.22 and 3.21. Then the new value of Z' is calculated for the hypothetical system by calling the subroutine CALCU.FOR, the interpolation subroutine. The error criterion of the trial and error process is the relative error $\left|1- Z'(old)/Z'(new)\right|$ to be less than 0.001. Otherwise, the new value is substituted for the trial value and the procedure is continued with the newly calculated β' and γ' values. For the recombination mode of termination, the procedure outlined in 2.5 is directly applicable.

It can be generally said that the inclusion of even a small value of k_{tp} results in rather drastic reduction of the deviation from the conventional kinetics. This explains the sudden stopping of the molecular weight increase at the onset of the Phase III, as demonstrated in Fig.3.2. The entanglement factor Z also increases very sharply as W decreases from 1. Thus the polymerization behavior of Phase III of vinyl polymerization can be understood as the period where the contribution from the residual termination increases steadily, and the deviation from conventional kinetics, known as the "gel effect" diminishes steadily, finally reaching

the conventional condition at high conversion. It is the author's belief that no other reasoning which does not count for the residual contribution can explain the polymerization behavior of Phase III in a logical way. Although the presented dangling chain end model may need further refining in the future studies, the concept of the residual termination first expressed in this thesis should be retained in the forseeable future.

3.6 CONCLUDING REMARKS

It has been postulated that the transition from the profound gel effect to more conventional kinetics experienced by many vinyl polymers in the 50-80% conversion range can be attributed to excess chain end mobility. Although the mathematical derivations may appear complex, it is based on the simple consideration that as translational movement of macroradicals becomes increasingly difficult, the contribution made by segmental motion derived solely from the propagation reaction will become the prevailing mechanism. The termination reaction is seen to change from chain length dependent to chain length independent during this trnsition period.

The test of the model proposed here can only be done within a complete theory of vinyl polymerization and the application to a variety of experimental data will be the subject of Chapter 5.

Chapter 4

FREE VOLUME PARAMETERS AND DIFFUSION CONTROLLED PROPAGATION

4.1 INTRODUCTION

This Chapter will deal with; 1.) the experimental determination of free volume parameters from viscosity measurements, 2.) diffusion controlled propagation reactions and their effect upon polymerization behavior, and 3.) limiting conversion and other phenomena which may characterize the last stage of the polymerization. The values of the free volume parameters determine the physical properties of the reaction medium and therefore determine the kinetics and molecular weight development of the reacting system during Phases II-IV of the polymerization. Using these readily measured physical constants in a kinetic model removes much of the empirical nature associated with the fitted constants of previous models (13,15).

Some time ago Melville and co-workers (26) reported that the propagation rate constants for methyl methacrylate and vinyl acetate decreased significantly at high conversions. However, excessive scatter in their data prevented any quantitative description. Soh (27) measured k_p values in seeded emulsion polymerizations for styrene and methyl methacrylate in the 40-60°C range. His results suggest that k_p remains constant up to at least 50% conversion. Saito (10), Hamielec (13) and the present author (28) independently proposed a semi-empirical relation for k_p which is written in terms of the fractional free volume, v_f,

$$k_p/k_{po} = \exp [C(1/v_{fc} - 1/v_f)] \qquad (4.1)$$

where v_{fc} is the free volume at which k_p begins to decrease, and both C and v_{fc} are adjustable constants. Hamielec and Saito used C = 1 while the present authors used C = 0.38 for both styrene and methyl methacrylate (28). Each group of workers used the following methods to compute v_f,

$$v_{fm} = 0.025 + 0.001\ (t-t_{gm}) \tag{4.2}$$

$$v_{fp} = 0.025 + 4.8 \times 10^{-4}\ (t-t_{gp}) \tag{4.3}$$

$$v_f = v_{fm}\ \phi_m + v_{fp}\ (1-\phi_m) \tag{4.4}$$

The numerical coefficients used in equations 4.2 and 4.3 are the "universal constants" from the WLF equation. It should be noted that experimental measurements of v_{fp} for individual polymers yield numerical coefficients somewhat different than the universal constants(14) and it may be preferable to use values specific to each polymer. Also, the previously mentioned models for k_p (13,26,28) have used equation 4.3 at temperatures below the glass transition temperature of the pure polymer where it is not strictly applicable (14). The method employed here overcomes these problems by introducing the free volume thermal expansion ratio used by Vrentas and Duda (19) as presented in 4.2.

4.2 DETERMINATION OF FREE VOLUME PARAMETERS

Estimation of free volume parameters is necessary for the calculation of k_{tvf} shown in Chapter 2 and of the propagation rate constant proposed in this Chapter. Although the free volume theory for diffusivity of polymer chains and monomer molecules is only an approximation, it is perhaps the only theory readily available and known to agree with experimental data reasonably well. There are two versions of free volume theory which are applicable to monomer-polymer systems. The theory of Fujita (29) assumes the following forms for the diffusivity of a chain segment D_s and of an organic penetrant D_m,

$$\frac{D_s}{kT} = \frac{1}{\zeta_s} = A \exp\left(-\frac{B}{v_f}\right) \tag{4.5}$$

$$\frac{D_m}{kT} = \frac{1}{\zeta_m} = A_d \exp\left(-\frac{B_d}{v_f}\right) \tag{4.6}$$

where the temperature dependence is generally neglected and the value of B is taken as unity. The value of B_d lies somewhere between 0.4 and 1.0 depending on the relative size of the organic penetrant to the polymer segment. Vrentas and Duda (19) defined the free volume more precisely and equated the ratio B_d/B in equations 4.5 and 4.6 to ξ, the relative size ratio of the organic solvent molecule and a polymer segment. The constant B was equated to the more fundamental constant $\gamma\hat{V}_p(0)/\hat{V}_o$ which can be estimated from the WLF equation constants (19). The values of ξ calculated using the data of Bondi (30) and estimation methods of Sugden or Biltz (31) are generally close to unity for monomer-polymer pairs. Sample calculation for styrene is given in Appendix H.

When considering monomer/polymer pairs, Vrentas and Duda (19) showed that their approach was identical to that of Fujita(29). They also recommended that the free volume parameters for the polymer and solvent be obtained from viscosity or diffusivity data of these materials in their pure states. This may be satisfactory for the polymer, but there is evidence (32) that the viscosity data of pure solvents deviate markedly from the free volume theory at temperatures in the range of interest for polymerization. Because of this conflict, the authors decided to obtain the free volume parameters for both polymer and monomer from viscosity data derived from concentrated monomer/polymer solutions. For this work, Fujita's simpler formulation was used (i.e. the value of B in equation 4.6 was taken as unity) but Vrentas and Duda's theory was used as a guide when the temperature was lower than the glass point of the pure polymer (see below).

Fujita's experiments(29) show that the free volume contribution from the polymer in a solvent/polymer mixture is identical for different solvents, and that for temperatures above t_s (which is slightly below t_{gp}) the free volume of the polymer can be expressed as

$$v_{fp} = v_{fs} + \alpha_p (t-t_s), \quad t \geq t_s \tag{4.7}$$

For temperatures below t_s, only data points were given and these do not strictly conform to equation 4.8. However, Vrentas and Duda (19) proposed the following relations for v_{fp},

$$v_{fp} = v_{fg} + \alpha_p (t-t_{gp}), \quad t \geq t_{gp} \tag{4.8}$$

$$v_{fp} = v_{fg} + \lambda\alpha_p (t-t_{gp}), \quad t < t_{gp} \tag{4.9}$$

where λ is a constant related to the ratio of thermal expansion co-

efficients below and above t_{gp}. The author decided to combine the above two approaches and to express v_{fp} as follows,

$$v_{fp} = v_{fs} + \alpha_p (t-t_s), \quad t \geq t_s \tag{4.10}$$

$$v_{fp} = v_{fs} + \lambda\alpha_p (t-t_s), \quad t < t_s \tag{4.11}$$

Theoretically, t_s should be equal to t_{gp}. But it should be noted that the glass transition, being second-order thermodynamic transition, depends on the rate by which it is measured. Thus the descripancy between t_s and t_{gp} can be understood as a manifestation of the "characteristic rate" of the viscosity measurements used.

Fujita presented viscosity data for concentrated solutions of polystyrene and polymethylmethacrylate at temperatures above and below the respective t_{gp}'s. Kishimoto reported poly (vinyl acetate) data using the same method (29). The slopes of the v_{fp} vs. t plots were used to determine the individual α_p's from the data above the t_{gp}'s. Fujita's reported values of α_p were accepted so that only the λ, t_s and v_{fs} values needed to be evaluated from the data below t_{gp}. This was done by fitting the data in the lower temperature ranges with a straight line intersecting the one for the higher temperatures as determined by Fujita. This is shown in Fig. 4.1 where the data well above t_{gp} have not been plotted and the upper section of each curve is Fujita's fit without modification. The intersection of the two lines determines t_s and v_{fs} , while the slop of the line below t_s determines λ. These values are shown in Table 4.1 which also shows the "universal values" commonly used. The λ values obtained from

Fujita's data and Kishimoto's data are close to or somewhat higher than the theoretical upper bound reported by Vrentas and Duda (19). Vrentas and Duda (19) also reported λ values obtained from various solvent-polymer systems where the solvent molecule is significantly smaller than the monomeric unit of the polymer ($\xi<1$). These values were smaller than the theoretical upper bound and are also shown in Table 4.1. Our λ value for poly (vinyl acetate) is significantly above the upper limit of Vrentas and Duda, but this will have no consequence in our kinetic work since vinyl acetate polymerization is usually done at temperatures above t_s where λ is not needed. The important point of Table 4.1 is that the λ values are in the range of 0.2-0.4 and shows that neglecting them at temperatures below t_s may lead to significant errors.

The free volume parameters for the monomer were obtained from viscosity measurements done in this laboratory for monomer/polymer solutions with solid contents in the 20-50% range. The monomers contained inhibitor to prevent reaction during the measurements which were carried out in the 30-60^{o}C temperature range in a Brookfield viscometer with temperature control. The solid contents were measured gravimetrically and the viscosities were determined at several shear rates to check for possible shear thinning, but no extrapolation was necessary to obtain the zero shear viscosity. Fujita (29) showed that the solution viscosity is related to the free volumes of the monomer and polymer as

$$\ln \eta/(1-\phi_m) = E + 1/(\beta\phi_m + v_{fp}) \qquad (4.12)$$

where $$\beta = v_{fm}-v_{fp} \qquad (4.13)$$

Table 4.1

FREE VOLUME PARAMETERS OF POLYMERS

polymer	v_{fs} this work	α_p $(°C)^{-1}$ Fujita (29)	t_s, °C this work	t_s, °C Fujita(29)	$t_s = t_{gp}$, °C Vrenta (19)	λ this work	λ* Vrentas (19)	λ theoretical upper bound (19)
PMMA[1]	0.0194	3.0×10^{-4}	105	100	115	0.428	0.33∿0.38	0.41
PSTY[2]	0.0238	4.5×10^{-4}	82	85	100	0.306	0.20∿0.24	0.30
PVAC[3]	0.0218	5.0×10^{-4}	26.5	30	32	0.535	0.16∿0.20	0.37
PMA[4]	-	5.3×10^{-4}	_	3	3	-	0.24∿0.39	0.39
Universal values (14)	0.025	4.8×10^{-4}	t_{gp}	-	t_{gp}			

[1] polymethyl methacrylate

[2] polystyrene

[3] polyvinyl acetate

[4] polymethyl acrylate

*values obtained for solvent-polymer pairs where $\xi<1$

The temperature dependence of v_{fm} was taken to be linear (a routine assumption analogous to equation 4.2),

$$v_{fm} = \alpha_o + \alpha_m t \qquad (4.15)$$

The values of v_{fp} were determined by using the values of Table 1 and the constants E, α_o and α_m were determined by nonlinear regression of the viscosity data according to equation 4.12. A packaged computer subroutine, NONREG.FOR of the University System of New Hampshire Statistical Programs, was used for this purpose. The "universal" values for α_o and α_m were used as starting points for the regression. The results of these regression analyses are shown in Figs. 4.2-4.4 and Table 4.2. The Figures show the comparison of equation 4.12 (computed with the parameters of Table 4.2) and the actual data. The styrene data in Fig. 4.2 are well described by equation 4.13 those for methyl methacrylate in Fig. 4.3 conform reasonably well, while those for vinyl acetate (not shown) show significantly poorer correlation. Additional data were obtained for methyl methacrylate at 40 and 60° C to confirm the concentration dependence and these comparisons are shown in Figure 4.4. The parameters displayed in Table 4.2 were used to generate the curves in this figure.

Recently, Fedors (33) proposed an estimation method for the glass transition temperature of simple liquids which is based upon their melting points (t_m) and their boiling points (t_b). This relationship may be rewritten as

$$t_g = 0.87t_m - 0.13t_b - 71.0 \qquad (4.15)$$

when all temperatures are written as ^{o}C. The author used this method to calculate t_{gm} for the monomers described in Table 4.2, and also calculated the fractional free volume of these monomers at those calculated glass points using those values of t_{gm}. Both of these quantities are shown in Table 4.2 contrasted with the universal values.

It should be noted that the values given in Table 4.1 and 4.2 are strictly valid only in the temperature range of the viscosity measurements. Bondi (30) showed that significant changes of thermal expansion coefficients, hence the free volume parameters, are expected when the temperature range is wide. However, the values shown in Table 4.1 and 4.2 may be used at conventional polymerization temperatures as they are reasonably close to the temperatures employed for the viscosity experiments. Appendix I and J give the detailed description and the tabulation of the data points and the viscosity average molecular weight measurements of the sample polymers.

Table 4.2

FREE VOLUME PARAMETERS OF SEVERAL MONOMERS

monomer	E	α_o	$\alpha_m(°C)^{-1}$	$t_{gm}(°C)$ (33)	v_f at t_{gm}
STY	-0.58	0.112	6.2×10^{-4}	-116.5	0.040
MMA	-4.48	0.149	2.9×10^{-4}	-126	0.011
VAC	1.42	0.154	5.1×10^{-4}	-164	0.070
universal value	-	-	10.0×10^{-4}	eq'n 4.16	0.025

Polymers used:

PMMA — Matheson, Coleman & Bell Co., $\bar{M}_v$ = 53,000 (measured in acetone solution at 25°C)

PSTY — Aldrich Chemical Co., $\bar{M}_v$ = 140,000 (measured in cyclohexane solution at 35°C)

PVAC — K&K Laboratories, $\bar{M}_v$ = 130,000 (measured in acetone solution at 25°C)

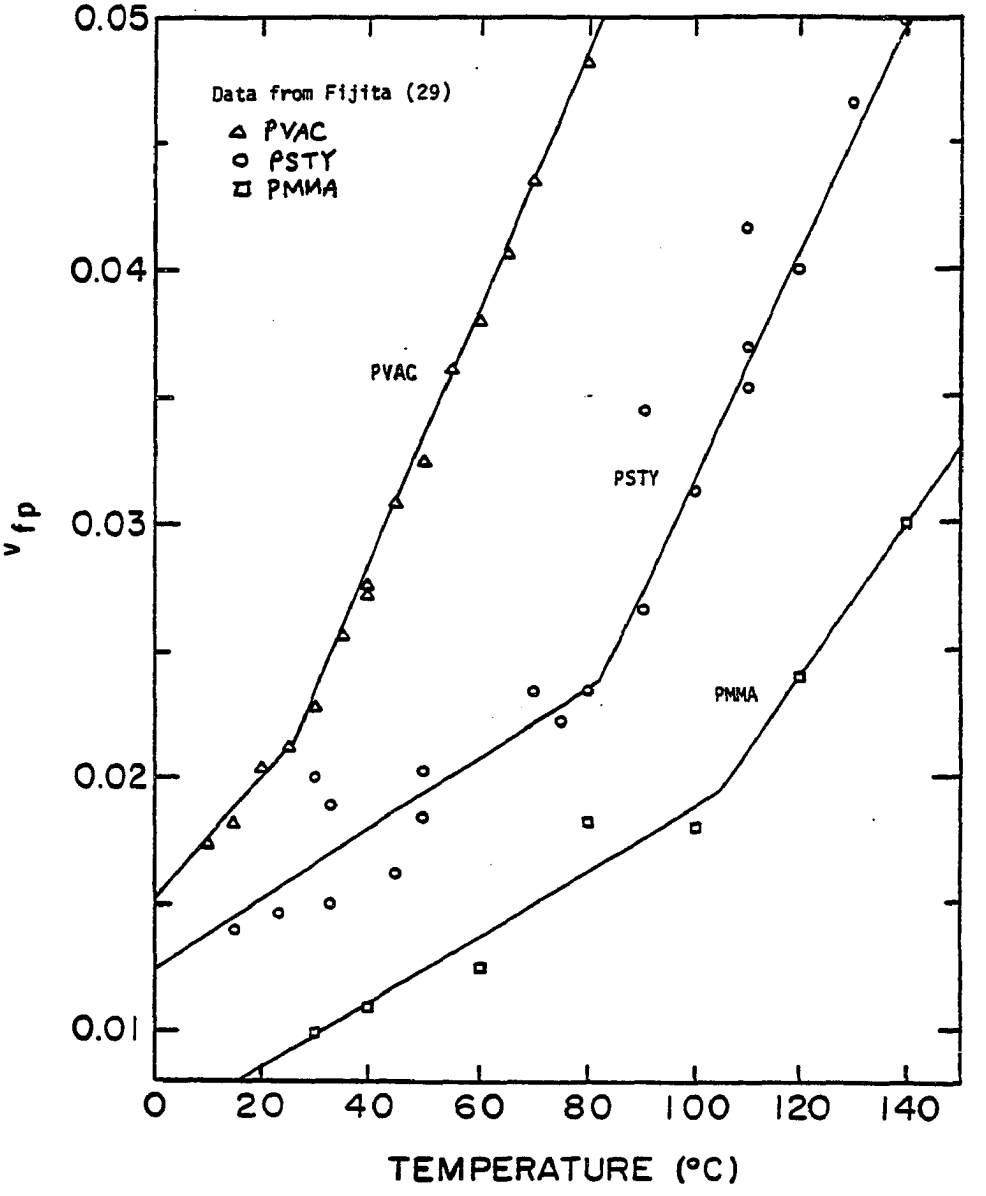

Fig 4.1 Free Volume Parameters of Polymers.

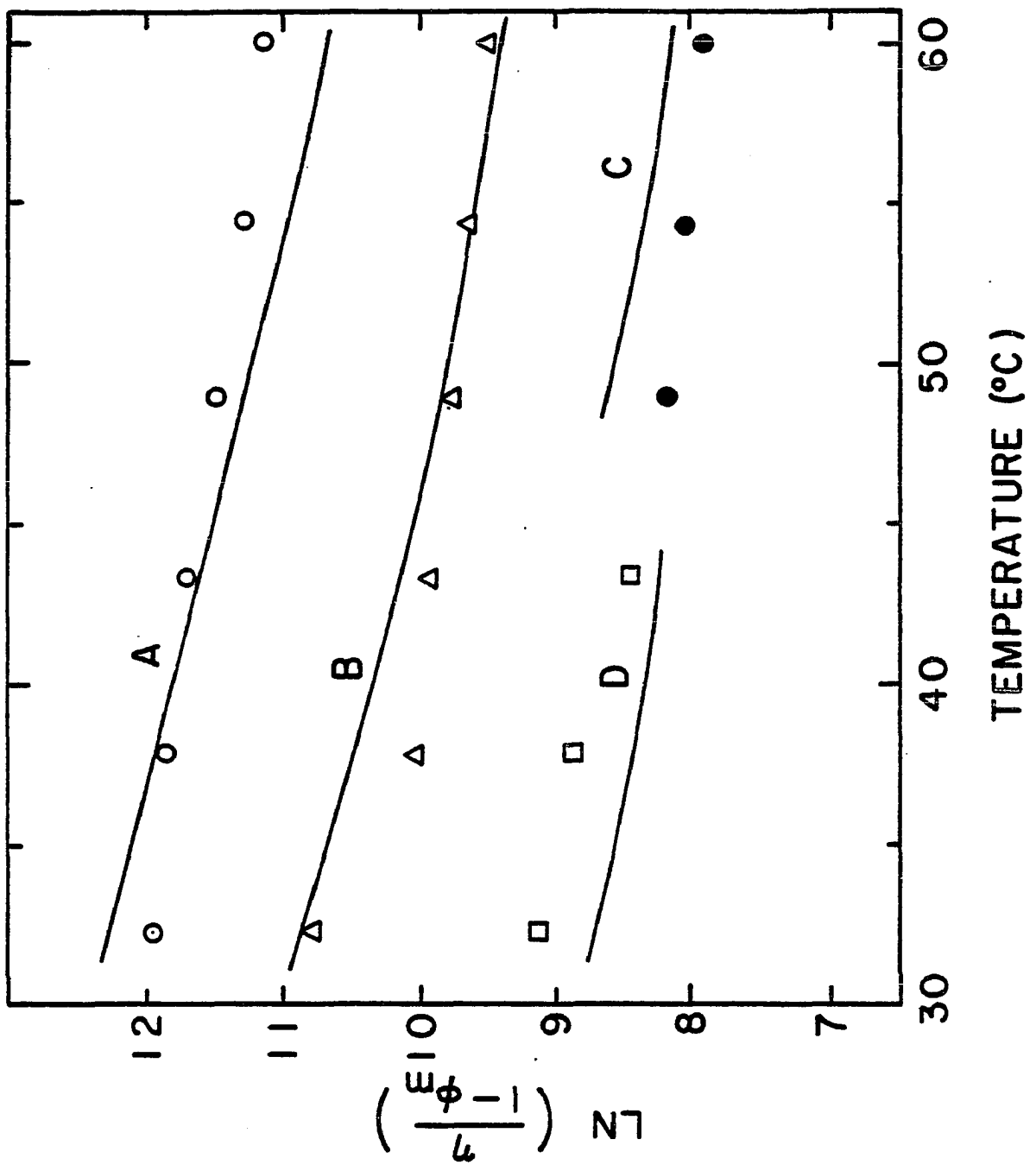

Fig. 4.2 Viscosity of Styrene-Polystyrene Systems

A: ◇=0.52, B: △=0.61, C: ●=0.73, D: □=0.79

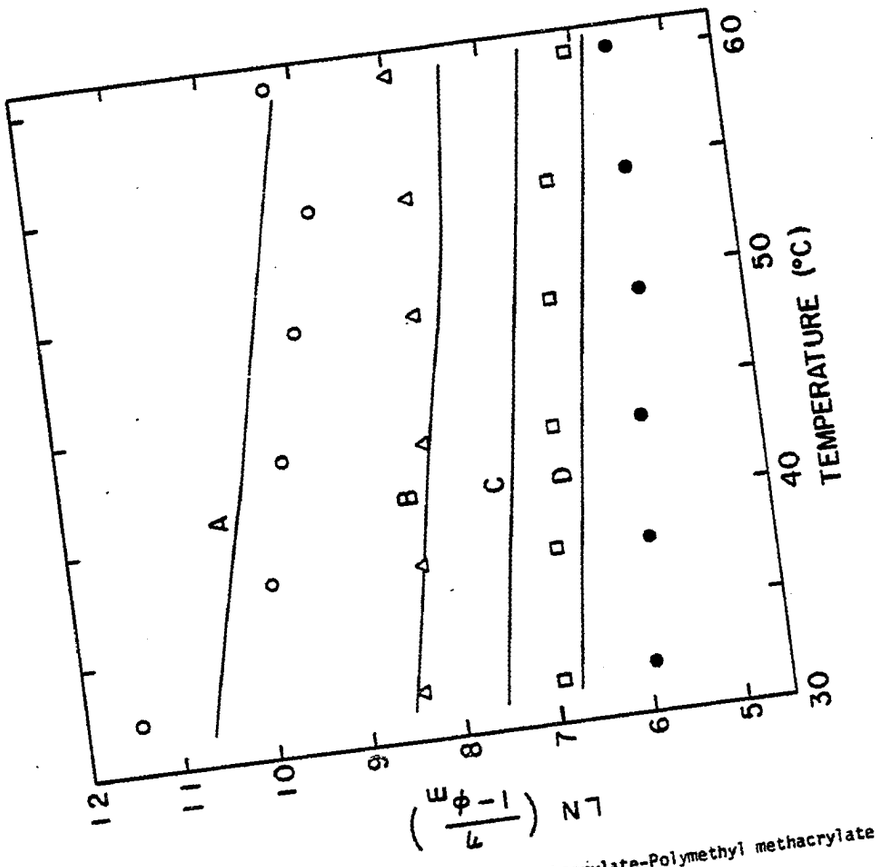

Fig. 4.3 Viscosity of Methyl methacrylate-Polymethyl methacrylate Systems
A: ○=0.56, B: △=0.67, C: □=0.73, D: ●=0.78

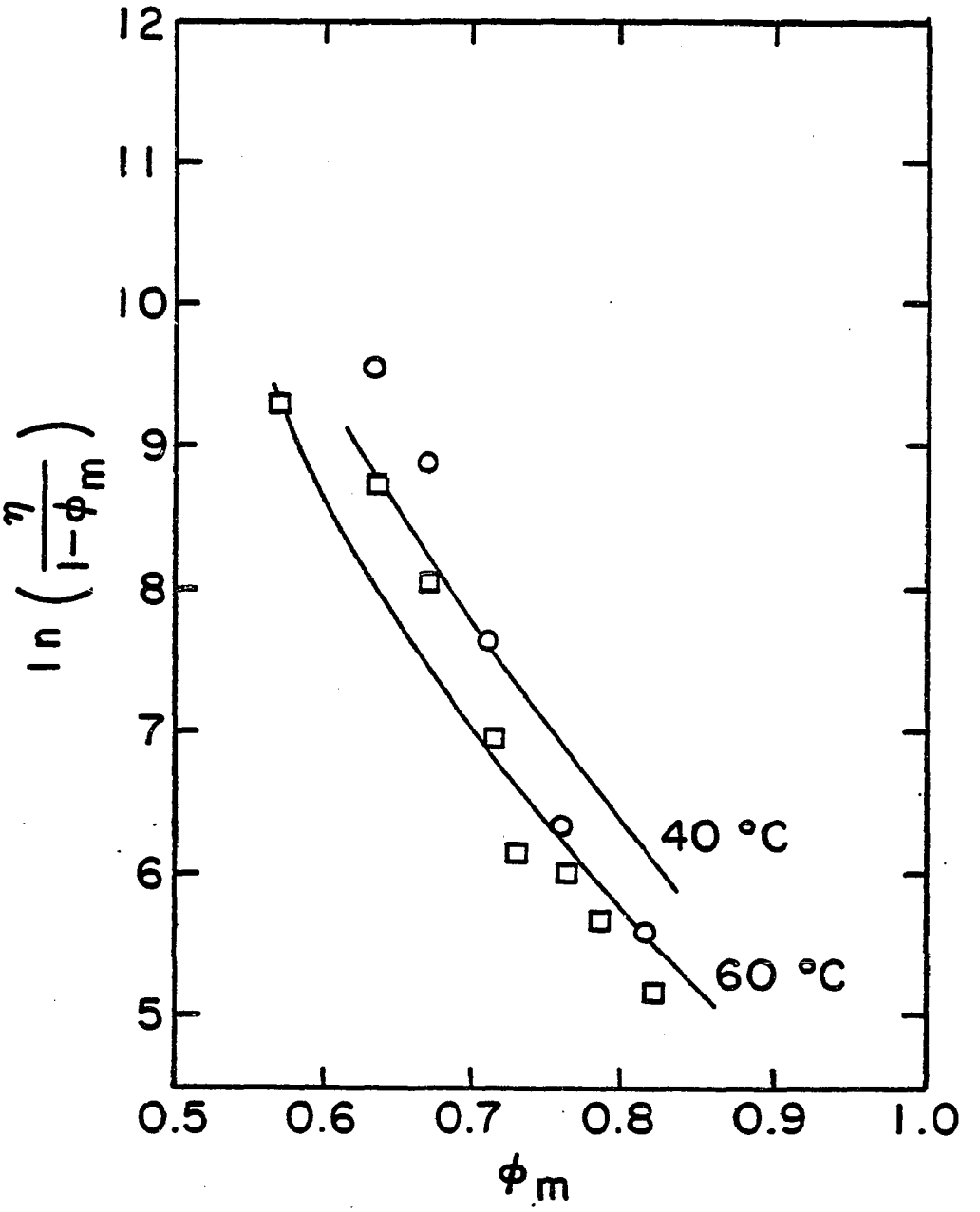

Fig. 4.4 Viscosity of MMA/PMMA Systems

o :40°C, □:60°C

4.3 DIFFUSION CONTROLLED PROPAGATION REACTIONS

As was mentioned earlier, the propagation rate constant is known to be affected by the restricted diffusion of individual monomer molecules at high conversions, or more correctly at low free volumes. The method of describing this phenomenon via equation 4.1 requires the designation of a critical free volume at which the decrease in k_p begins. In order to remove the empirical nature of fitting this v_{fc} to the experimental data, it was decided to write the effective propagation rate constant in terms of the two limiting cases associated with no diffusional resistance, k_{po}, and absolute diffusional control of the reaction, k_{pvf}. In the latter case, the reaction is seen to be instantaneous upon encounter. This description of k_p will take the form,

$$1/k_p = 1/k_{po} + 1/k_{pvf} \qquad (4.16)$$

The value of k_{po} is to be equal to the literature value measured at low polymer concentration, but k_{pvf} needs further investigation.

The treatment of diffusion controlled reactions between small molecules was summarized by Allen and Patrick (21). The Rabinowich model, the "volume-swept-out" model, and the Smoluchowski model predict comparable results for the same systems, but vary in the basic assumptions made. It may first appear that the existing models are not applicable to the propagation reaction because propagation is a reaction between a macroadical and a monomer molecule, much different in size. This is not the case as the mobility of the active center of a

macroradical and of a monomer molecule is considered to be identical (20). This is justified by identifying the segment of a chain as a monomeric unit. Considering that the active center of a macroradical is located at the end of a chain, and that a chain end behaves as if it were a segment of unentangled chain in the short-range motion which is necessary in a propagation reaction, the justification is quite straightforward. It is also expected that the structure of the polymer-monomer mixture can be visualized as a quasi-crystalline lattice due to the same size of the reactants (the active center as a monomeric unit and the monomer molecule). Therefore the basic assumptions of the Rabinowich treatment are satisfied for the propagation reaction, and k_{pvf} is predicted to be

$$k_{pvf} = 6D_m z/(\bar{\ell}^2 M_o) \qquad (4.17)$$

where the molar concentration of pure monomer, M_o, is used by neglecting the volumetric contraction with polymerization. The error associated with this choice will be small as the conversion will be quite high at the start of this period. The jump distance, $\bar{\ell}$, is usually taken to be the average intermolecular spacing in the quasi-crystalline lattice and approximated as

$$\bar{\ell} = (M_o N_{Av}/1000)^{-1/3} \qquad (4.18)$$

The coordination number, z, is taken to be approximately 8 for organic liquids. Combining these relationships and the numerical value of Avogadro's number into equation 4.17 one obtains

$$k_{pvf} = 3.4 \times 10^{15} D_m/M_o^{1/3}, \text{ lit/mol, sec} \qquad (4.19)$$

where the units of cm^2/sec and mol/lit should be used for D_m and M_o,

respectively. Equations 4.17 and 4.20 can provide a value of k_p at any conversion level provided that D_m is known.

Considering the general unavailability of diffusivity data for monomers in polymer solutions, the author proposes the following estimation method for D_m. This method is based on the assumption that the friction coefficients ζ_s and ζ_m of equations 4.6 and 4.7 are the same, and assuming that B and B_d of the same equations are the same and equal to unity. This is equivalent to assuming that A = Ad. Experimental data(14) support these assumptions as shown in the Table 4.3 where the segmental (molecular) friction coefficients of a chain unit and of small molecules are tabulated for comparison. Table 4.3 shows that even when the diffusing unit is chemically different from the chain unit, the friction coefficient of the diffusing unit (ζ) is nearly identical to the segmental friction coefficient ζ_s if the molecular weights of the two units are similar. For monomer-polymer pairs where chemical similarity and molecular identity is assured, the assumption of the same friction coefficients is expected to be excellent. Once ζ_s has been obtained for the pure polymer at the temperature of interest, ζ_m is computed at the conversion level of interest by using equation 4.7 to correct for the conversion level through the free volume. As such,

$$\zeta_m = \zeta_s = (\zeta_s)_{v_{fp}} \exp(1/v_f - 1/v_{fp}) \qquad (4.20)$$

Then D_m is computed as kT/ζ_m via equation 4.7 .

In summary, the proposed method of estimating the propagation rate constant can be outlined as follows:

1.) the value of k_{po} is obtained as the normal value measured at low polymer concentration,

Table 4.3

MOLECULAR FRICTION COEFFICIENTS OF VARIOUS DIFFUSING UNITS (14)

polymer	temp°K	diffusing unit (mol. wt.)	log ζ	log ζ_s (mol. wt.)
polyisobutylene	298	n-butane (58) i-butane (58) n-pentane (72) n-hexadecane (226)	-4.46 -4.11 -4.42 -4.17	-4.35 (56)
hevea rubber	303 298	n-butane (58) i-butane (58) n-pentane (72) n-hexadecane (226)	-6.74 -6.56 -6.74 -6.27	-6.90 (68)
polymethylacrylate	323	ethyl alchol (58)	-3.69	-3.15 (86)
poly(vinylacetate)	313	n-propyl alchol (60) n-propyl chloride (79)	-1.41 -1.49	1.75 (86)
poly-n-hexyl methacrylate	298	n-hexadecane (226)	-4.96	-0.75 (170)
poly-n-octyl methacrylate	298	n-hexadecane (226)	-5.58	-2.29 (198)
poly-n-dodecyl methacrylate	298	n-hexadecane (226)	-5.75	-4.69 (254)
Polydimethyl siloxane	298	n-hexadecane (226)	-7.59	-8.05 (74)
1,4-polybutadiene	298	n-hexadecane (226)	-6.73	-6.75 (54)
styrene-butadiene rubber	298	n-hexadecane (226)	-5.81	-6.11 (65.5)
1,2-polybutadiene	298	n-hexadecane (226)	-4.36	-4.11 (54)

2.) the value of $(\zeta_s)_{vfp}$ at the appropriate reaction temperature is obtained from Table 12-III in Ferry(14) or from Table 4.3(taken (taken from Ferry (14)). When the appropriate temperature cannot be found in Ferry's table, use is made of equation 4.5 with B set equal to unity. Using the values of the parameters shown in Table 1, v_{fp} is calculated for the temperature at which ζ_s is known, and both used in equation 4.5 to give the value of ζ_s at the desired temperature (v_{fp} having been calculated as before at this temperature).

3.) the free volume at any conversion is calculated from equations 4.4,4.10 or 4.11 and equation4.14, along with the free volume parameters in Tables 4.1 and 4.2.

4.) the monomeric friction coefficient ζ_m is obtained from equation 4.20,

5.) D_m is calculated as kT/ζ_m

6.) k_{pvf} is computed from equation 4.19.

7.) the effective rate constant, k_p, is calculated from 4.16.

As a check on whether the free volume parameters obtained from Fjita's viscosity measurements(29) for polymer solutions will predict the correct temperature dependence of the friction coefficient of the pure polymers, we have plotted the values of ζ_s (at different temperatures) obtained from Ferry(14) against the fractional free volume of the polymer as calculated from equation 4.10 or 4.11 and the free volume parameters listed in Table 4.1.As can be seen from eqn 4.5, a plot of log ζ_s vs $1/v_{fp}$ should yield a straight line with a slope of 1/2.303, or 0.434 (for B = 1.0). Fig. 4.5 is such a plot for three different polymers and shows acceptable linear behavior with slopes within 13% of the theoretical

value. This lends credence to the use of the free volume parameters obtained in this work.

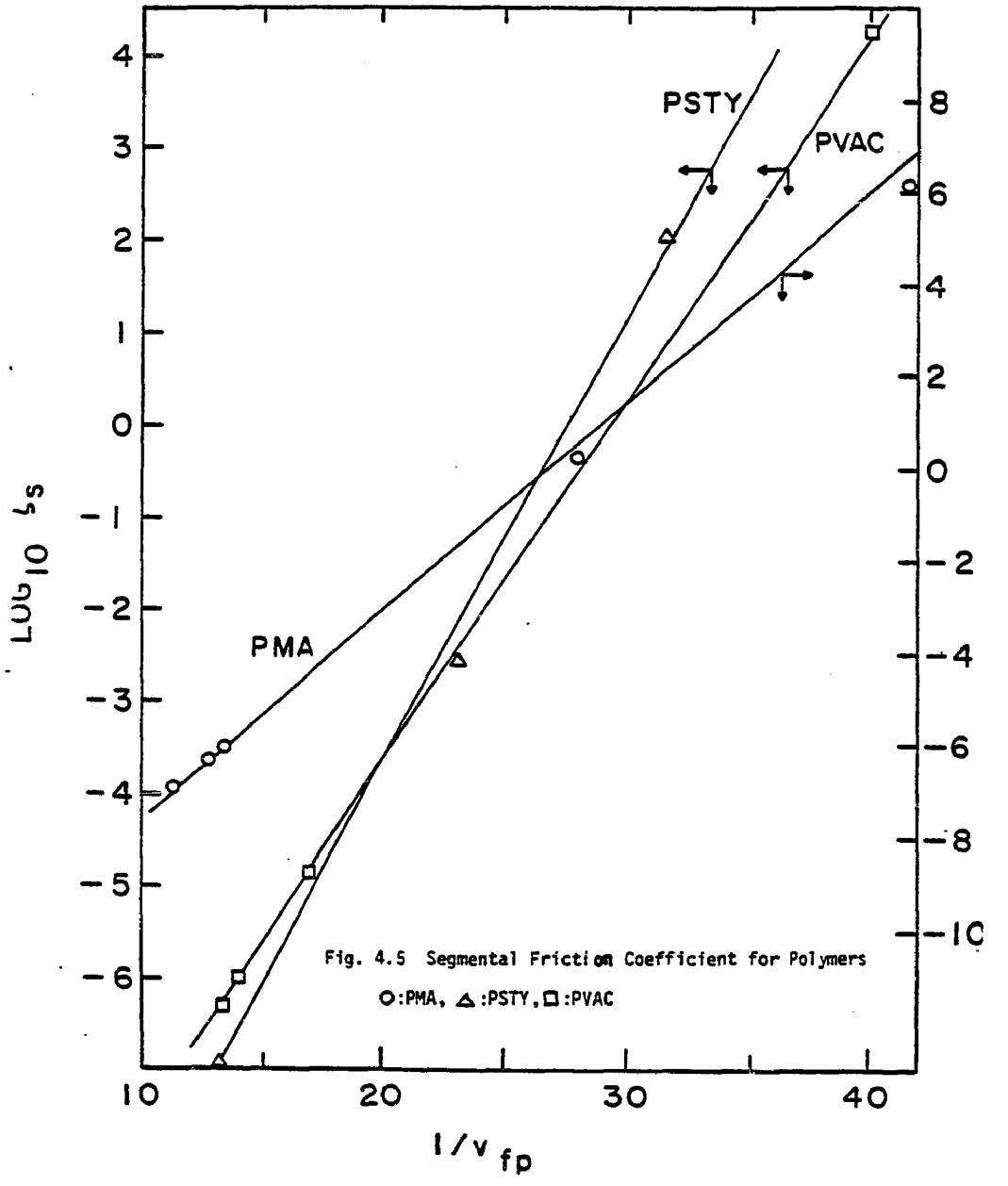

Fig. 4.5 Segmental Friction Coefficient for Polymers
○:PMA, △:PSTY, □:PVAC

4.4 LIMITING CONVERSION

The events which characterize the very last stage of the polymerization reaction are certainly the least understood and least discussed in the literature. It has often been noted that polymerizations carried out at temperatures significantly below the glass transition temperature of the pure polymer do not appear to reach full conversion. Such behavior has been reported by a number of investigators and there have been several articles devoted to its behavi [6,34,35]. However, there are other studies which report essentially full conversion for the same systems at these temperatures [11]. Accurate measurements of conversion can be difficult above 90% conversion and that may explain some of the discrepancies between reported experiments, but on the whole it does appear that limiting conversions are real.

Various researchers have treated this portion of the polymerization in very different ways. As already mentioned in Chapter 3, O'Driscoll [15] used the entire experimental polymerization conversion profile to fit the constants for his model but did not really address the mechanism by which the conversion is limited. Hamielec [13] paid particular attention to this section of the reaction by treating propagation as a diffusion controlled process and correlating it with free volume. His treatment required the use of an adjustable constant, the free volume at which the propagation rate constant begins to decrease. This rate constant was allowed to decrease exponentially with free volume, and by the appropriate choice of the adjustable constant, any limiting conversion could be shown. Soh and Sundberg [28] previously

used the same approach as Hamielec to treat the emulsion polymerization data of styrene and methylmethacrylate and had reasonable success in correlating the limiting conversion.

The results of this thesis have lead the author to believe that this portion of the polymerization is significantly more complex than the above treatments described. The author has strived to remove the necessity of employing adjustable constants. The treatment proposed for k_p, as shown in equations 4.20 and 4.21 in the previous section, is free of adjustable parameters as it uses the free volume of pure polymer as the reference free volume. However, as shown in Chapter 5, the values of k_p computed by this procedure display significant reduction in levels only above 90% conversion, even for styrene and methylmethacrylate polymerized at 50°C. Even when limiting conversions are predicted, the levels are sometimes higher than those shown experimentally. It is felt that the treatment of k_p given here is more correct than those described earlier, and this leads to conclude that other phenomena must be significantly contributing to decreased reaction rate during this period. The overall treatment of termination behavior already takes chain transfer reaction to monomer into account in deriving the chain length probability distribution function, but the effect of the monomeric radical formed by the chain transfer to monomer reentering the chain length growth sequence was not considered with the assumption that it is much smaller than the rate of monomeric radical generation by the initiator decomposition and the subsequent reaction with the monomer. To explain the polymerization behavior during the Phase IV in a quantitative way, one must consider the effect of restricted diffusion upon the initiator dissociation rate,

and chain transfer reactions to monomer and possibly polymer. The diffusion controlled initiator decomposition would lead to decreased production of free radicals (due to local recombination of initiator radical fragments) and such a model has been proposed by Saito (10), but it does not appear to have received much attention. Chain transfer to monomer and the subsequent formation of a new unentangled active chain would provide additional mobility of the active chain end and retard the rate of decrease of the overall termination rate constant. Chain transfer to polymer would have the same effect, although to a much lower degree partly because the resulting active center has much less mobility. All of these mechanisms would lead to decreases in the rate of polymerization and, if employed, would improve the ability of the present model to predict the appropriate limiting conversion. However, the application of these ideas is left to future work, while noting that definitive work in this range of the conversion profile will be difficult. The suitability of the predictions made without these considerations will be discussed in Chapter 5.

4.5 CONCLUDING REMARKS

This Chapter concludes the theoretical description of the polymerization rate and molecular weight development for the bulk polymerization of vinyl monomers over the entire conversion range. It has been proposed that such reactions are comprised of four distinct phases in which the termination and propagation reaction steps may be controlled by different phenomena. The theory has been developed without the use of adjustable parameters and the transition from Phase II to Phase III and from Phase III to Phase IV occurs naturally within the theory. The transition from Phase I (classical kinetics) to Phase II which marks the onset of the gel effect must yet at this time be treated as an adjustable parameter. The conversion and molecular weight profiles are quite sensitive to the choice of this point of transition and significant discussion will be devoted to it in the last paper in this series. Thus, the theory as presented may be classified as a one adjustable parameter model, and contains fewer adjustable parameters than any other comprehensive model put forth at this time.

Chapter 5

COMPARISON OF THEORY AND EXPERIMENT

5.1 INTRODUCTION

This Chapter will deal with the application of the theory to a variety of bulk polymerization systems, including methylmethacrylate (MMA), ethylmethacrylate (EMA), ethylacrylate (EAC), propylacrylate (PAC), styrene (STY), and vinyl acetate (VAC). Polymerization rate and molecular weight data available in the literature are compared with the predictions of the model. The systems analyzed cover a wide variety of monomers and reaction conditions, and provide excellent tests for the general validity of the theory. Table 5.1 shows the selected polymerization systems and their important characteristics.

The format to be followed in the following discussion will be first to present an overview of the theoretical computations based upon the theory presented in Chapter 2-Chapter 4, and then to analyze each of the six polymerization systems in Table 5.1. Particular emphasis will be placed upon molecular weight development and those aspects of each system which makes its polymerization rate behavior different from the others.

Table 5.1

SELECTED POLYMERIZATION SYSTEMS

Monomer	Mode of termination[1]	Approximate t_{gp}, °C	Reaction temperature, °C	Type of data[2]	Reference
MMA	D	115	45-90	P,M	3,11
EMA	D	62	70-90	P,M	14
EAC	D	- 24	35	P	15
PAC	D	- 48	35	P	23
STY	R	100	45-100	P,M	10,11,43
VAC	R	35	50	P	41

1. D = disproportionation, R = recombination
2. P = polymerization rate, M = molecular weight

5.2 METHOD OF ANALYSIS

This section deals with the general computational procedures and the set of equations used for the modelling of vinyl polymerizations with the proposed theory. Only an outline is given below since the details of the theory have already been discussed.

The following equations constitute a set of governing relationships capable of predicting the polymerization rate and molecular weight development.

1. initiator decomposition: $R_i = 2f\, k_d[I]$ (5.1)

   where $[I] = \frac{[I]_o}{1-\varepsilon X} \exp(-k_d\theta)$

2. radical concentration: $[R\cdot] = (R_i/\bar{k}_t)^{1/2}$ (5.2)

3. polymerization rate: $dX/d\theta = k_p[R\cdot](1-X)/(1-\varepsilon X)$ (5.3)

4. instantaneous number average molecular weight:

   $$M_n = M_o k_p[M]/(\bar{k}_t[R\cdot]/r + k_{tr,m}[M]) \quad (5.4)$$

   where $[M] = [M]_o(1-X)/(1-\varepsilon X)$

   and $r = \begin{cases} 1 \text{ for disproportionation} \\ 2 \text{ for recombination} \end{cases}$

5. instantaneous higher order molecular weights:

   $$M_j = \ell_j M_n \quad (5.5)$$

   where j may refer to the w, z, z+1, etc. averages. The ℓ_j's are defined in Chapter 2.

6. cummulative molecular weight averages:

   $$X d\bar{M}_n/dX = \bar{M}_n(1-\bar{M}_n/M_n) \quad (5.6)$$

   $$X d\bar{M}_w/dX = M_w - \bar{M}_w \quad (5.7)$$

$$X d\bar{M}_j/dX = (M_j - \bar{M}_j) \prod_{k=w}^{j-1} (M_k/\bar{M}_k) \qquad (5.8)$$

for $j>w$, i.e., $j = z, z+1$, etc. where equations 5.6 and 5.7 are routinely used(36) and equation 5.8 is derived in Appendix A.

Among the reaction rate constants involved, only $\bar{k}_t$ and k_p were allowed to change with conversion. k_p can be calculated by the method developed in Chapter 4 of this thesis, but its value remains constant for most of the conversion range. The values of $\bar{k}_t$ and ℓ_j change significantly with conversion and those dependencies differ for each phase of the polymerization.

Phase I - Conventional Kinetics

For conventional kinetics, only the ratio $k_{po}/(k_{to})^{1/2}$ is required to predict the rate and molecular weight development, but for Phases II-IV the individual values of k_{po} and k_{to} are necessary. Values of k_{po} are usually available, but those for k_{to} are not. During Phase I, $\bar{k}_t = k_{to}$ and the ℓ_j's are constant at the values shown in Table 2.1.
As the kinetics and molecular weight development are adequately understood during Phase I, the data obtained during this period can be used to determine f and k_{to}. These are not usually known with much accuracy, but f/k_{to} can be determined from time-conversion data via equation 5.3, and fk_{to} can be found from the molecular weight data through equations 5.1,5.2 and 5.4-5.8. Combining these two independent values, it is possible to obtain separate values for f and k_{to}.

Phase II - Gel Effect

The transition between Phases I and II marks the start of the gel effect and the exact location of the starting point serves as the only adjustable parameter of the proposed model. In addition to the constants normally known (k_d, k_{po}) and those found from the data of Phase I (f, k_{to}), the free volume parameters (determined from viscosity measurements as shown in Chapter 4, and the entanglement chain length x_{co} are necessary. Free volume parameters for some systems are given in Chapter 4 and tabulation of x_{co} is given in the literature (p. 76 of reference 20, p. 409 of reference 14) The fractional free volume v_f and entanglement parameter x_c are calculated by the following equations.

$$\phi_m = (1-X)/(1-\varepsilon X) \tag{5.9}$$

$$v_f = v_{fp}(1-\phi_m) + v_{fm}\phi_m \tag{5.10}$$

$$x_c = x_{co}/(1-\phi_m) \tag{5.11}$$

The two dimensionless parameters β and γ are calculated by

$$\beta = x_c C_m \tag{5.12}$$

where $C_m = k_{tr,m}/k_p$

$$\gamma = x_c(R_i k_{tvf})^{1/2}/k_p[M] \tag{5.13}$$

where k_{tvf} is calculated as

$$k_{tvf} = k^*_{tvf} \exp(1/v_{fxc} - 1/v_f) \tag{5.14}$$

where v_{fxc} is the adjustable parameter which determines the starting point of the gel effect, or Phase II, and k^*_{tvf} is determined to satisfy the following equation

$$k^*_{tvf} Z \Big|_{v_f = v_{fxc}} = k_{to} \tag{5.15}$$

Now β and γ are determined with the aid of equations 5.14 and 5.15, the

dimensionless indices Z and ℓ_j's (j = w, z, z+1, etc.) are read from the master charts of **Chapter 2**, and $\bar{k}_t$ is calculated as

$$\bar{k}_t = k_{t_{vf}} Z \tag{5.16}$$

As Z accounts for the entanglement contribution to $\bar{k}_t$, it is equal to 1.0 when the polymer/monomer solution as a whole is not entangled. This consideration gives rise to the expectation that there should be two different kinds of gel effect behavior during Phase II. One type the authors have named the "true gel effect", where the entanglement condition is met from the start of Phase II. The criterion used to establish the entanglement point is

$$\bar{M}_w \Big|_{v_f = v_{fxc}} \geq M_o x_c \Big|_{v_f = v_{fxc}} \tag{5.17}$$

Actually the entanglement effect occurs gradually with increasing polymer concentration and/or molecular weight, and this transition is made more diffuse by broader molecular weight distributions(14). Also Turner (37) has proposed a "close-packing model" which predicts $(\bar{M}_w)^{1/2}$ dependence instead of the $\bar{M}_w$ dependence shown in equation **5.17**. More discussion is devoted to this subject in Appendix L. However, for conditions corresponding to the "true gel effect" where the existence of entanglement coupling is assured by both equation **5.17** and Turner's model, the choice does not affect the predictions of the model.

For the "true gel effect", as both k_{tvf} and Z of equation **5.16** decrease with increasing conversion, the rate of decrease of $\bar{k}_t$ will be much faster than the other type, which we will call the "pseudo gel effect". Here the condition for entanglement (equation **5.17**) is not met at the start of Phase II as

$$\bar{M}_w\Big|_{v_f=v_{fxc}} < M_o x_c\Big|_{v_f=v_{fxc}} \qquad (5.18)$$

For the pseudo gel effect, Z will be equal to 1.0, and equation 5.16 can be simplified to

$$\bar{k}_t = k_{tv_f} = k_{to} \exp\,(1/v_{fxc} - 1/v_f) \qquad (5.19)$$

The phrase "pseudo gel effect" is used because the ℓ_j's remain at the same values as during Phase I, and hence the polymerization kinetics and the molecular weight development are identical with the Phase I, except that the effective termination rate constant $\bar{k}_t$ decreases with conversion and rate acceleration is observed. For the pseudo gel effect, the polymerization system will eventually reach a point after the start of Phase II when the condition for the entanglement is met. From that point (with fractional free volume v^*_{fxc}), the system enters a period of "true gel effect". To retain the continuity of $\bar{k}_t$ at v^*_{fxc}, $\bar{k}_t$ should be calculated during the "true gel effect" period following the "pseudo gel effect" as

$$\bar{k}_t = k_{tvf}\, Z/Z\Big|_{v_f=v^*_{fxc}} \qquad (5.20)$$

From the analysis of a number of actual systems, styrene polymerization frequently shows pseudo gel effect behavior due to its short kinetic chain length formed during Phase I. For the pseudo gel effect, the location of the starting point of the entanglement coupling ($v_f=v^*_{fxc}$) does affect the subsequent polymerization behavior markedly. The predictions of the entanglement theory, as estimated by equations 5.17 and 5.18 were used to determine v^*_{fxc} during the computers computations, while hoping that better criterion will become available in the future.

Phase III - Limited Gel Effect

The termination rate constant during this period includes the consideration of the residual termination rate constant k_{tp}. The method proposed for its computation was developed in **Chapter 3** which is re-written here as

$$k_{tp} = \pi\sigma^2 a N_{Av} k_p [M] f_t / 1000 \qquad (5.21)$$

$$f_t = [P(1)-P(1)|_{X=0.5}]/[1-P(1)|_{X=0.5}] \qquad (5.22)$$

$$P(1) = \exp\{-\beta-\gamma\sqrt{Z}/2 - \gamma/(2\sqrt{Z})\} \qquad (5.23)$$

where σ is calculated by the methods proposed in **Chapter 3,** and the values of a are found in the literature (p. 24 of reference **20,p.362** of reference **14,** p. 40-42 of reference **25**). The parameter which indicates the contribution of the residual rate to the total termination rate behavior, W, is given as

$$W = k_{tvf}/(k_{tvf}+k_{tp}) \qquad (5.24)$$

The other dimensionless parameters, β and γ, are calculated by the method used during Phase II, while Z and the ℓ_j's are computed as functions of β, γ and W as shown in **Chapter 3.** $\bar{k}_t$ is then computed as

$$\bar{k}_t = (k_{tvf}+k_{tp})Z \qquad (5.25)$$

Sometimes the resulting $\bar{k}_t$ value calculated by equation **5.25** may increase with conversion during the early portion of Phase III. This is the result of the artificiality of equation **5.22,** and it was avoided here by setting $\bar{k}_t$ constant until the conversion is reached when equation **5.25** begins to predict a $\bar{k}_t$ value which decreases again with the increasing conversion.

Phase IV - Final Stages of Polymerization

During this period, $\bar{k}_t$ and all parameters other than k_p are calculated as in Phase III. The propagation rate constant was allowed to decrease by the method outlined in Chapter 4. This may be done for the entire conversion range if desired, but the effect is not at all significant until very late in the reaction.

Computer Modelling

The actual computations were done by the computer programs described in this section. Copies of the programs are found in the Appendix E.

The main program INT.FOR forst calls the subroutine COEFF.FOR which reads the interpolation coefficients necessary for the calculation of the entanglement factor, and the molecular weight indices are read from the data file CONST.DAT and GAMMA.DAT from the disk storage area. Then it accepts the values of the parameters which are most likely differ for each run from the terminal. The calculations which need be done only once for each run are done by calling the subroutine MONOM.FOR. The instantaneous values at any given conversion are calculated in the subroutine UPDATE.FOR, which will be called for each integration step in the IMSL integration subroutine DVERK.FOR which is called from INT.FOR and performs the sixth order Runge-Kutta variable step integration. For systems where the pseudo gel effect is expected, the subroutine MONPCK.FOR and UPDPCK. FOR replaces MONOM.FOR and UPDATE.FOR. The computation techniques involved in the preparation and interpolation of the master charts were described in Chapter 2 and 3. More descriptions of each program are found

in the comments of the listed programs in the Appendix E. Computer output for methyl methacrylate polymerization at 90° C and 0.5% AIBN concetration (Table 5.2) is also presented in Appendix E.

5.3 METHYL METHACRYLATE POLYMERIZATION

Balke and Hamielec (3) have presented the most extensive data for MMA to be found in the literature. This work includes both rate and molecular weight data obtained over a range of temperature and initiator levels. Ito (11) has shown similar results for a single polymerization temperature but covering a much broader rante of initiator levels. Both sources of data will be used in the following comparisons between theory and experiment.

The initiator dissociation rate constant for azobisisobutyronitrile (AIBN) used in the above experiments was taken from the literature (21) as

$$k_d = 1.5 \times 10^{15} \exp(-15450/T) \qquad (5.23)$$

The propagation rate constant was obtained in an absolute manner from seed emulsion polymerization data (27) as

$$k_{po} = 1.62 \times 10^{7} \exp(-3500/T) \qquad (5.24)$$

The chain transfer to monomer constant was taken to be temperature independent at a value of $C_M = 10^{-5}$, (38). Other physical property data used are;

$$x_{co} = 100 \qquad \text{reference (20)}$$

$$d_m = 0.973 - 1.164 \times 10^{-3} t$$

The expression for d_m was found by least squares linear regression of the density data tabulated in reference (39).

$$\varepsilon = 0.183 + 9.0 \times 10^{-4} t \qquad \text{reference (40)}$$

where t is the temperature as °C.

As indicated in the previous section, k_{to} and f were determined from the rate and molecular weight data of Phase I. The free volume parameters used are, from Chapter 4;

$$v_{fp} = 0.0194 + 3.0 \times 10^{-4}(t-105),\ t \geq 105$$
$$= 0.0194 + .13 \times 10^{-4}(t-105),\ t < 105$$
$$v_{fm} = 0.149 + 2.9 \times 10^{-4}\ t$$

The adjustable parameter v_{fxc} was selected to provide the best fit to the analyzed data of Phases II and III. It should be mentioned here that the calculated results are quite sensitive to the value of v_{fxc} and it must be determined carefully. Table 5.2 shows the k_{to}, f and v_{fxc} values used for the MMA calculations.

The fact that the k_{to} values found from Ito's data are different from those expected based on Hamieleis data may not have to be taken too seriously because only one set of molecular weight data was used to determine k_{to} and, more importantly, the molecular weight data were obtained from viscosity measurements, which were approximated to be equal to the weight average molecular weight by the authors. Also it may be noted that the contribution from recombination mode of termination may become more important at low temperature, which was not considered in this work. For the purpose of fitting the polymerization rate data alone, even 100% error in the value of k_{to} does not change the model prediction significantly as long as the same initial rate (determined by the ratio f/k_{to}) is used and v_{fxc} is adjusted as discussed above.

It appears that the value of v_{fxc} necessary to fit these data decreases slightly as the initiator concentration is increased. This may be expected since lower initiator concentration produces higher molecular

Table 5.2

CONSTANTS FOR MMA POLYMERIZATIONS

Data Source	Reaction Temp. (°C)	$[I]_o$	$k_{to} \times 10^{-7}$ (lit/mol,sec)	f	v_{fxc}
3	50	0.30 wt%	1.3	0.44	0.152
		0.39	1.2	0.42	0.151
		0.50	1.2	0.40	0.150
	70	0.30	2.2	0.44	0.149
		0.50	2.2	0.44	0.149
	90	0.30	3.0	0.48	0.138
		0.50	3.2	0.44	0.138
11	45	0.20 mol/lit	2.9	0.42	0.146
		0.10	2.9	0.42	0.149
		0.05	2.9	0.42	0.152
		0.025	2.9	0.42	0.153
		0.0125	2.9	0.48	0.154
		0.00625	2.9	0.48	0.155

weight, enabling the transition to Phase II to occur at an earlier stage of the reaction.

The results of the model predictions are compared with both rate and molecular weight data in Figs. 5.1-8. All data are explained remarkably well by the model until the very end of the polymerizations where limiting conversion behavior may occur. Disagreement in this region was expected and is discussed in Chapter 4.

It was noted in Chapter 2 of this thesis that if the time-conversion data are used to determine the adjustable parameter(s) in any particular model, the model will automatically fit the $\bar{M}_n$ data as good as the fit of the time-conversion data irrespective of the suitability of the particular model to describe the chain length dependency of k_t. Thus it is imperative to compare the predictions of any proposed model with the higher order molecular weight data in order to discriminate an acceptable model from unrealistic models.

It is in this vein that attention is drawn to Figs. 5.4-7 where the molecular weight averages $\bar{M}_n$, $\bar{M}_w$, $\bar{M}_z$ and $\bar{M}_{z+1}$ are shown with the model predictions. These figures clearly show that the molecular weights remain relatively unchanged during Phase I as conventional kinetics predict. During Phase II, higher order molecular weights ($\bar{M}_w$, $\bar{M}_z$, $\bar{M}_{z+1}$) increase very rapidly, with $\bar{M}_w$ increasing by about a factor of 5 during the 20-60% conversion range, and $\bar{M}_{z+1}$ increasing from 10-30 times in the same period. Strong agreement between theory and experiment is found for all of these cases.

The authors believe that this is the first reported attempt to predict higher order molecular weight development (especially $\bar{M}_z$ and $\bar{M}_{z+1}$) while considering the gel effect. The apparent agreement betwee

the theory and the data should be considered as supporting evidence for the validity of the model. Especially, the fact that $\bar{M}_w$ and higher molecular weights agree very well necessarily means that the theory, and in particular, the form of the chain length dependence function for the termination reaction, is valid.

Recently, Hamielec and Marten (13) presented a sophisticated model of diffusion controlled termination reactions which is based upon free volume theory. The model contains molecular weight dependence through the cumulative weight average molecular weight as follows;

$$k_t/k_{to} = (\bar{M}_w/\bar{M}_{wcr})^a \exp(A[1/v_f - 1/v_{fcr}])$$

where the subscript cr refers to the value at the start of the gel effect, and A and a are adjustable constants. They assumed that the instantaneous molecular weight distribution of newly formed polymer chains always conforms to that of the Schulz-Flory most probable distribution. In contrast, the model proposed in the present work treats the termination rate constant for each chain length separately and allows the distribution of newly formed polymer to deviate from the most probable distribution. The average value of k_t for all chains is partially determined by this distribution and may lead to different predictions than the relation used by Hamielec. In comparing these two models, it is found that both give nearly identical time-conversion curves (except near the limiting conversion where Hamielec's model shows better agreement with the data) partly because each use at least one adjustable constant which is (are) determined by fitting these same data. Since it is clear that a model which fits the rate data must also fit the $\bar{M}_n$ data, whatever differences exist between the models will only be visible from data for the higher

molecular weight averages ($\bar{M}_w$, $\bar{M}_z$, $\bar{M}_{z+1}$, etc). From Fig.5.6 and 5.7 it may be judged that both models give equivalent goodness of fit to the $\bar{M}_n$ data (only one curve is drawn through these data as both models predict the same values), except that the present model has only one adjustable constant compared to Hamielec's which has three. However, the real difference between the models becomes apparent for the weight average molecular weight predictions. Here it becomes evident that the chain length dependency of k_t of the present theory leads to a much more adequate description of the $\bar{M}_w$ data. It should also be noted that diffusion controlled propagation which may be important near the limiting conversion, does not appear to significantly affect the molecular weight data even during Phase IV.

The proposed model not only gives a good fit of the data, but also gives a fresh insight into the reason why MMA shows such profound gel effect. This is not because the polymethyl methacrylate chains have orders of magnitude lower diffusivity than the polymer chains which show less gel effect, but because the kinetic chain length produced from the conventional Phase I is much longer than the entanglement spacing. This enables the decrease of segmental mobility and the entanglement factor to work synergistically in an accelerating fashion to produce rapid polymerization rate and higher molecular weight. As will be discussed later, ethyl acrylate shows the same mechanism, resulting in the profound gel effect, while for polystyrene, the entanglement factor does not play a significant role until high conversion. This is due to the short kinetic chain length, resulting in a very moderate gel effect solely induced by the change of the segmental mobility, resulting in a pseudo-gel effect.

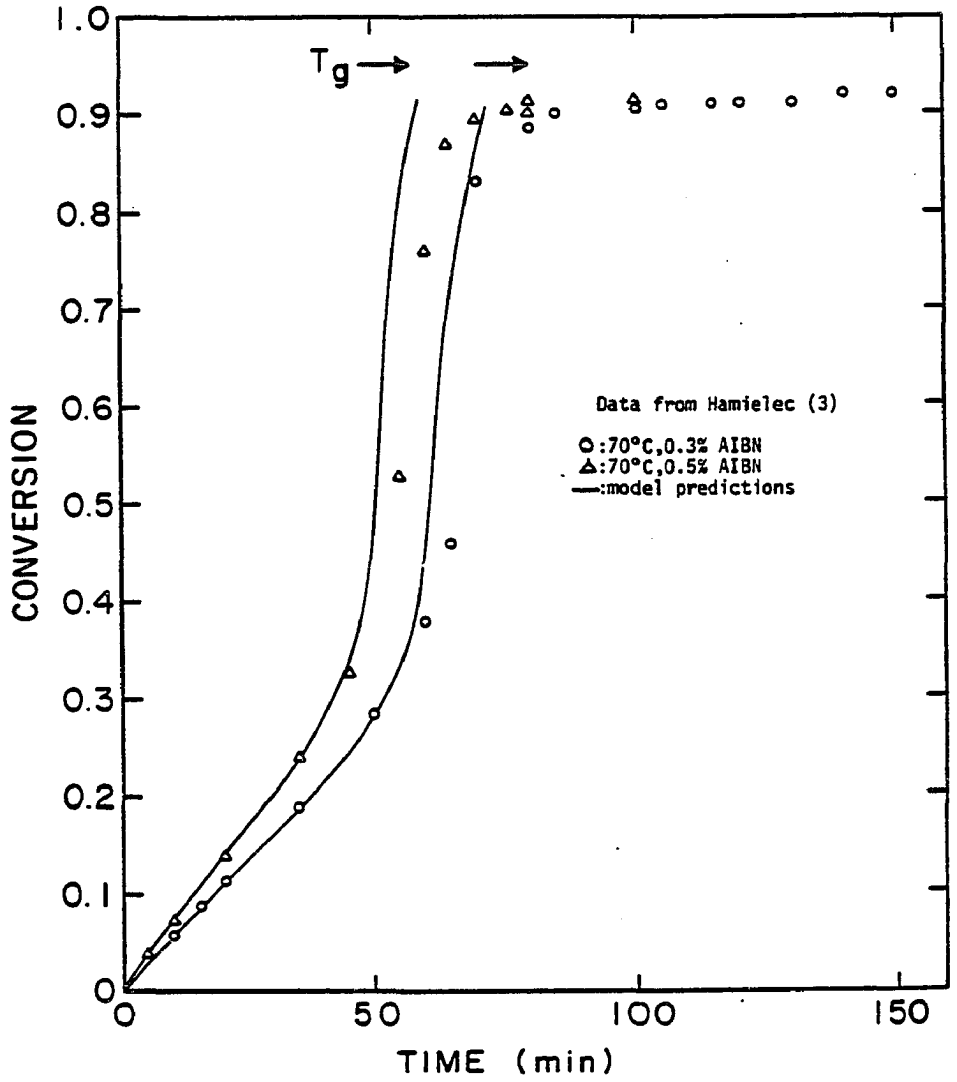

Fig. 5.1 Conversion-Time Profiles for MMA Polymerization

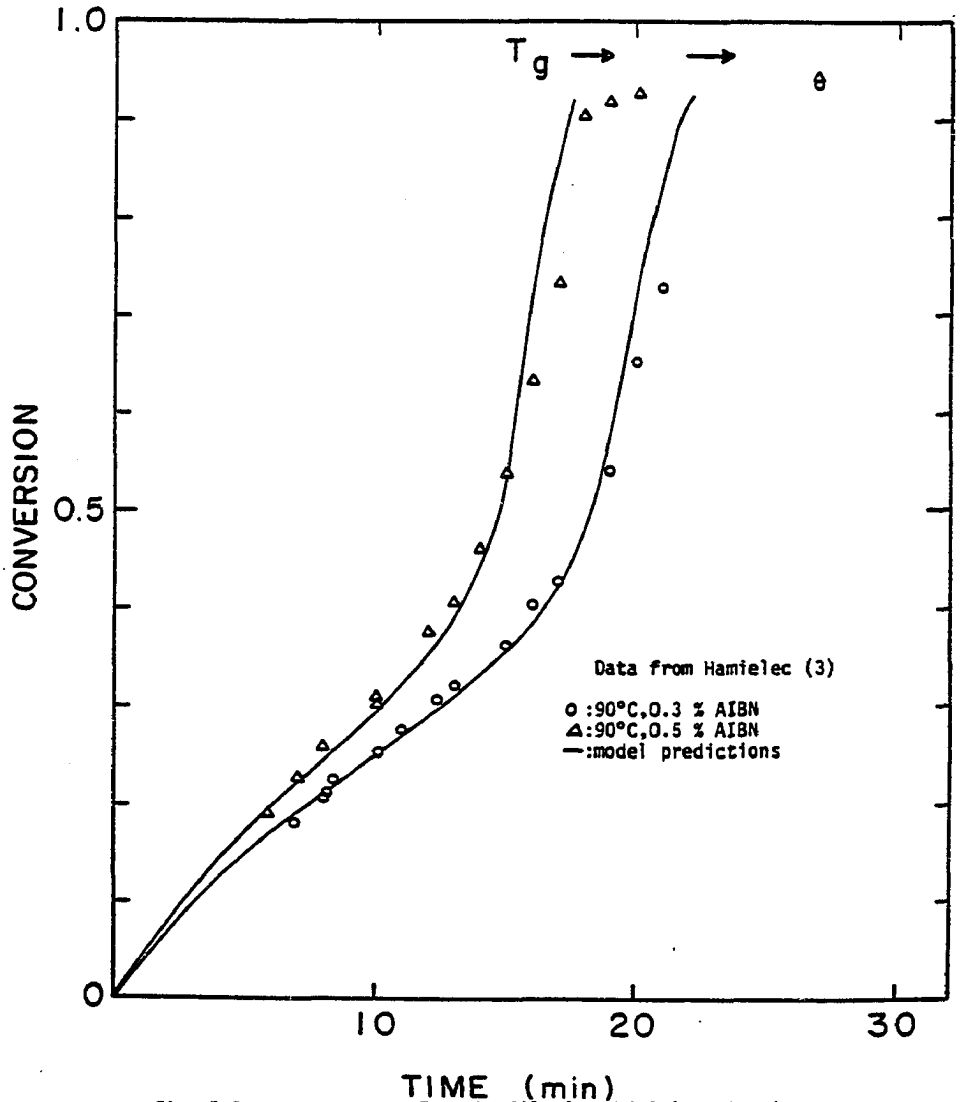

Fig. 5.2 Conversion-Time Profile for MMA Polymerization

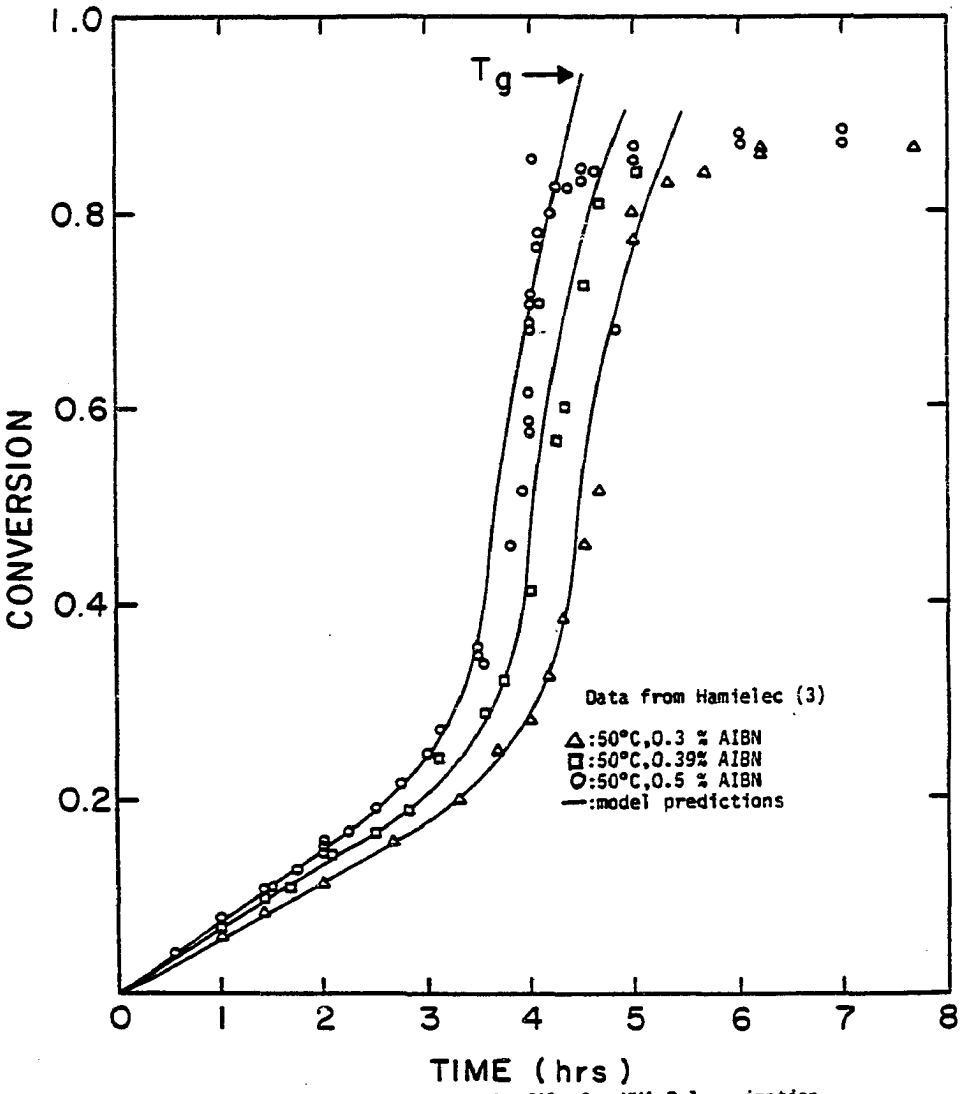

Fig. 5.3 Conversion-Time Profile for MMA Polymerization

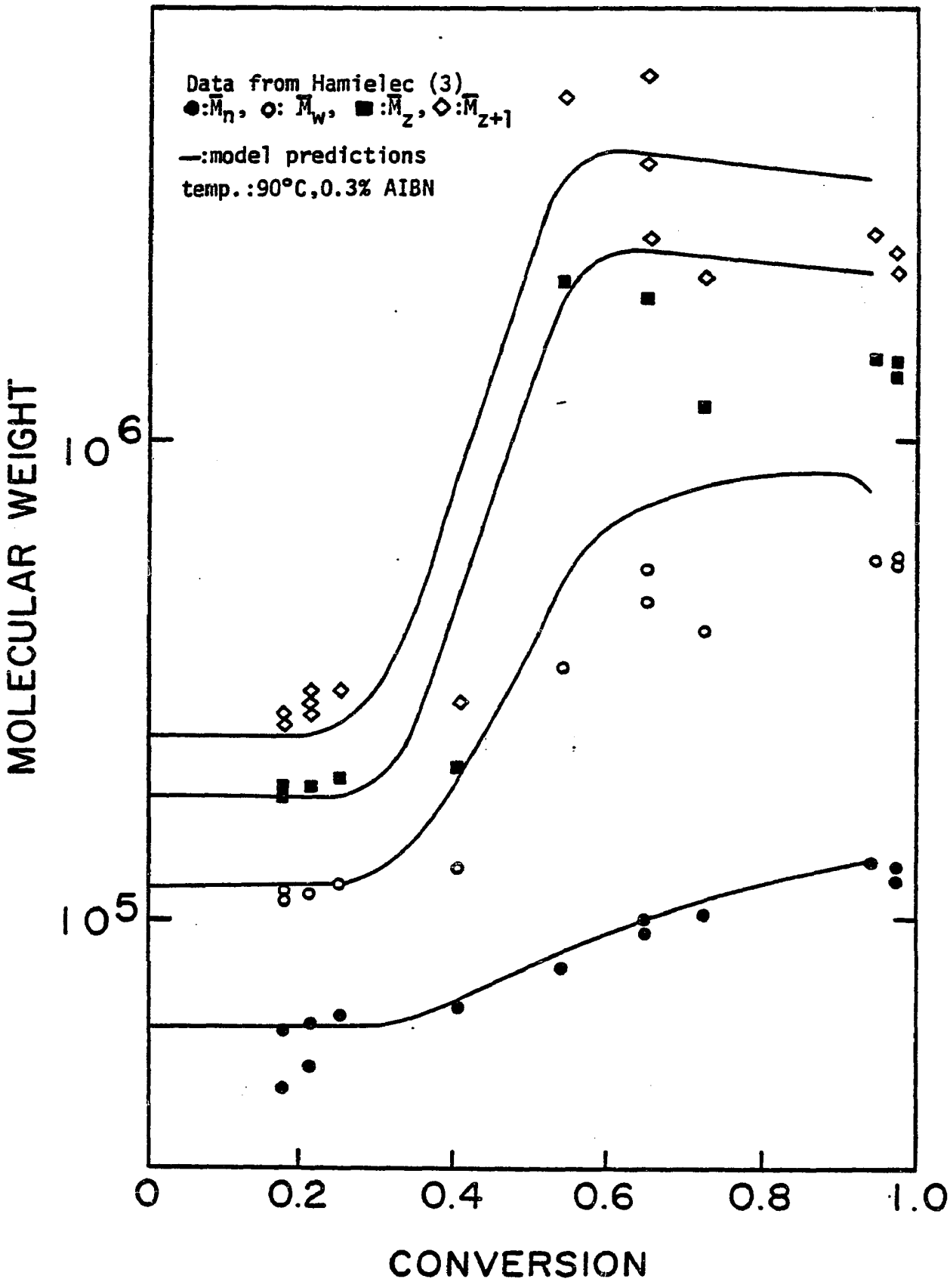

Fig. 5.4 Molecular Weight Development for MMA Polymerization

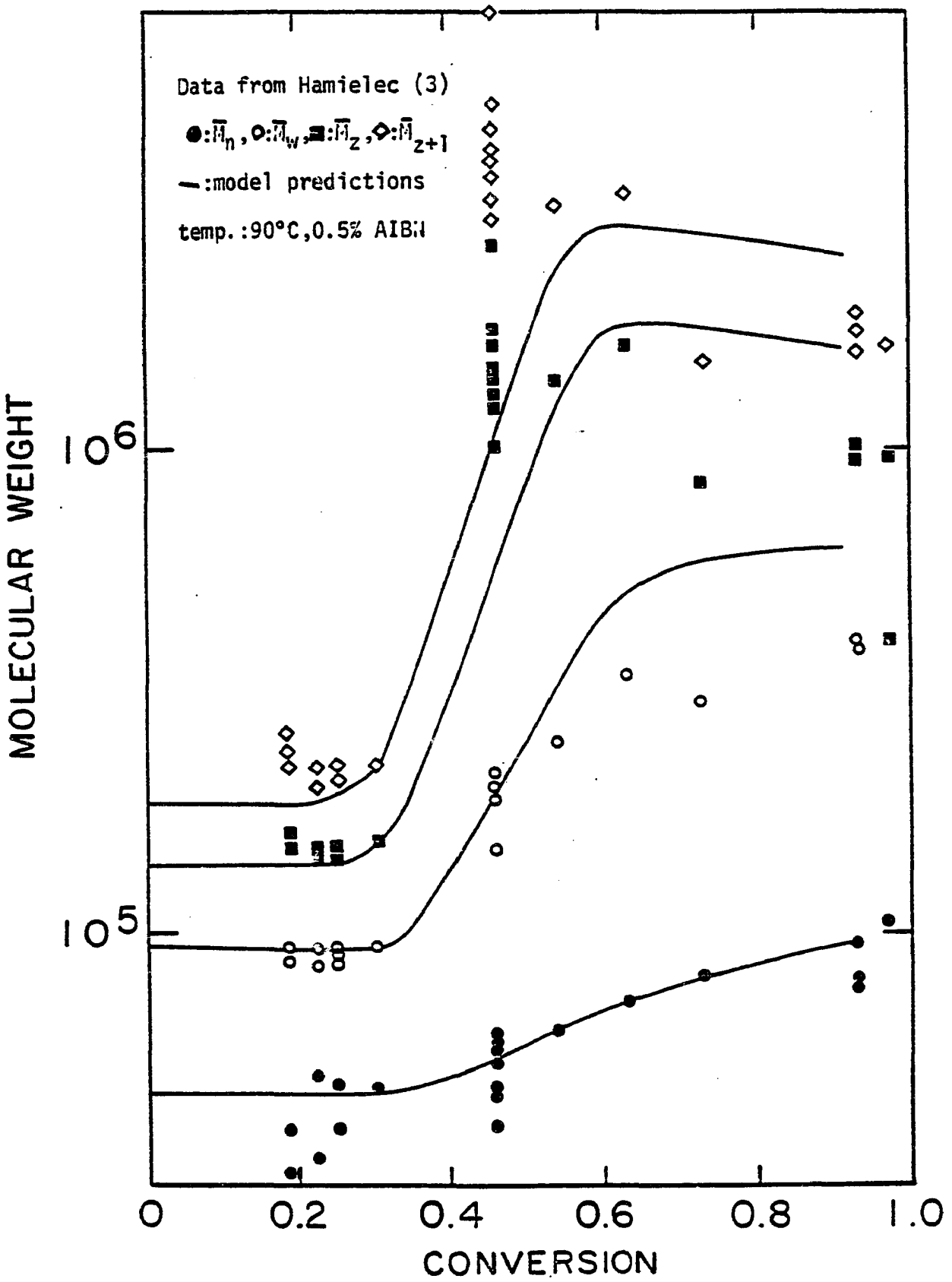

Fig. 5.5 Molecular Weight Development for MMA Polymerization

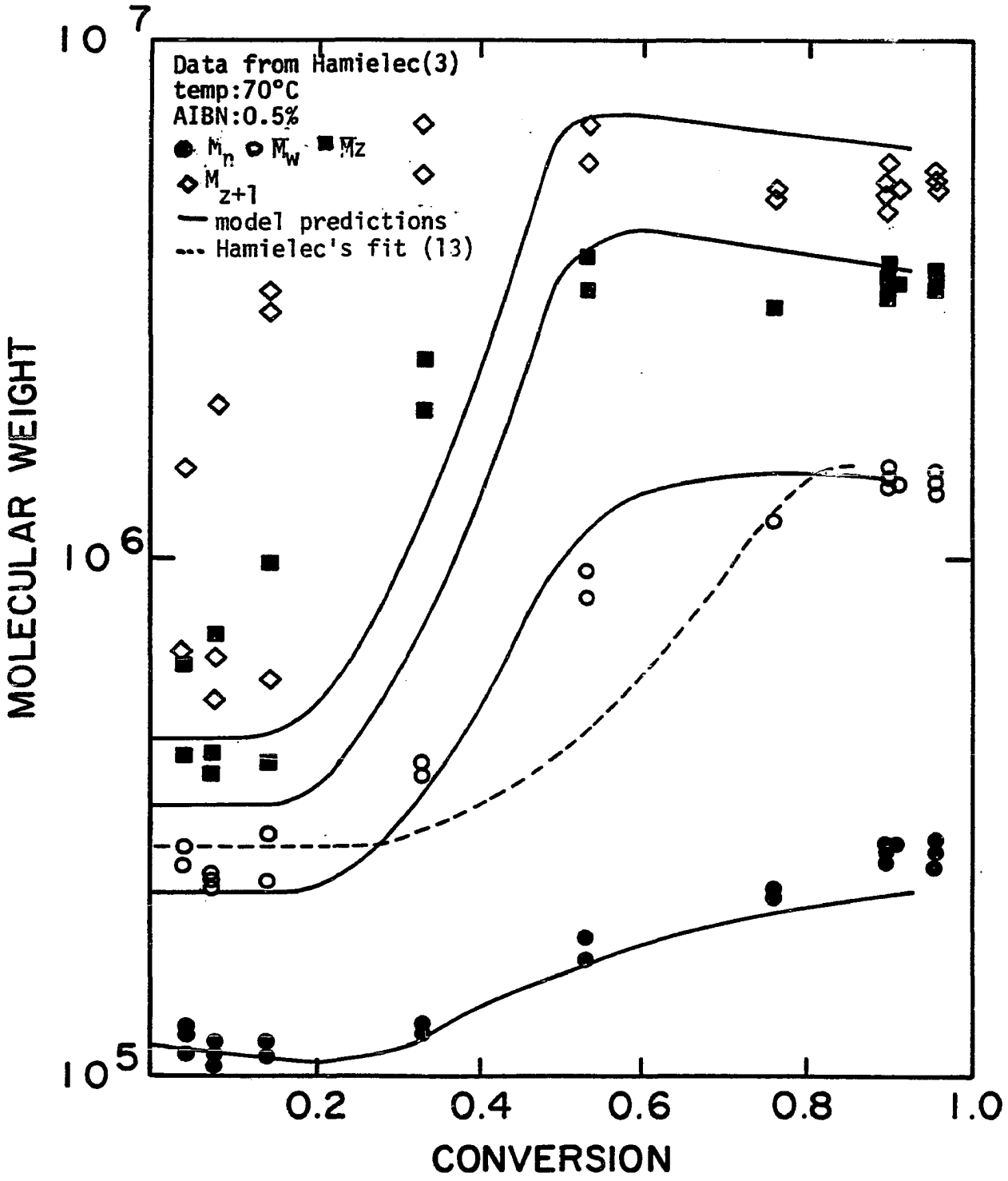

Fig. 5.6 MOLECULAR WEIGHT DEVELOPMENT FOR MMA POLYMERIZATION

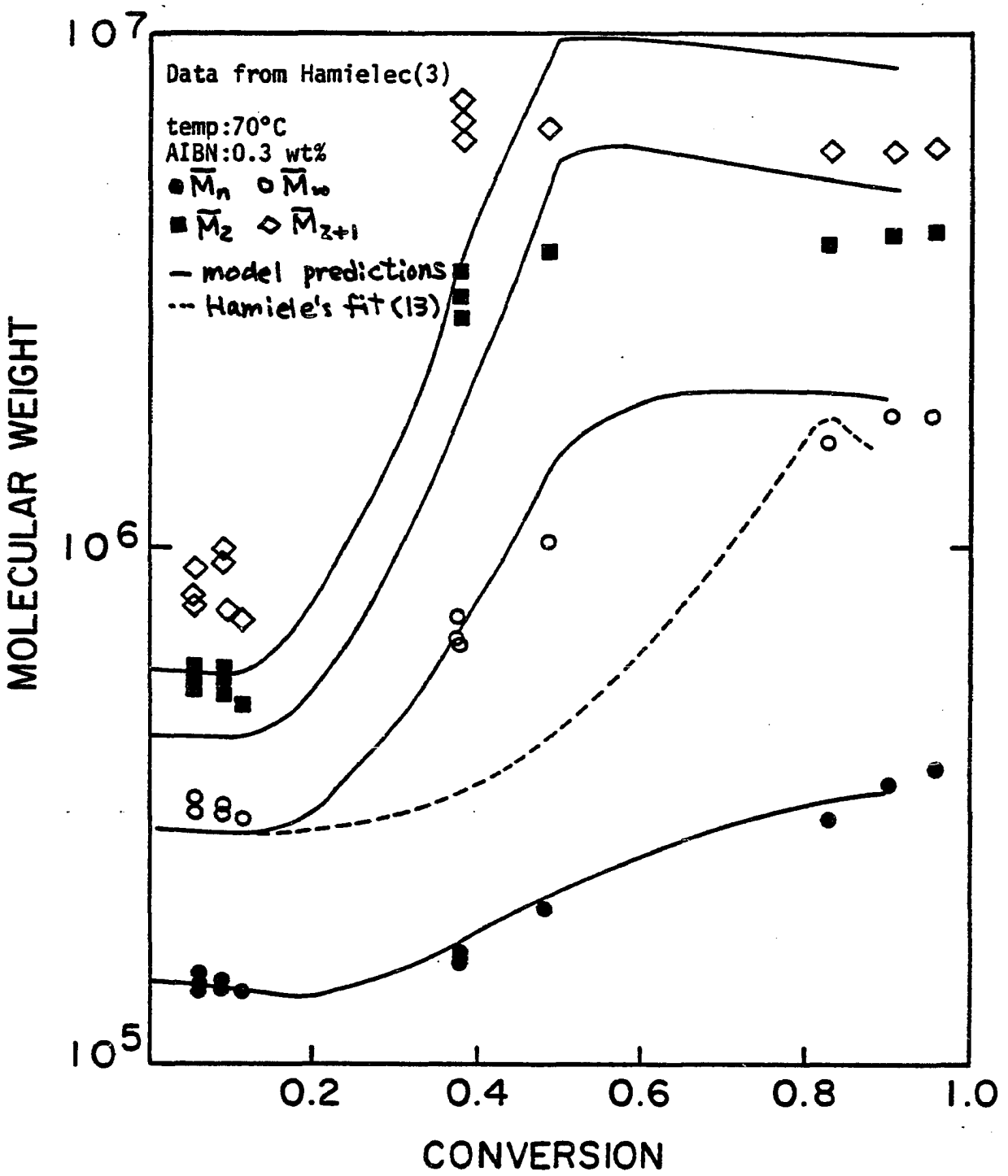

Fig. 5.7 MOLECULAR WEIGHT DEVELOPMENT FOR MMA POLYMERIZATION

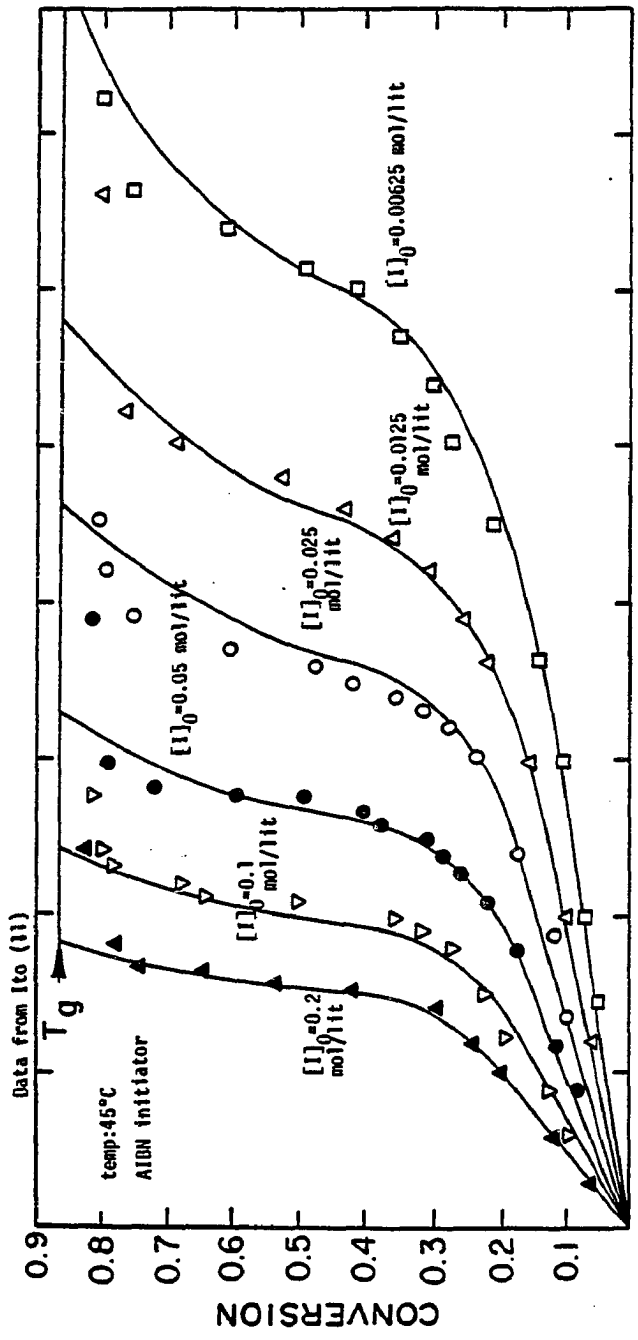

Fig. 5.8 CONVERSION-TIME PROFILES FOR MMA POLYMERIZATION

5.4 POLYMERIZATION OF ETHYL AND PROPYL ACRYLATE

Generally the acrylate series shows a very strong gel effect in spite of the fact that the polymerization is usually carried out well above their glass transition temperatures. Because the free volume remains relatively high throughout the reaction (due to the low t_{gp}) and cannot explain such a significant gel effect, entanglement coupling should be the main driving force for the rate acceleration. Patra's data (23) for ethyl acrylate (EAC) and n-propyl acrylate (PAC) at 35°C show that the gel effect causes rapid acceleration at very low conversions. This can only be explained by the high k_p values of acrylate monomers leading to high molecular weights rapidly exceeding the entanglement spacing. Computationally this is seen in the value of Z decreasing rapidly and causing a pronounced lowering of $\bar{k}_t$.

Since Patra's data do not include molecular weight results, it was not possible to obtain separate values for k_{to} and f from his data. Besides, reliable values of other rate constants and parameters were not readily available so that reasonable values of k_{po}, k_{to}, and C_M were used consistent with the values reported for their close homologues (38 and 39). The x_{co} value of 200 is the average value for many polymers (14). These values are;

Constant	Value at 35°C EAC	PAC
k_d(AIBN), sec^{-1} (21)	2.46×10^{-7}	2.46×10^{-7}
k_{po}, lit/mol,sec.	840	700
k_{to}, lit/mol,sec	2×10^6	2×10^6
C_M	10^{-5}	10^{-5}

Constant	Value at 35°C EAC	PAC
x_{co}	200	200
d_m, g/cm^3	0.978	0.959
ε	0.163	0.1565
t_{gp}, °C	-24	-48
t_{gm}, °C	-106	-106

The free volume calculations utilized the universal constants within the following expressions;

$$v_{fm} = 0.025 + 0.001\ (t-t_{gm}) \qquad (5.25)$$

$$v_{fp} = 0.025 + 4.8 \times 10^{-4}(t-t_{gp}) \qquad (5.26)$$

In a manner similar to that for MMA, the initiator efficiency was obtained from the initial polymerization rate and v_{fxc} was adjusted to coincide with the start of Phase II. The values determined for f and v_{fxc} are listed in Table 5.3.

Figs. 5.9-5.10 show the predicted behavior and the experimental data points. Very good agreement is found over the whole conversion range except for the runs utilizing the lowest concentrations of initiator, and those only deviate above 50% conversion. On the whole, however, the agreement is seen to be quite acceptable. The importance of presenting these data and their analyses is that it clearly establishes the role of polymer entanglements in bringing about significant gel effect behavior in systems where such behavior should be much less severe by the free volume changes alone. It would be interesting to test the effect of the addition of chain transfer agents in quantities capable of lowering the chain lengths below the entanglement spacing, x_{co}, and to view the anticipated reduction in the gel effect.

Table 5.3

Constants For EAC and PAC Polymerizations

Monomer	$[I]_o$, mol/lit	f	ν_{fxc}
EAC	0.04	0.584	0.1602
	0.03	0.584	0.1602
	0.02	0.584	0.1607
	0.014	0.475	0.1620
	0.008	0.428	0.1634
PAC	0.03	0.528	0.1617
	0.02	0.528	0.1622
	0.0121	0.428	0.1635
	0.008	0.428	0.1637

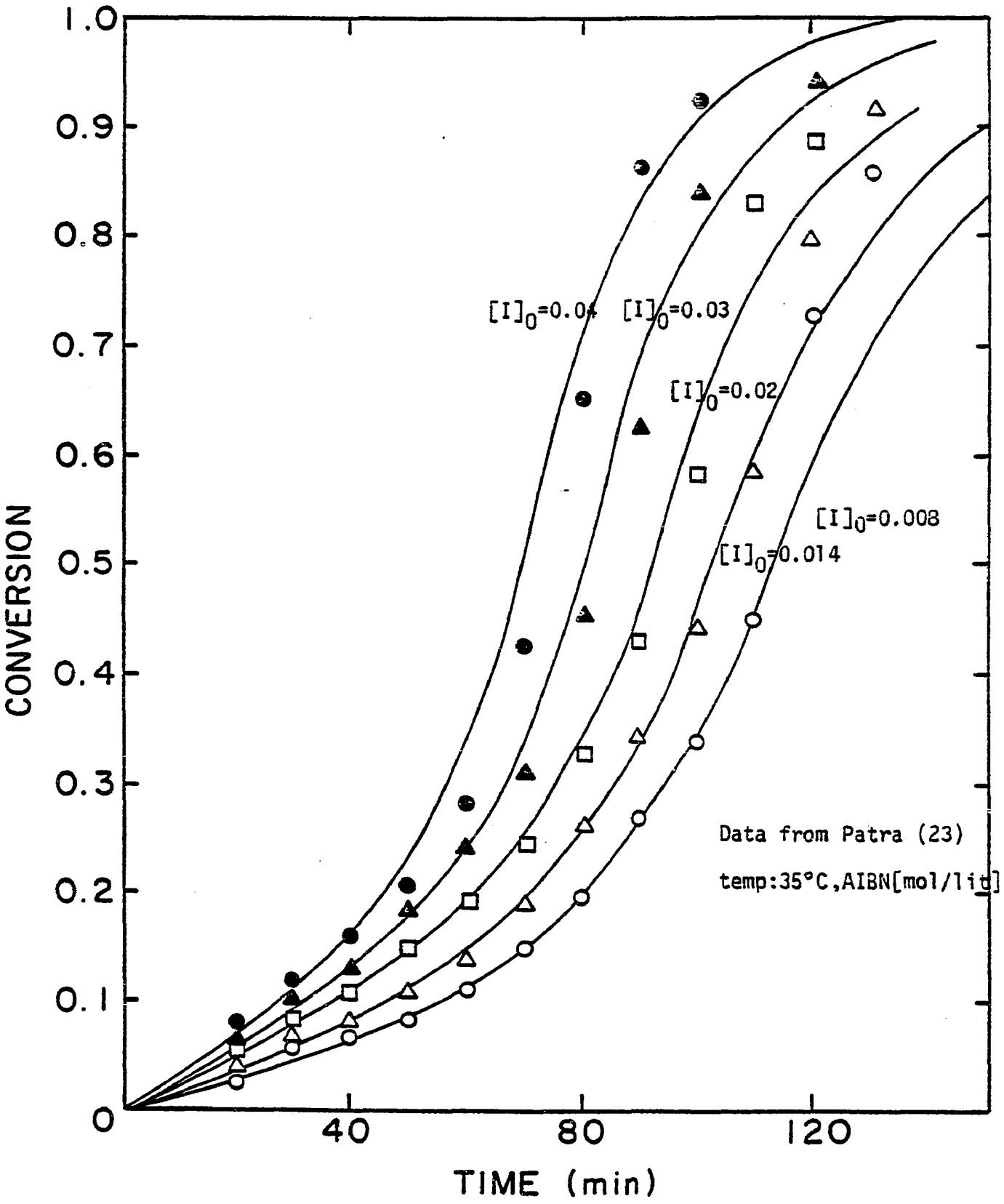

Fig. 5.9 CONVERSION-TIME PROFILES FOR EAC POLYMERIZATION

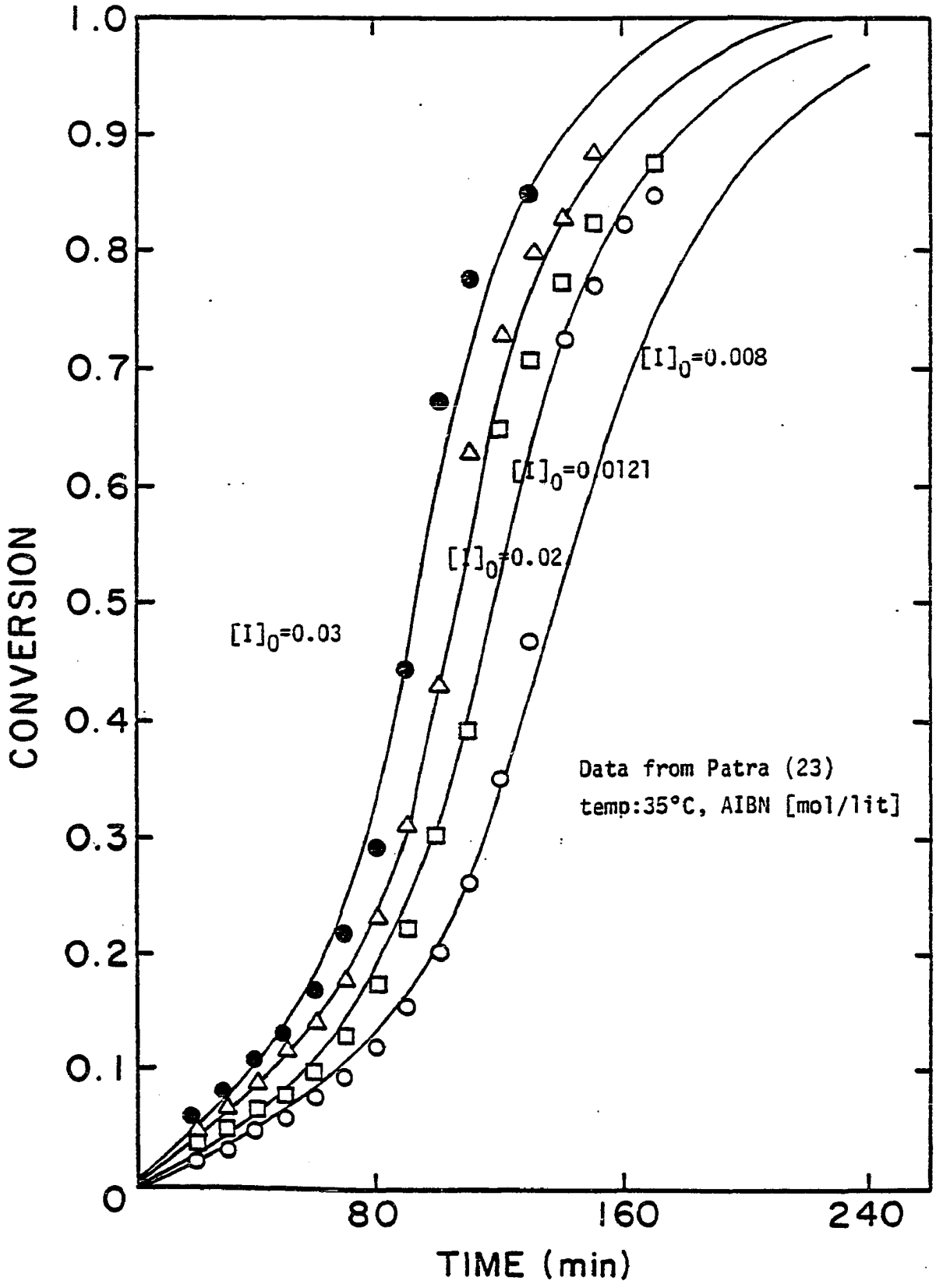

Fig. 5.10 CONVERSION-TIME PROFILES FOR PAC POLYMERIZATION

5.5 POLYMERIZATION OF VINYL ACETATE

It was suggested in the preceeding sections that for MMA the free volume effect and the entanglement coupling combine to produce a profound gel effect, while for EAC and PAC, entanglement coupling is the main driving force for their strong gel effect. VAC gel effect is also expected to be driven mainly by the entanglement factor as most polymerizations are done above its glass transition temperature.

The data of Friis (41) at 50°C was used for comparison in this case. Unfortunately this work only reports the results at a single initiator level and contains no molecular weight measurements. Consequently the values of f and k_d are left as a combined parameter which was determined from the initial rate data.

Thus the literature values are used in the calculation and fk_d value was found from the Phase I portion of the data. The remaining constants used are as follows;

Constant	Value at 50°C	Reference
k_{po}, lit/mol,sec.	3500	41
k_{to}, lit/mol,sec.	2×10^8	41
C_M	10^{-4}	38
fk_d, sec.$^{-1}$	3.01×10^{-6}	this work
x_{co}	256	14
d_m, g/cm^3	0.89	39
ε	0.247	39

The free volume calculations utilized the parameters reported in Chapter 4 with the following expressions;

$$v_{fp} = 0.0218 + 5.0 \times 10^{-4}(t-26.5),\ t \geq 26.5$$

$$= 0.0218 + 2.7 \times 10^{-4}(t-26.5),\ t < 26.5$$

$$v_{fm} = 0.154 + 5.1 \times 10^{-4}t$$

An inhibition time of 22 minutes was chosen as it appeared that Friis did not compensate for it in the plot of his data. The inhibition time was found by extrapolating the initial rate data to zero conversion as shown in Fig. 5.11. The v_{fxc} value was adjusted to coincide with the onset of the gel effect, and was found to be 0.13. As shown in Fig. 5.11, the relative mildness of the gel effect is due to the short duration of Phase II. As the polymerization system reaches the Phase III before a strong gel effect is developed, and as the decrease of $\bar{k}_t$ during the Phase III is slow at best, VAC shows a mild gel effect although the other kinetic parameters point towards a strong gel effect comparable to EAC and PAC. The success of the proposed theory lies in the fact that the theory correctly accounted for such vast differences in controlling parameters without any modification particular to each system.

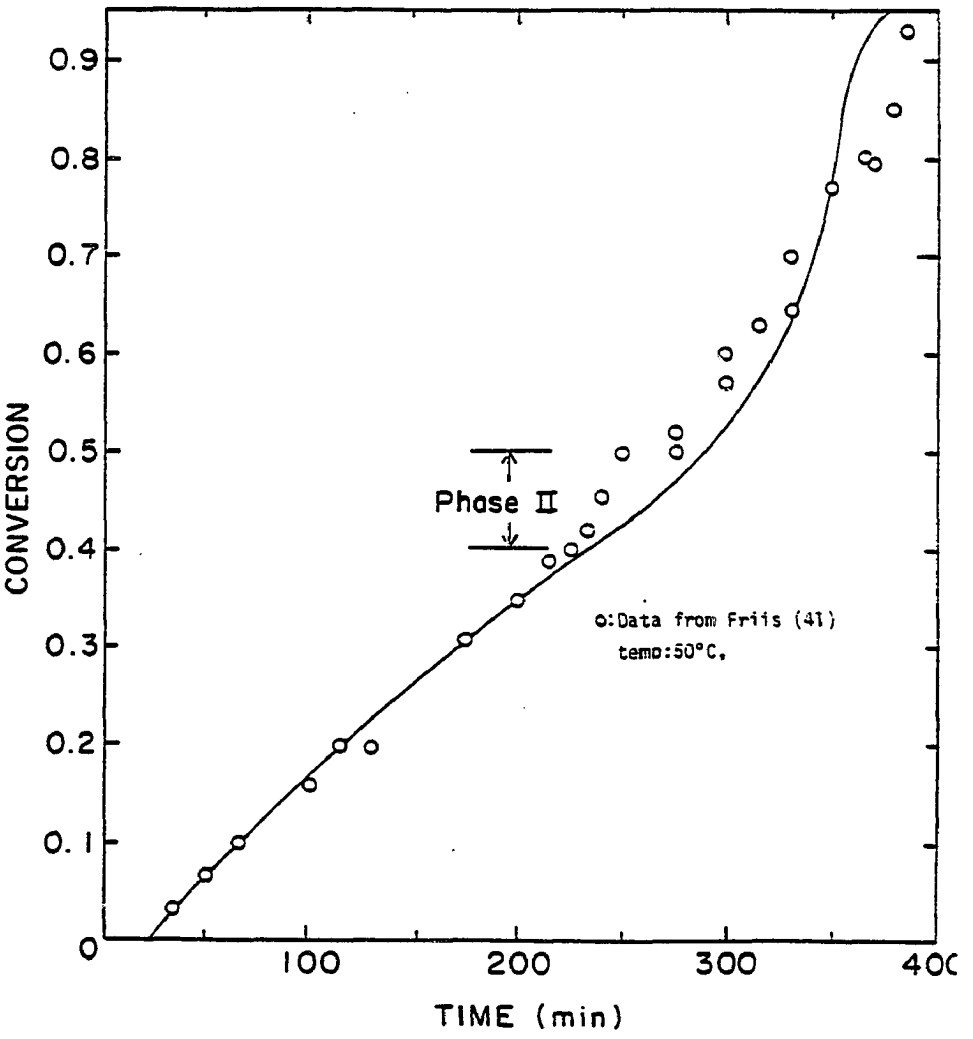

Fig. 5.11 CONVERSION-TIME PROFILES FOR VAC POLYMERIZATION

5.6 POLYMERIZATION OF ETHYL METHACRYLATE

Considering that the glass transition temperature of polyethyl methacrylate is 62°C (38), the EMA gel effect is expected to be less severe than MMA, its close homolog. O'Driscoll's data (15) at 70°C and 90°C were used with the following parameters:

$k_{po} = 1.01\ (10^7)\ \exp\ (-3253/T)$	reference (15)
$C_M = 2.71\ (10)^{-2}\ \exp\ (-2440/T)$	reference (15)
$\varepsilon = 0.18 + 0.001\ t$	reference (39)
$d_m = 1.081 - 3.36\ (10)^{-3}\ t$	reference (39)
$x_{co} = 200$	average value
$t_{tp} = 62°C$	reference (38)
$t_{gm} = -106°C$	universal value

Free volume parameters were calculated using equation 5.25 and 5.26.

The values of k_{to}, f and the adjustable parameter v_{fxc} calculated in the manner previously described are listed in Table 5.4. The reason that the last value of f in Table 5.4 is so different from the others is not known. However, since the data for $I_o = 0.0098$ did not include molecular weight measurements, its f value is not certain either. An adjustment for inhibition time was made for the data at 90°C and I_o = 0.0032 mol/lit.

The predicted rate and molecular weight values are compared to O'Driscoll's experimental data in Figures 5.12-5.15. Agreement with these data is considered to be excellent and demonstrates the general validity of the proposed model.

The most significant difference between EMA and MMA polymerizations is that the pronounced gel effect in EMA occurs at significantly higher conversions, and that the molecular weight changes follow different paths. $\bar{M}_w$ and higher molecular weight averages for MMA rapidly increase early in the reaction and level off or begin decreasing at about 50-60% conversion. Those for EMA do not level off until 80-90% conversion for nearly identical experimental conditions. These differences are due to the combined differences in the entanglement spacing, x_{co}, free volume levels at equivalent conversions, and starting points for Phase II (v_{fxc}), all leading to a delayed and less significant gel effect. Since $\bar{k}_t$ does not decrease as fast as that for MMA, the value of $W(\equiv k_{tvf}/[k_{tvf}+k_{tp}])$ remains close to 1.0 until quite high conversions and thereby prevents significant contribution from the residual termination reaction. It has been previously shown that it is the influence of k_{tp} (via W) which causes the leveling off or decreasing of molecular weight, and that point is not reached for EMA polymerizations until quite late in the reaction.

Table 5.4

Constants For Ethyl Methacrylate Polymerization

Temp (°C)	$[I]_o$ (mol/lit.)	f	$k_{to} \times 10^{-7}$ lit./mol,sec.	v_{fxc}
70	0.05	0.42	2.5	0.167
70	0.02	0.42	2.5	0.167
90	0.0098	0.44	2.2	0.167
90	0.0032	0.71	2.2	0.163

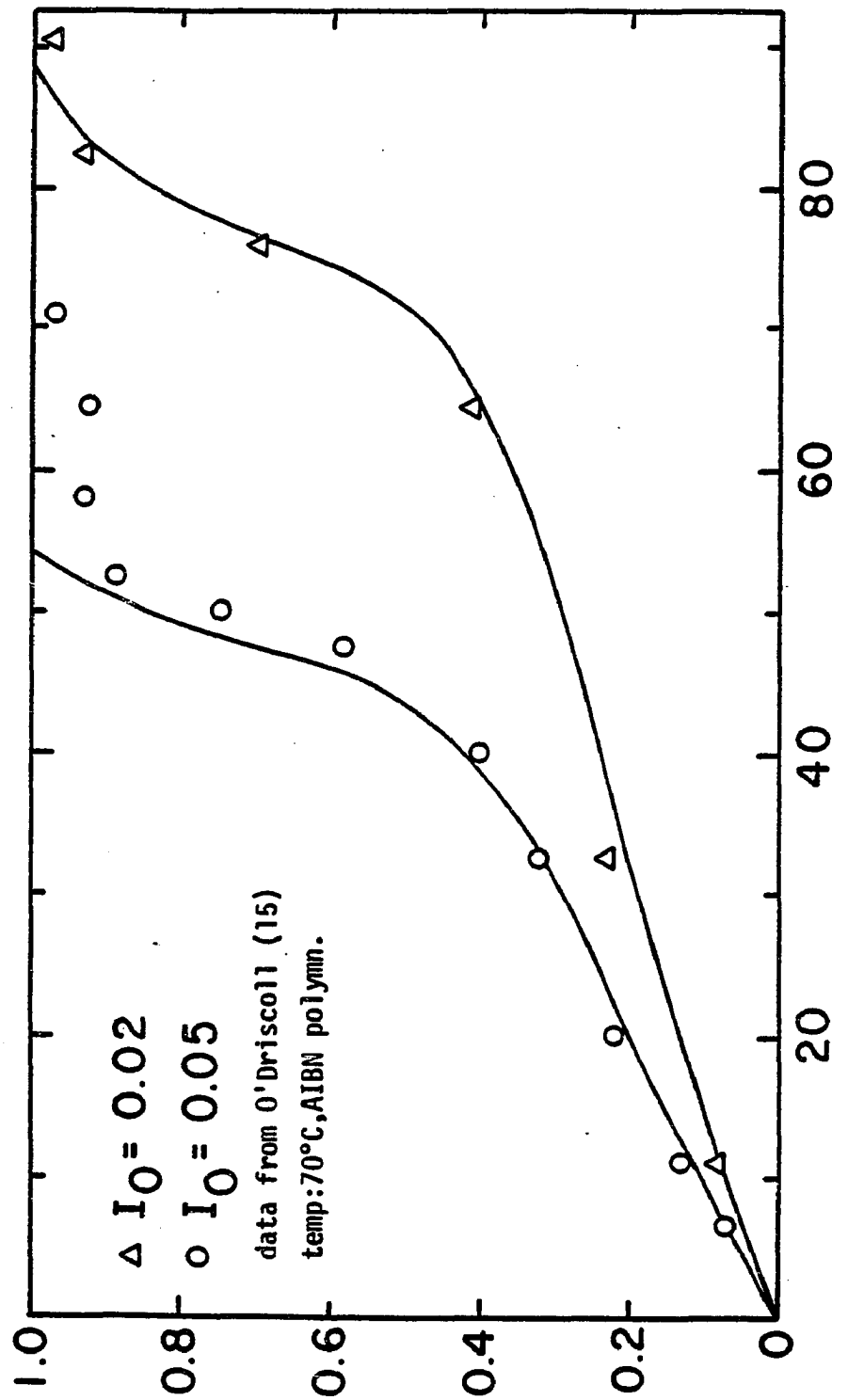

Fig. 5.12 CONVERSION-TIME PROFILES FOR EMA POLYMERIZATION

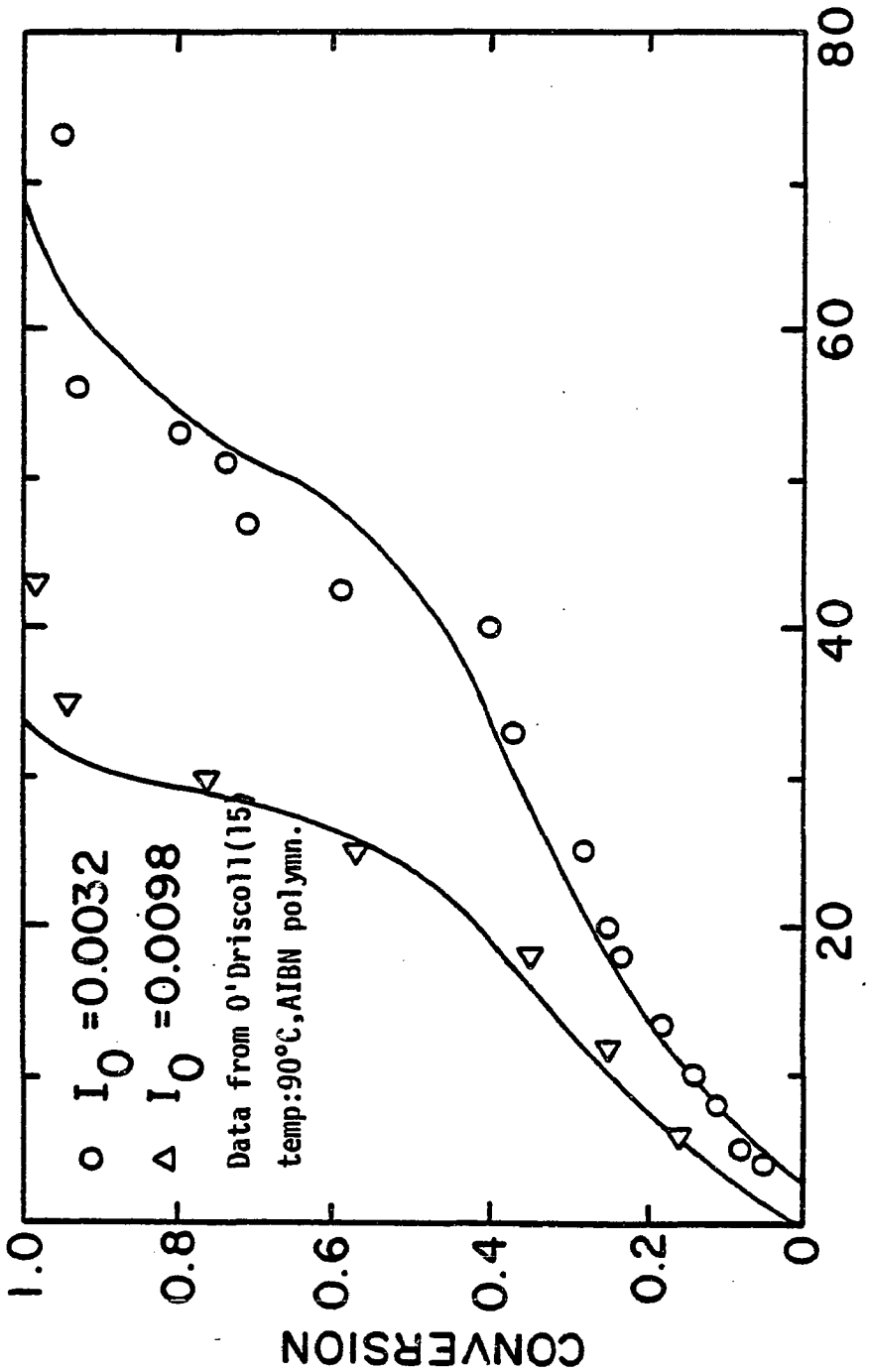

Fig. 5.13 CONVERSION-TIME PROFILES FOR EMA POLYMERIZATION

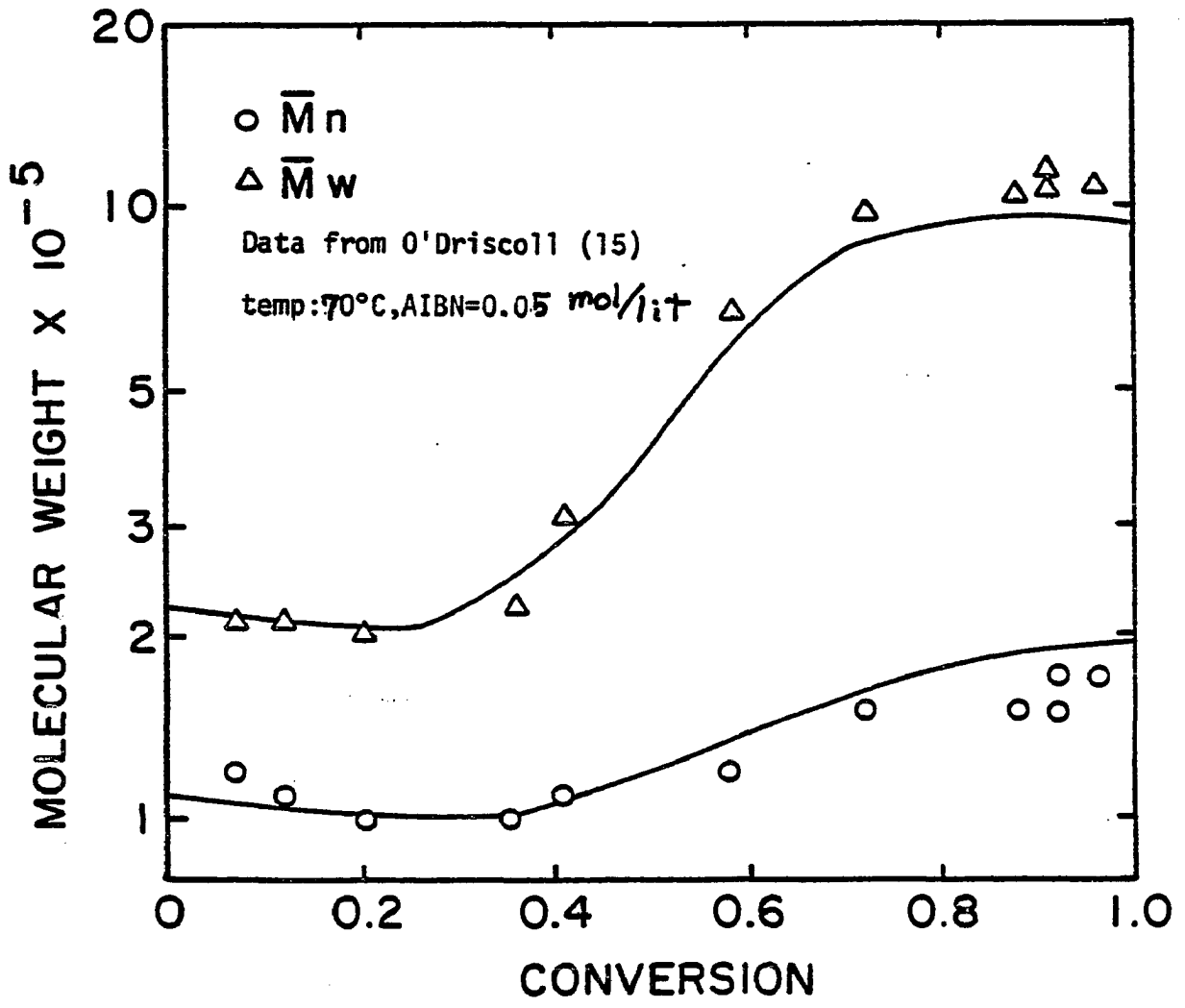

Fig. 5.14 MWD FOR EMA POLYMERIZATION

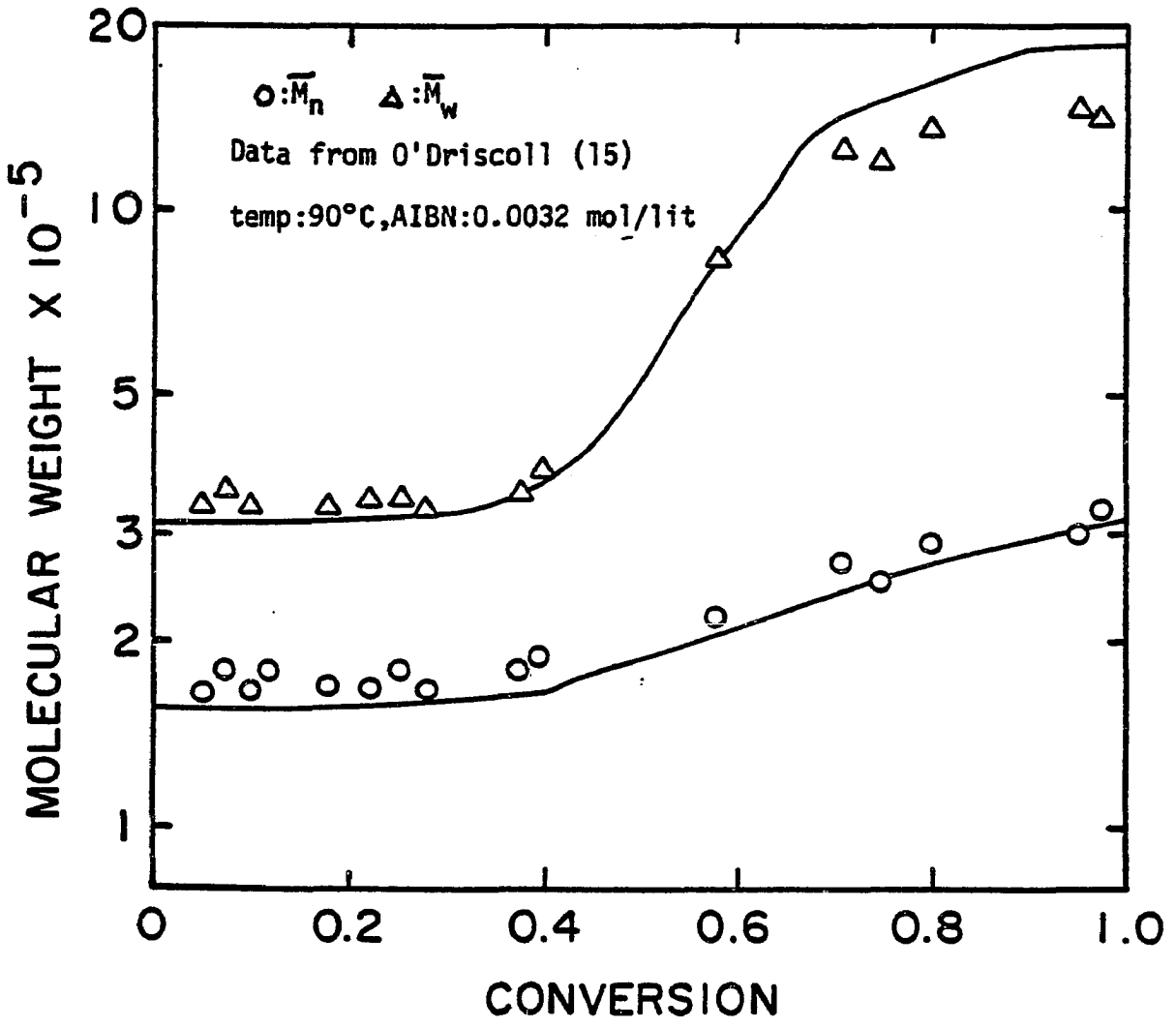

Fig. 5.15 MWD FOR EMA POLYMERIZATION

5.7 POLYMERIZATION OF STYRENE

The bulk polymerization of styrene is known to display conventional kinetics up to quite high conversions. It will be shown in the following discussion that this is due to the relatively short kinetic chain length which prevents the occurrence of entanglement of the conversion range. The mild gel effect seen below the entanglement point is due to free volume change alone, this having been named the "pseudo gel effect" earlier in this paper.

The following constants were used for the model calculations, all of them being available in the literature or determined independently earlier in the present work.

Constant	Reference
$k_{po} = 2.17 \times 10^{7} \exp(-3905/T)$	42
$C_M = 8.0 \times 10^{-5}$	38
$d_m = 0.9236 - 8.87 \times 10^{-4} t$	39
$\varepsilon = 0.137 + 4.4 \times 10^{-4} t$	39
$x_{co} = 385$	14
$v_{fp} = 0.0245 + 4.5 \times 10^{-4}(t-82)$, $t \geq 82$	
$= 0.0245 + 1.4 \times 10^{-4}(t-82)$, $t < 82$	Chap. 4
$v_{fm} = 0.112 + 6.2 \times 10^{-4} t$	Chap. 4

The other constants necessary (f, k_{to} and v_{fxc}) were determined in the manner described earlier by using data reported by a number of researchers. First, Tobolsky's rate data (43) at 90 and 100°C were analyzed with the assumption that f = 1.0. At these conditions used by Tobolsky, the reactions display "dead end polymerization" behavior due to premature

Table 5.5

Constants for Styrene Polymerization

temp °C	Initiator	$[I]_o$ [a]	k_{to} x10^{-7} [b]	f	v_{fxc}	Data source
100	AIBN	0.0337	6.16	1.0	0.142	43
100	AIBN	0.0093	6.16	1.0	0.142	43
90	AIBN	0.021	4.6	1.0	0.1261	43
80	AIBN	0.0212	4.8	1.0	0.11	43
80	BPO	0.0347	4.8	0.63	0.105	Appendix K
70	AIBN	0.0214	6.0	1.0	0.11	43
70	BPO	0.104	6.0	1.0	0.105	Appendix K
60	AIBN	0.0992	5.2	0.49	0.103	10
60	AIBN	0.0268	5.2	0.81	0.105	10
60	AIBN	0.0164	5.2	0.64	0.119	10
60	AIBN	0.00858	5.2	0.81	0.115	10
45	AIBN	0.2	3.3	0.52	0.085	11
45	AIBN	0.1	2.75	0.545	0.085	11
45	AIBN	0.05	2.75	0.545	0.093	11
45	AIBN	0.025	2.75	0.545	0.097	11
45	AIBN	0.0125	2.75	0.545	0.103	11

a mol/lit

b lit/mol,sec.

depletion of the initiator. These data and the model predictions are shown in Fig.5.16. As the reaction temperature is lowered, the gel effect becomes more appreciable. Tobolsky's data at 70 and 80°C obtained with AIBN, and some data obtained with benzoyl peroxide were also used. The dissociation rate constant for benzoyl peroxide was taken as

$$k_d = 8.5*10^{14} \exp(-15200 / T), \text{ sec}^{-1}$$

Appendix K shows the experimental procedures used.

Saito (10) reported rate and molecular weight data at 60°C and as such, both k_{to} and f values can be determined independently. Ito's data (11) at 45°C included viscosity average molecular weights. Although these are not simply related to either $\bar{M}_n$ or $\bar{M}_w$, they are usually fairly close to $\bar{M}_w$ and were assumed identical to $\bar{M}_w$ for this analysis. The resultant values for f, k_{to} and v_{fxc} are shown in Table 5.5.

To examine the acceptability of the k_{to} values shown in Table 5.5 they were plotted in an Arrhenius form as in Fig.5.17. Included in this plot are k_{to} values derived from Tobolsky's (k_{po}^2/k_{to}) values (45) by using the k_{po} relation suggested by Matheson (42). The plot shows reasonable agreement of all k_{to} values and a least squares fit to all of the data shows

$$k_{to} = 8.2 \times 10^9 \exp(-1747/T)$$

Fig 5.18 shows the agreement between the model predictions and Saito's rate data at 60°C, while Fig 5.19 makes the same comparison for the data of Tobolsky and Soh at 70 and 80°C. Note that the gel effect is very mild until the conversion reaches about 50%. This is in marked contrast to the acrylates and methacrylates and is due to the delay of

chain entanglements. Ito's rate data at 45°C show this delayed gel effect very clearly in Fig. 5.20. A close analysis of the model's response shows that better agreement could have been obtained with these data if the starting point for the "true gel effect" ($v_f = v^*_{fxc}$) is delayed slightly. If one uses Turner's criterion (Appendix 1) for obtaining the critical polymer concentration for entanglement, the onset of the "true gel effect" appears too late to explain the experimental data. Adjusting v^*_{fxc} to be mid-range between Turner's criterion and that suggested here (equation 5.17) can yield very good fits to all data used here, but that was not done.

Ito (11) presented his molecular weight data as plots in the form of $1/\bar{M}_w$ vs. conversion. He noted that these plots reached a maximum and due to the fact that he felt the data above 70% conversion were not useful for his purpose, he did not report them. The available data and the model predictions are presented in Fig. 5.22 and it is evident that there is reasonable agreement. The maximum in these curves clearly marks the points at which $\bar{M}_w$ begins to increase after decreasing during the first 50% conversion. This is due to the transition from the "pseudo gel effect" to the "true gel effect" at the point of occurence of polymer chain entanglement.

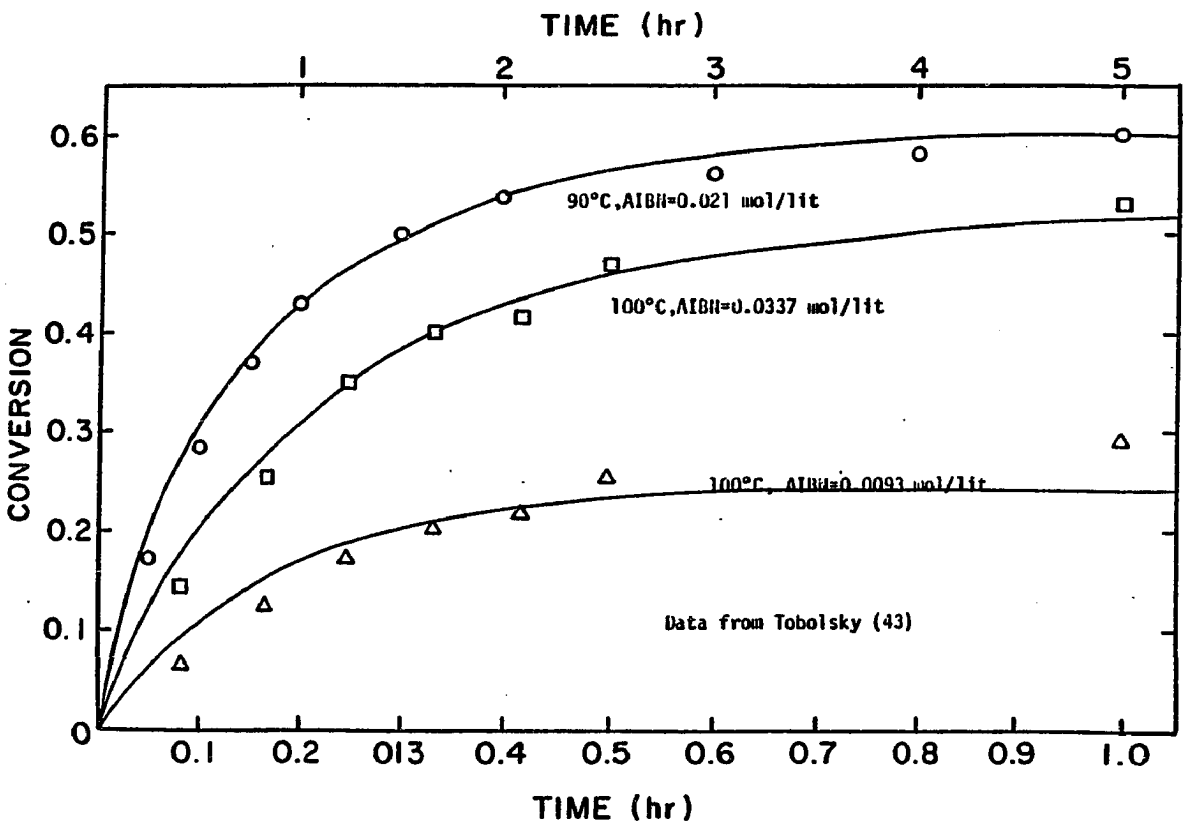

Fig. 5.16 CONVERSION-TIME PROFILES FOR STY POLYMERIZATION

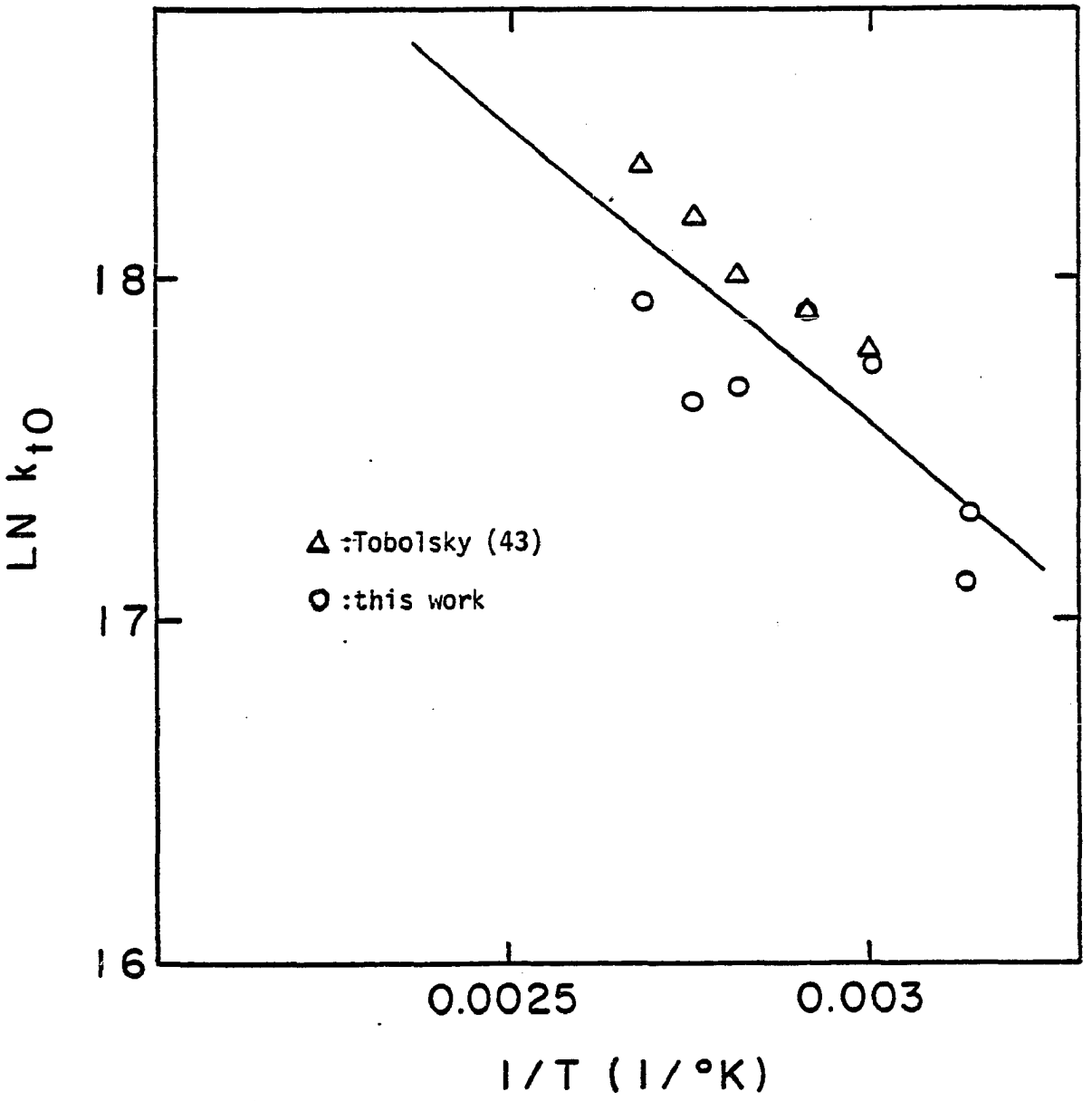

Fig. 5.17 ARRHENIUS PLOT OF k_{tO} VALUES

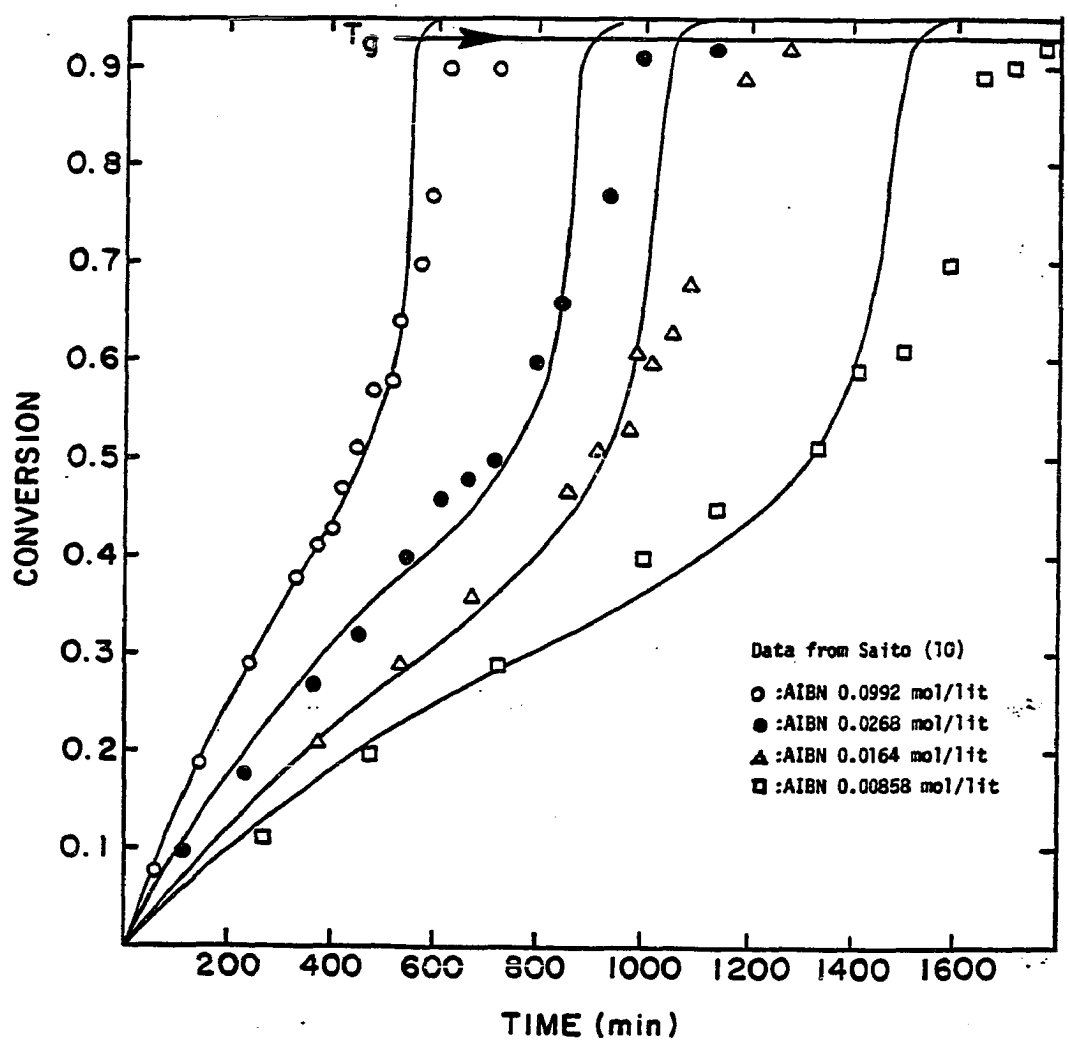

Fig. 5.18 CONVERSION-TIME PROFILES FOR STY POLYMERIZATION

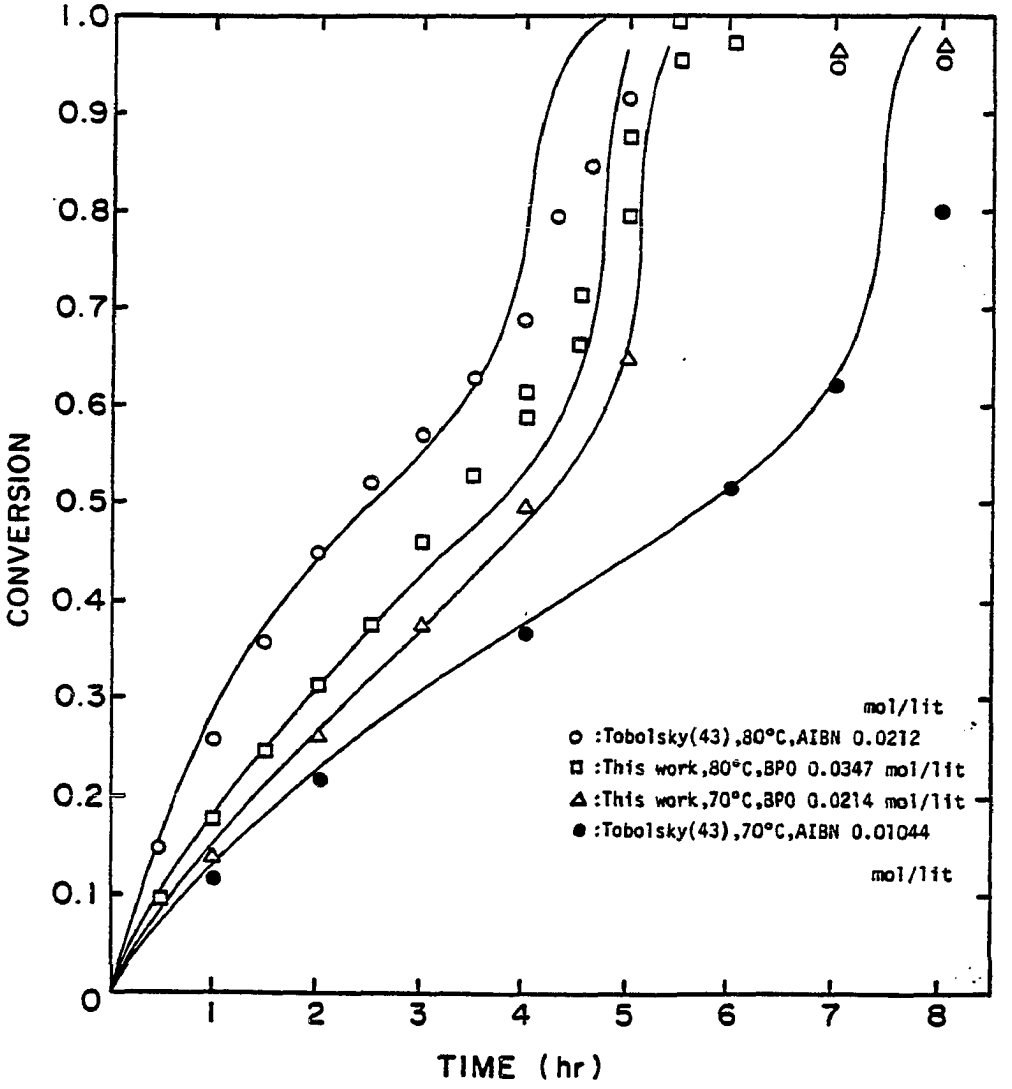

Fig. 5.19 CONVERSION-TIME PROFILES FOR STY POLYMERIZATION

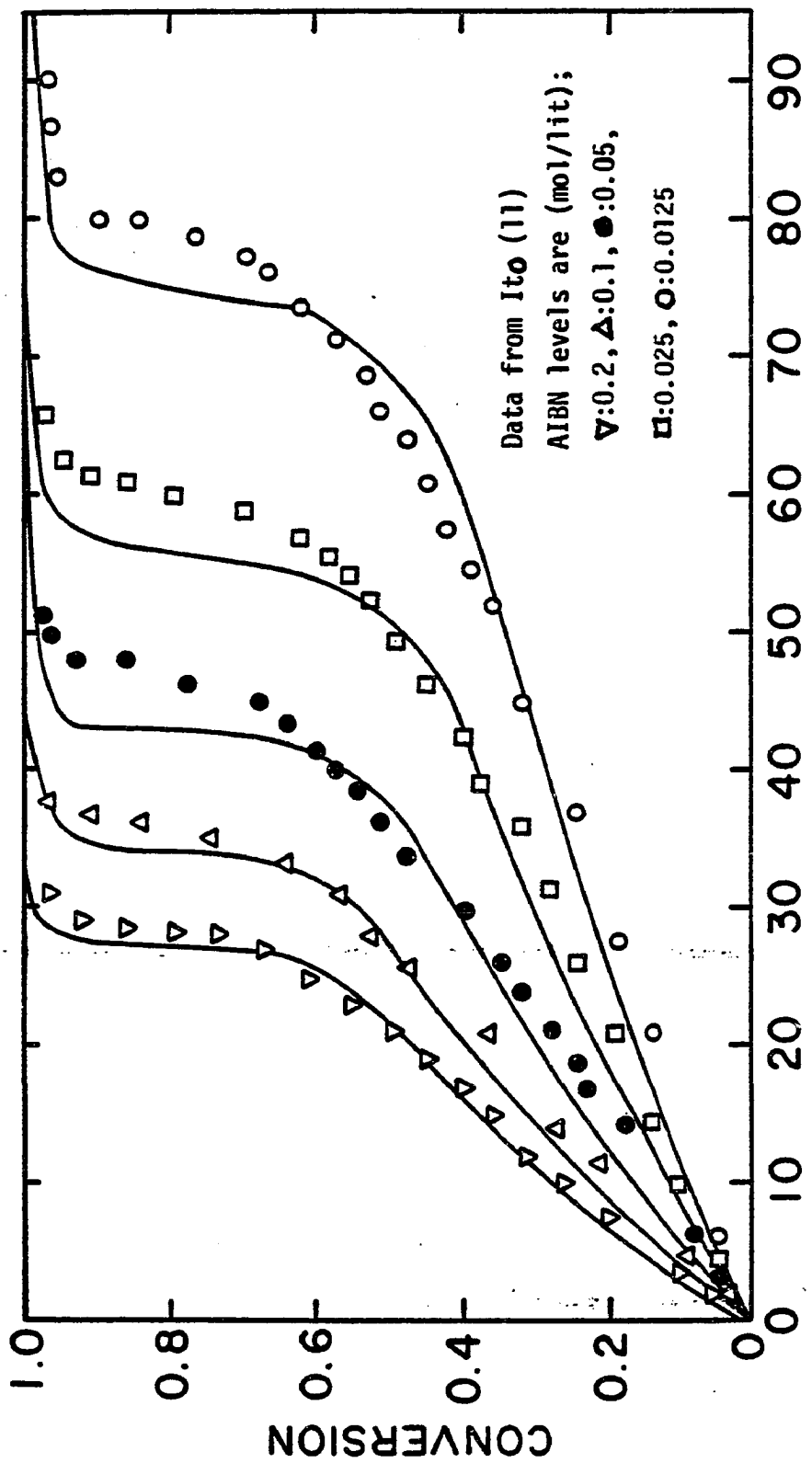

Fig. 5.20 CONVERSION-TIME PROFILES FOR STY POLYMERIZATION

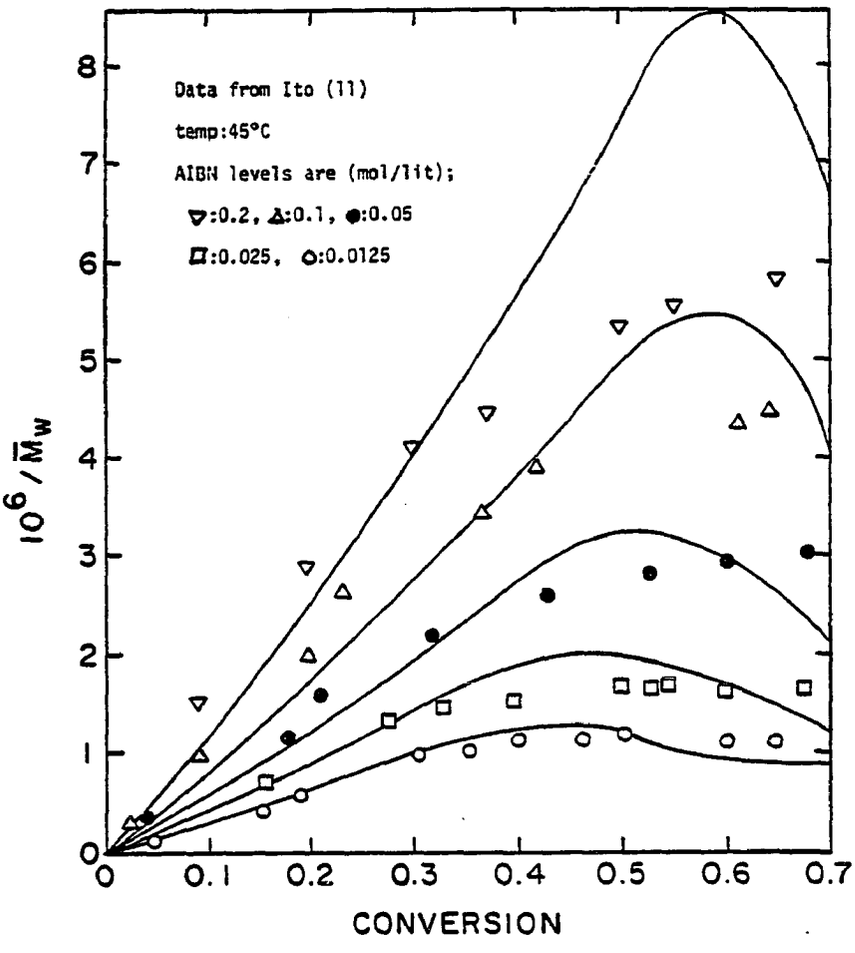

Fig. 5.21 MWD FOR STY POLYMERIZATION

5.8 CONCLUDING REMARKS

The six different polymerization systems analyzed in this Chapter have been shown to display a wide variety of non ideal behavior, all of which are related to the diffusional characteristics of the reacting species. The reaction model proposed in this work has been shown to explain this range of behavior by using only one adjustable parameter. Especially important are the model's ability to predict higher order molecular weight averages ($\overline{M}_w$, $\overline{M}_z$, etc.] and to explain the controlling primary reaction steps responsible for the different types of behavior displayed by these polymerization systems. Central to the development of this capacity is the consideration of chain length dependent and residual termination reactions. Residual termination reactions will require the most refinements due to the various assumptions involved in the derivation of their governing equations. However, the general success of the model should justify its use as a guideline for future studies.

Chapter 6

CONCLUSIONS AND RECOMMENDATIONS

6.1 CONCLUSIONS

Many of the minor conclusions which can be drawn from the theoretical derivations and the applications to the experimental data have already been discussed at the ends of Chapters 2-5. In this section the most significant conclusions which the author believes to have far-reaching implications on the modelling of polymerization kinetics are included. They are;

1) The existence of the chain length dependence of the termination has been established.

2) The existence of the residual contribution has been established.

3) It was demonstrated that a general method of dealing with the chain length dependent polymerization kinetics is possible without specifying the functional form of the chain length dependence.

4) It was demonstrated that a set of models can explain a variety of polymerization systems. This may seem trivial, but this work may be the first to show working examples.

6.2 RECOMMENDATIONS

The success of the presented method of dealing with the chain length dependent termination reaction and the proposed models based on the free volume concept and the entanglement coupling concept gives rise to the expectations of successful applications to more complex systems such as solution polymerization, copolymerization, and emulsion polymerization systems. Applications to these systems require the generalization of the present models to three component systems, but it is expected to be straightforward and may produce, if successful, very valuable criteria for the solvent selection in solution polymerization and the analysis of the copolymerization reactor performance.

In copolymerization studies, the change of copolymer composition with the overall conversion level is not expected to be influenced by the occurrence of the chain length dependent termination. However, the polymerization rate and the molecular weight development are expected to be profoundly affected by the gel effect and subsequent diffusion controlled reaction kinetics. It is difficult to speculate on the total effect as there exists surprisingly little information in the literature.

The presented theories are also expected to be applicable to emulsion polymerization, but the analysis will be complecated by the radical distribution within the latex particles and more detailed investigation is necessary to speculate about the result.

The general methodology used in this thesis is free from any particular assumptions regarding the chain length dependence of the termination reaction rate constant, and should be useful for all future works which

may employ different specific physical models. Regarding the particular models used in this work, several improvements may be made. These are;

1) conceptual developments about the segmental diffusion-translational diffusion transition period. This thesis treated it by an adjustable parameter, but also produced more fundamental questions about the nature of the transition as already discussed in Chapter 2.

2) transition from pseudo-gel effect to the true gel effect. This requires precise definition of the entanglement point in the presence of the molecular weight distribution. The predictions of the classical entanglement theory and Turner's criteria need to be examined closely, but it is the subject of polymer physics rather than polymerization kinetics.

3) residual termination. Although the model proposed here established the existence of such a mechanism which can lead to residual termination behavior, it is still far from a precise and quantitative description as pointed out already in Chapter 3, and requires major investigation. This thesis is at this point content with the establishment of such phenomenon and providing rather crude estimation method.

4) diffusion controlled propagation. This work provided for the first time an estimation method, which the author feels to be good at least within an order of magnitude. An experimental measurements are necessary and will help to explain the abnormalities of the high conversion polymerization. The main difficulty of propagation rate constant measurement at high conversion

is the necessity of holding the conversion level and the radical concentration as constant as possible to obtain reasonable data. This can be extremely difficult in mass polymerization and batch emulsion polymerization. The most promising technique is the semi-continuous emulsion polymerization where theoretically one can keep both the polymer:monomer ratio and the radical concentration constant. However, more study is necessary to realize such ideal conditions in an experimental setup.

LIST OF SYMBOLS

ALPHABETICAL

A	proportionality constant
a	average r.m.s. length per monomer unit [cm]
a_c	shift factor
B	proportionality constant
C	numerical constant
C_M, C_m	chain transfer constant to monomer
C(M)	constant determined by the molecular weight distribution w(M)
D	diffusivity
D_{AB}	mutual diffusivity between A and B
D_i	diffusivity of polymer chain of d.p. i
D_m	diffusivity of monomer
D_s	diffusivity of a chain segment
d_m	density of monomer [g/cc]
d_p	density of polymer [g/cc]
F	numerical constant
f	initiator efficiency
f_t	efficiency factor for residual termination
f_1, f_2	dimensionless ratios

F_i	moment defined in chapter 2
f(i), f(y)	chain length defendence function corresponding to chain length i or y
[I]	concentration of initiator [mol/lit]
i	chain length or integer variable
i_c	critical degree of polymerization
j	integer variable or chain length
j_c	entanglement spacing
K	numerical constant
k	Boltzmann's constant
K	constant
k_d	initiator decomposition rate constant [lit/sec]
k_p	propagation rate constant [lit/mol,sec]
k_{p0}	propagation rate constant at zero conversion [lit/mol,sec]
k_{pvf}	diffusion controlled propagation rate constant [lit/mol,sec]
k_t	termination rate constant [lit/mol,sec]
$\bar{k}_t$	apparent termination rate constant [lit/mol,sec]
k_{tc}	termination rate constant between entangled and unentangled macroradicals [lit/mol,sec]
k_{te}	termination rate constant between entangled macroradicals [lit/mol,sec]
k_{tij}	termination rate constant between macroradicals of chain length of i and j [lit/mol,sec]
k_{tp}	residual termination rate constant [lit/mol,sec]

$k_{tr,M}$ chain transfer reaction rate constant to monomer [lit/mol,sec]

$k_{tr,S}$ chain transfer reaction rate constant to chain transfer agent S [lit/mol,sec]

$(k_t)_{tr}$ translational diffusion contribution of termination rate constant [lit/mol,sec]

k_{tvf} unentangled termination rate constant [lit/mol,sec]

k^*_{tvf} k_{tvf} value @ $v_f = v^*_f$ [lit/mol,sec]

k_{t0} termination rate constant at zero conversion [lit/mol,sec]

$\bar{k}^o_t$ hypothetical value defined in Chapter 3 [lit/mol,sec]

k^o_{tvf} hypothetical value defined in Chapter 3 [lit/mol,sec]

$\bar{l}$ average intermolecular spacing, or jump distance [cm]

l^d_i, l^r_i index of molecular weight distribution of corresponding order

l_w weight index of molecular weight distribution

l_z z of molecular weight distribution

l_{z+1} z+1 of molecular weight distribution

l_{z+i} z+i of molecular weight distribution

[M] concentration of monomer [mol/lit]

M molecular weight

m numerical constant

M_c critical molecular weight for entanglement

M_0 molecular weight of monomer

M_i molecular weight of polymer chain of degree of polymerization i

M_e entanglement spacing in unit of molecular weight

M_i instantaneous average molecular weight of order i
i may be substituted by n,w,z,z+1 etc.

$\bar{M}_i$ cumulative average molecular weight of order i
i may be substituted by n,w,z,z+1, etc.

N_{Av} Avogadro's number, $6.023*10^{23}$

$N_d(i)$ numer molecular weight distribution funtion for disproportionation mode of termination. i may be substituted by y to denote continuous variable

$N_r(i)$ number molecular weight distributon function for recombinaitor mode of termination. i may be substituted by y to denote continuous variable
moment of the corresponding number molecular weight distribution function

$p(i), p(y)$ probability of propagation at the specified chain length

$P(i), P(y)$ probability distributon function for macroradical of the specified chain length

$P^o(y), P'(y)$ hypothetical function defined in Chapter 3
moment of $P(y)$

p_f probability defined by Turner (15)

$\dot{q}$ rate of heat dissipation [cal/sec]

Q_e entanglement factor

r node-to-chain end distance [cm]

r	coefficient equal to 1 for disproportionation, 2 for recombination
$[R\bullet]_i$	total free radical concentration [mol/lit]
$[R\bullet]_{local}$	concentration of i-mer radicals
$[R\bullet]_{local}$	effective concentration defined in Chapter 3
R_i	initiation rate [mol/lit/sec]
R_{hi}	hydrodynamic radius of i-mer polymer chain [cm]
$R_h(y)$	hydrodynamic radius corresponding to chain length y [cm]
$\langle \vec{R}^2 \rangle$	average mean square rode-to-end distance [cm]
$\langle \vec{r}^2 \rangle$	average root-mean-square chain distance [cm]
R_t	termination rate [mol/lit/sec]
R_p	polymerization rate [mol/lit/sec]
R_i	radius of polymerization reactor [cm]
r_i	I.D. of polymerization reactor [cm]
r_o	O.D. of polymerization rector [cm]
[S]	concentration of chain transfer agent [mol/lit]
s	slippage factor for polymer chain segmen
T	temperature [deg. K]
t	temperature [deg. C]
t	dummy integration variable
t_b	boiling point [deg. C]
t_g	glass transition point [deg. C]
t_{g_m}	glass transition point of monomer [deg. C]
t_{gp}	glass transition point of polymer [deg. C]
t_m	melting point [deg. C]
t_o	temperature @ reactor center [deg. C]

t_w	temperature @ reactor wall [deg. C]
u(i)	unit step function
V	volume of the system [cm^3]
v_f	fractional free volume
v_f^*	critical fractional free volume
v_{fg}	fractional free volume @ glass transition point
v_{fm}	fractional free volume of monomer
v_{fp}	fractional free volume of polymer
v_{fs}	fractional free volume @ t_s deg. C
v_{fxc}	fractional free volume at the onset of gel effect
v_{fxc}^*	fractional free volume at the entanglement point
$\hat{v}_0$	occupied volume [cm^3/mol]
$\hat{v}_p(0)$	occupied volume of polymer @ 0 deg. K [cm^3/mer-mol]
W	dimensionless parameter defined in Chapter 3
w(M)	weight molecular weight distribution function
w(r)	chain end distance distribution function
x, X	fractional conversion
Xi, Xj	mole fraction of the corresponding length macroradicals
x_n^d, x_n^r	the corresponding number average degree of polymerization
x_{c0}	critical degree of polymerization for the entanglement of pure polymer
x_c	critical degree of polymerization for entanglement
Xc	conversion at the onset of entanglement
y	reduced chain length

$y_{n'}^{d}$, y_{n}^{r}	the corresponding number average degree of polymerization in continuous chain length variable
Z	entanglement factor for termination
Z^{o}, Z'	hypothetical Z value of phase III
z	coordination number

GREEK LETTERS

α_m	thermal expansion coefficient of free volume for monomer
α_p	thermal expansion coefficient of free volume for polymer
α_0	fractional free volume of monomer @ 0 deg. C
β, γ	dimensionless parameter defined in Chapter 2
β', γ'	dimensionless parameter defined in chapter 3
γ	overlap factor defined in Chapter 4
ϵ	volume shrinkage factor, equal to $dp/dm - 1$
ζ_i	friction coefficient of i-mer chain
ζ_m	friction coefficient of monomer
ζ_s	friction coefficient of polymer chain segment
η	viscosity of solution [cp]

η_0	viscosity of monomer [cp]
θ	time of reaction [sec]
λ	numerical constants
μ_j	j-th moment of w(M)
ν	kinetic chain length
ξ	size ratio of polymer segment and penetrant
ρ_c	density of the polymerization medium @ x=x_e
ρ	parameter of chain end distribution defined in Chapter 3
σ	collision radius for termination [cm]
ϕ	jump frequency [1/sec]
ϕ_m	volume fraction of monomer
ϕ_p	volume fraction of polymer

SUBSCRIPTS

A	compound A
B	compound B
c	critical degree of polymerization
d	initiator decomposition, or disproportionation
d	penetrant

e	entanglement
f	free volume
g	glass transition
h	hydrodynamic
i	degree of polymerization, initiation, or integer
j	degree of polymerization, or integer
k	degree of polymerization, or integer
M,m	monomer
n	number average, or integer
p	propagation
r	recombination
S	chain transfer agent
s	reference temperature near t deg. C
s	polymer segment
vf	unentangled state
w	weight average
z	z-average
z+1	z+1-average
[ ]	concentration @ X=0
0	value @ X=0

SUPERSCRIPTS

d	disproportionation
m	mode of termination, d or r
r	recombination
*	a constant
0	phase III
'	value of hypothetical system defined in Chapter 3

LIST OF REFERENCES

1. John H. Seinfeld and L. Lapidus, Mathematical Methods in Chemical Engineering, Vol. 3, Process Modelling, Estimation, and Identification, Prentice Hall, Inc., 1974.

2. M. J. R. Cantow ed., Polymer Fractionation, Academic Press, 1967.

3. S. T. Balke and A. E. Hamielec, J. of Appl. Pol. Sci., 17, 905 (1973).

4. A. M. North, "The Kinetics of Free Radical Polymerization", Vol. 1 of Topic 17, The International Encyclopedia of Physical Chemistry and Chemical Physics, Pergamon Press (1966).

5. L. H. Peebles, Jr., "Molecular Weight Distribution in Polymers", page 7, Vol. 18 of Polymer Reviews, Interscience Publishers (1971).

6. N. Friis and A. E. Hamielec, "Emulsion Polymerization", ACS Symp. Ser., No. 24, 82 (1976).

7. S. W. Benson and A. M North, J. Am. Chem. Soc., 81, 1339 (1959), ibid., 84, 935 (1962).

8. A. M. North and G. A. Reed, Trans. Faraday Soc., 57, 859 (1961), J. Polymer Sci., A1, 1311 (1963).

9. F. C. Goodrich, "The Numerical Analysis and Kinetic Interpretation of Molecular Weight Distribution Data", in M. J. R. Cantow ed., Polymer Fractionation, Academic Press (1967).

10. K. Arai and S. Saito, J. of Chem. Eng. of Japan, 9, 302 (1976).

11. K. Ito, J. of Pol. Sci., A1, 7, 3387 (1969), ibid, 8, 1313 (1970), ibid, 10, 1481 (1972), ibid., Polymer Chem. Ed., 13, 401 (1975).

12. R. T. Ross, Jr. and R. L. Lawrence, AIChE Symp. Ser., 72,No. 160, 74 (1976).

13. F. L. Marten and A. E. Hamielec, ACS Symp. Ser., 104, 43 (1978).

14. J. D. Ferry, Viscoelatic Properties of Polymers, John Wiley Sons, Inc.(1970).

15. J.N. Cardenas and K.F. O'Driscoll, J. Pol. Sci., Polymer Chem. Ed., 14, 883 (1976), ibid., 15, 1883, 2097 (1977).

16. K. Ito, J. Pol. Sci., Polymer Chem. Ed., 12, 1991 (1974), ibid., 13, 401 (1975), ibid., 15, 1759 (1977), ibid., 18, 701 (1980).

17. E. Morawetz, Macromolecules in Solution, page 273, Interscience Publishers (1965).

18. E. Fujita and A. Kishimoto, J. of Chem. Phys., 34, 393 (1961).

19. J.S. Vrentas and J.L. Duda, Macromolecules, 9, 785 (1976), J. Pol. Sci., Polymer Phys. Ed., 15, 403, 417, 441 (1977), J. Appl. Pol. Sci., 21, 1715 (1977), ibid., 22, 2325, ibid., 25, 1793, 1297 (1980).

20. F. Bueche, Physical Properties of Polymers, Interscience Publishers (1962).

21. P.E.M. Allen and C.R. Patrick, Kinetics and Mechanisms of Polymerization Reactions, Chapter 2, John Wiley Sons, Inc. (1974).

22. N.M. Atherton, H. Melville and D.H. Whiffen, J. Pol. Sci., 34, 199 (1959).

23. D. Mangaraj and S.K. Patra, Makromol. Chem., 104, 125 (1967).

24. J.L. Gardon, J. Pol. Sci., A1, 6, 2851 (1968).

25. P.J. Flory, Statistical Mechanics of Chain Molecules, Interscience Publishers, 1969.

26. P. Hayden and H.W. Melville, J. Pol. Sci., 43, 201 (1960) and W.I. Benbough and H.W. Melville, Pro. Roy. Soc. of London, 230, 429 (1955).

27. S.K. Soh, J. Appl. Sci., 25, 2993 (1980).

28. D.C. Sundberg, S.K. Soh, J.Y. Hsieh and R.F. Baldus, ORPL Preprints, 43, 520 (1980).

29. H. Fujita and A. Kishimoto, J. Chem. Phys., 34, 393 (1961), A. Kishimoto, J. Pol. Sci., A2, 1421 (1964), H. Fujita, A. Kishimoto and K. Matsumoto, Trans. Faraday Soc., 56, 424 (1960).

30. A. Bondi, J. Pol. Sci., A2, 3159 (1964).

31. R.N. Howard, J. Macromol. Sci., Reviews Macromol. Chem., C4(2), 191 (1970).

32. A.J. Barlow, J. Lamb and A.J. Matheson, Proc. Roy. Soc. of London, A-292, 322 (1966).

33. R.F. Fedors, J. Pol. Sci., Polymer Letters Ed., 17, 719 (1979).

34. N. Friis and A.F. Hamielec, J. Pol. Sci., Polymer Chem. Ed., 12, 251 (1974).

35. D.C. Sundberg and D.R. James, J. Pol. Sci., Polymer Chem. Ed., 16, 523 (1978).

36. F.T. Wall, J. Am. Chem. Soc., 67, 1929 (1945).

37. D.T. Turner, Macromolecules, 10, 221, 226, 231 (1977).

38. J. Brandrup and E.M. Immergut Eds., Polymer Handbook, 2nd Ed., Interscience Publishers (1975).

39. M.F. Mark et al., eds., Encyclopedia of Polymer Science and Technology, Interscience Publishers, 1964.

40. S.T. Balke, Ph.D. Thesis, McMaster University, 1972.

41. N. Friis and I. Nyhagen, J. Appl. Pol. Sci., 17, 2377 (1973).

42. M.S. Matheson et al., J. Am. Chem. Soc., 71, 497 (1949).

43. A.V. Tobolsky, C.F. Rogers and R.D. Brickman, J. Am. Chem. Soc., 82, 1277 (1960).

44. N. Ototake, F. Ueno, H. Tarada and Y. Uragnich, J. Chem. Eng. of Japan, 1, 67 (1968).

45. J. Offenbach and A.V. Tobolsky, J. Pol. Sci., 16, 322 (1955).

46. J.M. Dionisio and K.F. O'Driscoll, J. Pol. Sci., Polymer Chem. Ed., 18, 3199 (1980).

47. J.P. Holman, Heat Transfer, 4th Ed., International Student Ed., 1976.

APPENDIX A

INSTANTANEOUS AND CUMULATIVE MOLECULAR WEIGHT AVERAGES

The definition of $\bar{M}_{z+i}$ (i = 0,1,2, etc) can be written as

$$\bar{M}_{z+i}\Big|_X = \frac{\int_0^\infty M^{i+2}\, w(M)\Big|_X\, dM}{\int_0^\infty M^{i+1}\, w(M)\Big|_X\, dM} \qquad \text{(A-1)}$$

where M is the molecular weight as an integration variable and w(M) is a weighting function at a fractional conversion X. Similarly at a conversion of $X + \Delta X$,

$$\bar{M}_{z+i}\Big|_{X+\Delta X} = \frac{\int_0^\infty M^{i+2}\, w(M)\Big|_{X+\Delta X}\, dM}{\int_0^\infty M^{i+1}\, w(M)\Big|_{X+\Delta X}\, dM} \qquad \text{(A-2)}$$

Let us assume w (M) is normalized in such a way as to satisfy

$$\int_0^\infty w(M)\Big|_X\, dM = X \qquad \text{(A-3)}$$

The instantaneous value $M_{z+i}\Big|_X$ is defined as

$$M_{z+i}\Big|_X = \frac{\int_0^\infty M^{i+2}\, \Delta w(M)\, dM}{\int_0^\infty M^{i+1}\, \Delta w(M)\, dM} \qquad \text{(A-4)}$$

where $\Delta w(M) = w(M)\Big|_{X+\Delta X} - w(M)\Big|_X$ (A-5)

Substracting equation (A-1) from equation (A-2) gives an expression for $\Delta\bar{M}_{z+i}$ $(\equiv \bar{M}_{z+i}\Big|_{X+\Delta X} - \bar{M}_{z+i}\Big|_X)$

$$\Delta\bar{M}_{z+i} = \frac{\mu_{i+2} + \mu'_{i+2}}{\mu_{i+1} + \mu'_{i+1}} - \frac{\mu_{i+2}}{\mu_{i+1}} \tag{A-6}$$

$$= \frac{\mu'_{i+2}\mu_{i+1} - \mu_{i+2}\mu'_{i+1}}{\mu_{i+1}(\mu_{i+1} + \mu'_{i+1})}$$

where $$\mu_j = \int_0^\infty M^j w(M)\Big|_X \, dM \tag{A-7}$$

and $$\mu'_j = \int_0^\infty M^j \Delta w(M) \, dM \tag{A-8}$$

The difference between the instantaneous and averaged z+i molecular weights is

$$M_{z+i}\Big|_X - \bar{M}_{z+i}\Big|_X = \frac{\mu'_{i+2}}{\mu'_{i+1}} - \frac{\mu_{i+2}}{\mu_{i+1}}$$

$$= \frac{\mu'_{i+2}\mu_{i+1} - \mu_{i+2}\mu'_{i+1}}{\mu_{i+1}\mu'_{i+1}} \tag{A-9}$$

Substituting equation (A-9) into (A-6) gives

$$\Delta\bar{M}_{z+i} = \left(M_{z+i}\Big|_X - \bar{M}_{z+i}\Big|_X\right) \frac{\mu'_{i+1}}{\mu_{i+1} + \mu'_{i+1}} \tag{A-10}$$

As a mathematical identity, μ'_{i+1} can be written as

$$\mu'_{i+1} = \left[\int_0^\infty w(M)dM\right]\left[\frac{\int_0^\infty M\Delta w(M)dM}{\int_0^\infty \Delta w(M)dM}\right] \cdots\cdots \left[\frac{\int_0^\infty M^{i+1}\Delta w(M)dM}{\int_0^\infty M^i \Delta w(M)dM}\right] \tag{A-11}$$

From equation (A-3) the first term on the right hand side is simply ΔX, while the second term is M_w, the third M_z, etc. Thus

$$\mu'_{i+1} = \Delta X\{(M_w)(M_z)(M_{z+1}).....(M_i)\} \tag{A-12}$$

Likewise,

$$\mu_{i+1} = \left[\int_0^\infty w(M)dM\right]\left[\frac{\int_0^\infty Mw(M)dM}{\int_0^\infty w(M)dM}\right] \cdots\cdots \left[\frac{\int_0^\infty M^{i+1}w(M)dM}{\int_0^\infty M^{i}w(M)dM}\right]$$

$$= X\{(\bar{M}_w)(\bar{M}_z)(\bar{M}_{z+1}) \cdots\cdots (\bar{M}_i)\} \qquad \text{(A-13)}$$

When (A-12) and (A-13) are substituted into equation (A-10),

$$\Delta\bar{M}_{z+i} = (\Delta X/X)(M_{z+1}\big|_X - \bar{M}_{z+1}\big|_X)\left\{\frac{\prod_{k=w}^{i} M_k}{(\prod_{k=w}^{i}\bar{M}_k) + \frac{\Delta X}{X}\prod_{k=w}^{i} M_k}\right\}$$

Rearranging and taking the limit as ΔX goes to zero yields the following differential;

$$X\, d\bar{M}_j/dX = (M_j - \bar{M}_j)\left(\prod_{k=w}^{j-1}\frac{M_k}{\bar{M}_k}\right) \qquad \text{(A-14)}$$

for j = z, z+1, or higher.

APPENDIX B

DERIVATION OF MOMENT RELATIONSHIPS

B.1 EVALUATION OF ZEROTH MOMENTS

To derive the recurrence relationships, it is necessary to evaluate the zeroth moments as follows;

From the definition of eq'n 2.31, which can be written for i=0 and m=d,

$$N_0^d = \int_0^\infty N_d(y)dy \tag{B.1}$$

The expression for $N_d(y)$, eq'n 2.29 is substituted to eq'n B.1

$$x_c N_0^d = \int_0^\infty [\beta+\gamma(Z+f(y))/2/\sqrt{Z}]P(y)dy \tag{B.2}$$

$$P'(y)=-[\beta+\gamma\{Z+f(y)\}/2/\sqrt{Z}] \tag{B.3}$$

Eq'n B.2 can be integrated by parts with the aid of eq'n B.3.

$$x_c N_0^d = \int_0^\infty P'(y)P(y)dy$$

$$= -P(y)_0^\infty$$

$$=1 \tag{B.4}$$

Another expression for N_0^d can be obtained from eq'n B.2 as

$$x_c N_0^d = \int_0^\infty N_d(y)dy$$

$$= \int_0^\infty [\beta+\gamma\{Z+f(y)\}/2\sqrt{Z}]P(y)dy$$

$$= \int_0^\infty (\beta+\gamma\sqrt{Z}/2)\,P(y)dy+\int_0^\infty \gamma/2/\sqrt{Z}f(y)P(y)dy \tag{B.5}$$

Considering the definition of Z given by eq'n 3.18,

$$\int_0^\infty \frac{\gamma}{\gamma/2/\sqrt{Z}} f(y)P(y)dy = \gamma\sqrt{Z}/2 \int_0^\infty P(y)dy \qquad (B.6)$$

Substituting eq'n B.6 into eq'n B.5 yields

$$x_c N_0^d = (\beta+\gamma\sqrt{Z}/2) \int_0^\infty P(y)dy + \gamma\sqrt{Z}/2 \int_0^\infty P(y)dy$$

$$= (\beta+\gamma\sqrt{Z}) \int_0^\infty P(y)dy \qquad (B.7)$$

Combining eq'n B.4 and B.7,

$$P_0 = \int_0^\infty P(y)dy = 1/(\beta + \gamma\sqrt{Z}) \qquad (B.8)$$

Substituting eq'n B.8 into eq'n 2.18 gives the expression for F_0 .

$$F_0 = \int_0^\infty f(y)P(y)dy \; / \int_0^\infty P(y)dy \; * \int_0^\infty P(y)dy$$

$$= Z/(\beta+\gamma\sqrt{Z}) \qquad (B.9)$$

An expression for N_0^d is obtained directly from eq'n B.4.

$$N_0^d = 1 / x_c \qquad (B.10)$$

An expression for N_0^r is obtained as follows;

From eq'n 2.30,

$$x_c N_0^r = \int_0^\infty [\beta P(y) + \frac{(\beta+\gamma\sqrt{Z})}{\sqrt{Z}} \int_0^{y/2} (f(t)+f(y-t))/2*P(t)P(y-t)dt]dy \qquad (B.11)$$

$$= \beta \int_0^\infty P(y)dy + \frac{(\beta+\gamma\sqrt{Z})}{\sqrt{Z}} \int_0^\infty \int_0^{y/2} (f(t)+f(y-t))/2*P(t)P(y-t)dtdy \qquad (B.11)$$

The first term in eq'n B.11 bas already been evaluated and only the second term needs be evaluated to obtain an expression for N_0^r.

The first integration can be done as follows;

$$\int_0^y \frac{f(t)+f(y-t)}{2} P(t)P(y-t)dt$$

$$= \frac{1}{2}\int_0^{y/2} f(t)P(t)P(y-t)dt + \frac{1}{2}\int_0^{y/2} f(y-t)P(t)P(y-t)dt \qquad (B.12)$$

The second integration in eq'n B.12 can be transformed by changing the dummy variable t to y-t.

$$\int_0^{y/2} f(y-t)P(t)P(y-t)dt = -\int_0^{y/2} f(t)P(y-t)P(t)dt$$

$$= \int_{y/2}^{y} f(t)P(t)P(y-t)dt \qquad (B.13)$$

Substitution of eq'n B.13 into eq'n B.12 gives,

$$\int_0^{y/2} \frac{f(t)+f(y-t)}{2} P(t)P(y-t)dt = \frac{1}{2}\int_0^{y} f(t)P(t)P(y-t)dt \qquad (B.14)$$

Eq'n B.14 can be evaluated by using the Laplace transform with the aid of the convolution theorem (1).

$$L\left[\int_0^y f(t)P(t)P(y-t)dt\right] = L[f(t)P(t)]\ L[P(t)] \qquad (B.15)$$

Substitution of eq'n B.14 into the second term of eq'n B.11 gives the integral,

$$\int_0^{\infty}\int_0^{y} f(t)P(t)P(y-t)dtdy \qquad (B.16)$$

Using the relationship B.15, eq'n B.16 becomes

$$\int_0^{\infty}\int_0^{y} f(t)P(t)P(y-t)dtdy = L[f(t)P(t)]_{@s=0}\ L[P(t)]_{@s=0} \qquad (B.17)$$

As $$L[f(t)P(t)]_{@s=0} = \int_0^{\infty} f(t)P(t)dt = Z\int_0^{\infty} P(t)dt = Z/(\beta+\gamma\sqrt{Z}) \qquad (B.18)$$

And $$L[P(t)]_{@s=0} = \int_0^\infty P(t)dt = 1/(\beta+\gamma\sqrt{Z}) \qquad (B.19)$$

Substituting eq'n B.18 and B.19 into eq'n B.16 gives

$$\int_0^\infty \int_0^y f(t)P(y-t)P(t)dtdy = \frac{Z}{\beta+\gamma\sqrt{Z}} \frac{1}{\beta+\gamma\sqrt{Z}} = \frac{Z}{(\beta+\gamma\sqrt{Z})^2} \qquad (B.20)$$

Substituting eq'n B.20 into eq'n B.11 gives the desired expression.

$$\begin{aligned} x_c N_0^r &= \beta \int_0^\infty P(y)dy + \frac{-(\beta+\gamma\sqrt{Z})}{2\sqrt{Z}} \cdot \frac{Z}{(\beta+\gamma\sqrt{Z})^2} \\ &= \frac{\beta}{\beta+\gamma\sqrt{Z}} \cdot + \frac{Z/2}{\beta+\gamma\sqrt{Z}} \\ &= \frac{\beta+\gamma\sqrt{Z}/2}{\beta+\gamma\sqrt{Z}} \end{aligned} \qquad (B.21)$$

B.2 EVALUATION OF MOMENT F_i

Substituting eq'n 2.26 into eq'n 2.33 gives

$$\begin{aligned} F_i &= \int_0^\infty y^i f(y)P(y)dy \\ &= \int_0^\infty y^i f(y)\exp[-(\beta+\gamma\sqrt{Z}/2)y]\exp[-\frac{\gamma}{2\sqrt{Z}}\int_0^y f(y)dy]\,dy \end{aligned} \qquad (B.22)$$

Using the relationship

$$f(y)\exp[-\frac{\gamma}{2\sqrt{Z}}\int_0^y f(y)dy] = \frac{d}{dy}[-\frac{2\sqrt{Z}}{\gamma}\exp(-\frac{\gamma}{2\sqrt{Z}}\int_0^y f(y)dy] \qquad (B.23)$$

$$F_i = \int_0^\infty y^i \exp[-(\beta+\frac{\gamma\sqrt{Z}}{2})y]\frac{d}{dy}[-\frac{2\sqrt{Z}}{\gamma}\exp(-\frac{\gamma}{2\sqrt{Z}}\int_0^y f(y)dy]\,dy \qquad (B.24)$$

Integrating eq'n B.24 by parts,

$$F_i = y^i\exp[-(\beta+\gamma\sqrt{Z}/2)y]\Big|_0^\infty + \frac{2\sqrt{Z}}{\gamma}\int_0^\infty [y^i\exp[-(\beta+\frac{\gamma\sqrt{Z}}{2})y]'*$$

$$\exp[-\frac{\gamma}{2\sqrt{Z}}\int_0^y f(y)dy]dy \qquad \text{(B.25)}$$

As the first term of eq'n B.25 disappears, F_i is equal to the second term of eq'n B.25, and can be further simplified as follows;

$$F_i = \frac{2\sqrt{Z}}{\gamma}\int_0^\infty [i\int_0^\infty y^{i-1}p(y)dy - (\beta+\frac{\gamma\sqrt{Z}}{2})\int_0^\infty y^i P(y)dy]$$

$$= \frac{2\sqrt{Z}}{\gamma}[iP_{i-1} - (\beta+\gamma\sqrt{Z}/2)P_i] \qquad \text{(B.26)}$$

Eq'n B.26 is identical to eq'n 2.36.

B.3 EVALUATION OF MOMENT N_i

The eq'n 2.34 for N_i^d can be easily obtained from eq'n 2.29 as

$$x_c N_i^d = \int_0^\infty y^i x_c N_d(y)dy$$

$$= \int_0^\infty (\beta + \gamma/2*\sqrt{Z})y^i P(y)dy + \int_0^\infty \frac{\gamma}{2\sqrt{Z}} y^i f(y)P(y)dy$$

$$= (\beta+\gamma\sqrt{Z}/2)P_i + \gamma/2/\sqrt{Z}*F_i \qquad \text{(B.27)}$$

Substituting eq'n B.26 gives

$$x_c N_i^d = i P_{i-1} \qquad \text{(B.28)}$$

The expression for N_i^r (eq'n 2.35) requires more calculations as shown below;

Substitution of eq'n 2.30 to eq'n 2.31 yields

$$x_c N_i^r = \int_0^\infty y^i x_c N_r(y)dy$$

$$= \int_0^\infty \beta y^i P(y)dy + \frac{\gamma(\beta+\gamma\sqrt{Z})}{2\sqrt{Z}}\int_0^\infty\int_0^y y^i f(t)P(t)P(y-t)dtdy \qquad \text{(B.29)}$$

Note that the exprssion B.14 has been used in deriving eq'n B.29.

The second term of eq'n B.29 can be evaluated by using Laplace transform properties shown in eq'n B.15.

$$\int_0^\infty y^i \int_0^\infty f(t)P(t)P(y-t)dtdy = (-1)^i \frac{d^i}{ds^i} [L(P(t))]L(f(t)P(t)]_{@s=0} \quad \text{(B.30)}$$

Considering that $(-1)^n \frac{d^n}{ds^n} L(P(t))_{@s=0} = P_n$ (B.31)

And that $(-1)^n \frac{d^n}{ds^n} L(f(t)P(t))_{@s=0} = F_n$ (B.32)

Eq'n B.30 can be expanded into the eq'n B.33.

$$\int_0^\infty y^i \int_0^y f(t)P(t)P(y-t)dtdy = \sum_{j=0}^{i} \binom{i}{j} F_j P_{i-j} \quad \text{(B.33)}$$

Substituting eq'n B.33 into eq'n B.29 yields eq'n 2.35.

APPENDIX C

DERIVATION OF y_n^d AND y_n^r

The term y_n^d is defined as

$$y_n^d = \frac{N_1^d}{N_0^d} \tag{C.1}$$

In eq'n C.1, N_0^d is equal to $1/x_c$ by eq'n B.10 and the expression for N_1^d can be obtained by setting i=1 in eq'n B.28.

$$x_c N_1^d = P_0 \tag{C.2}$$

As P_0 is equal to $\frac{1}{\beta+\gamma\sqrt{Z}}$ by eq'n B.8, eq'n C.1 can rewritten as

$$y_n^d = 1/(\beta+\gamma\sqrt{Z}) \tag{C.3}$$

Also from the definition of y_n^r,

$$y_n^d = N_1^r / N_0^r \tag{C.4}$$

In eq'n C.3, N_0^r is equal to $\frac{\beta+\gamma\sqrt{Z}/2}{x_c(\beta+\gamma\sqrt{Z})}$ by eq'n B.21 and an expression for N_1^r can be obtained by substituting i=1 in eq'n 2.35.

$$x_c N_1^r = \beta P_1 + \gamma/2/\sqrt{Z} * (\beta+\gamma\sqrt{Z}) * (F_0 P_1 + F_1 P_0) \tag{C.5}$$

As

$$F_0 = Z/(\beta+\gamma\sqrt{Z}) \tag{C.6}$$

$$F_1 = 2\sqrt{Z}/\gamma * (P_0 - (\beta+\gamma\sqrt{Z})/2 * P_1) \tag{C.7}$$

$$P_0 = 1/(\beta+\gamma\sqrt{Z}) \tag{C.8}$$

Eq'n C.5 can be transformed as

$$x_c N_1^r = \beta P_1 + \gamma/2/\sqrt{Z} * (ZP_1 + 2\sqrt{Z}/\gamma * P_0 - 2\sqrt{Z}/\gamma * (\beta+\gamma\sqrt{Z}/2) * P_1)$$

$$= 1/(\beta+\gamma\sqrt{Z}) \qquad \text{(C.9)}$$

Substituting eq'n C.9 and the expression for N_0^r into eq'n C.4 gives

$$y_n^r = \beta + \gamma\sqrt{Z}/2 \qquad \text{(C.10)}$$

APPENDIX D

EVALUATION OF l_i's

D.1 EVALUATION OF l_i^d

Eq'n 2.41 can be rewritten as

$$l_i^d = M_i^d / M_n^d = y_i^d / y_n^d \qquad (D.1)$$

As $$y_n^d = \int_0^\infty y N_d(y)dy \; / \; \int_0^\infty N_d(y)dy \qquad (D.2)$$

From eq'n C.3, $$y_n^d = 1/(\beta+\gamma\sqrt{Z}) \qquad (D.3)$$

Similarly, $$y_i^d = \int_0^\infty y^i N_d(y)dy \; / \; \int_0^\infty y^{i-1} N_d(y)dy = iP_i/(i-1)/P_i \qquad (D.4)$$

Thus, $$l_i^d = y_i^d / y_n^d = (\beta+\gamma\sqrt{Z})i/(i-1)*P_i/P_{i-1} \qquad (D.5)$$

Substituting i=2 for l_w^d, i=3 for l_z^d, and i=z+n for l_{z+n}^d gives Table 2.2.

D.2 EVALUATION OF l_i^r

F_0 has been evaluated in eq'n B.9 and the higher moments F_i can be expressed in terms of P_i by setting i=1,2,3, etc. in eq'n B.26.

$$F_0 = Z/(\beta+\gamma\sqrt{Z}) \qquad (D.6)$$

$$F_1 = 2\sqrt{Z}/\gamma*(P_0-(\beta+\gamma\sqrt{Z}/2)P_1) \qquad (D.7)$$

$$F_2 = 2\sqrt{Z}/\gamma*[2P_1-(\beta+\gamma\sqrt{Z}/2)P_2] \qquad (D.8)$$

$$F_3 = 2\sqrt{Z}/\gamma*[3P_2-(\beta+\gamma\sqrt{Z}/2)P_3] \qquad (D.9)$$

Evaluating P_i in terms of l_i^d's from the left column of Table 2.2,

$$P_1 = l_w^d/2/(\beta+\gamma\sqrt{Z})^2 \qquad (D.10)$$

$$P_2 = 2l_z^d P_1/3/(\beta+\gamma\sqrt{Z})$$

$$= 1_w^d \, 1_z^d \, / \, 3 / \, (\beta+\gamma\sqrt{Z})^3 \tag{D.11}$$

$$P_3 = 3 \, 1_{z+1}^d \, P_2 \, / \, 4 \, / (\beta+\gamma\sqrt{Z}) = 1_w^d 1_z^d 1_{z+1}^d / 4 / (\beta+\gamma\sqrt{Z})^4 \tag{D.12}$$

Similarly, the recurrence relationship D.13 can be derived.

$$P_i = \prod_{j=2}^{i+1} 1_j^d \, / (i+1) / (\beta+\gamma\sqrt{Z})^{i+1} \tag{D.13}$$

It should be noted that

$$1_2^d = 1_w^d \tag{D.14}$$

$$1_3^d = 1_z^d \tag{D.15}$$

$$1_{3+i}^d = 1_{z+i}^d \tag{D.16}$$

Substituting eq'ns D.10-D.13 into eq'n D.6-D.9, along with the definition of f_1 as shown in the footnote of Table 2.2 gives

$$F_0 = \sqrt{Z} \, / (\beta + \gamma\sqrt{Z}) \tag{D.17}$$

$$F_1 = 2\sqrt{Z} \, (1 - f/2) / \gamma / (\beta+\gamma\sqrt{Z}) \tag{D.18}$$

$$F_2 = 2\sqrt{Z} \, (1 - f1_w^d/3) / \gamma / (\beta+\gamma\sqrt{Z})^2 \tag{D.19}$$

$$F_3 = 2\sqrt{Z} \, (1 - f1_z^d/4) / \gamma / (\beta+\gamma\sqrt{Z})^3 \tag{D.20}$$

Similarly, for an arbitrary integer i,

$$F_i = 2\sqrt{Z} \, (1 - f1_i^d/(i+1)) / \gamma / (\beta+\gamma\sqrt{Z})^i \tag{D.21}$$

Now eq'ns D.17-D.21 can be resubstituted into eq'n 2.35.

$$N_0^d = \beta P_0 + \gamma(\beta+\gamma\sqrt{Z})/2/\sqrt{Z} * F_0 \, P_0$$

$$=P_0[\beta+\gamma(\beta+\gamma\sqrt{Z})/2/\sqrt{Z}*Z/(\beta+\gamma\sqrt{Z})]$$

$$=f \qquad (D.22)$$

$$N_1^d=\beta P_1+\gamma/2/\sqrt{Z}*(\beta+\gamma\sqrt{Z})*(F_1P_0+F_0P_1)$$

$$= P_1(\beta+\gamma\sqrt{Z}/2)+\gamma/2/\sqrt{Z}*F_1$$

$$= 1_w^d*f/2/(\beta+\gamma\sqrt{Z}) + \gamma/2/\sqrt{Z}*2\sqrt{Z}/\gamma*(1-f1_w^d/2)/(\beta+\gamma\sqrt{Z})$$

$$=1/(\beta+\gamma\sqrt{Z}) \qquad (D.23)$$

$$N_2^d=\beta P_2+\gamma/2/\sqrt{Z}*(\beta+\gamma\sqrt{Z})*(F_2P_0+2F_1P_1+F_0P_2)$$

$$= P_2(\beta+\gamma\sqrt{Z}/2) + 1_w^d(1-f1_z^d/3)/(\beta+\gamma\sqrt{Z})^2 + 2\gamma/2/\sqrt{Z}*(\beta+\gamma\sqrt{Z})*2\sqrt{Z}/\gamma*$$

$$(1-f1_w^d/2)/(\beta+\gamma\sqrt{Z})*1_w^d/2/(\beta+\gamma\sqrt{Z})^2$$

$$= 1_w^d(2-f1_w^d/2)/(\beta+\gamma\sqrt{Z})^2 \qquad (D.24)$$

$$N_3^d=\beta P_3+\gamma/2/\sqrt{Z}*(\beta+\gamma\sqrt{Z})*(F_3P_0+3F_2P_1+3F_1P_2+F_0P_3)$$

$$= f1_w^d1_z^d1_{z+1}^d/4/(\beta+\gamma\sqrt{Z})^3 + 1_w^d1_z^d(1-f1_{z+1}^d/4)/(\beta+\gamma\sqrt{Z})^3$$

$$+3\gamma/2/\sqrt{Z}*(\beta+\gamma\sqrt{Z})*1_w^d/2/(\beta+\gamma\sqrt{Z})^2*2\sqrt{Z}/\gamma*1_w^d/(\beta+\gamma\sqrt{Z})^2*(1-f1_z^d/3)$$

$$+3\gamma/2/\sqrt{Z}*(\beta+\gamma\sqrt{Z})*2\sqrt{Z}/\gamma*(1-f1_w^d/2)/(\beta+\gamma\sqrt{Z})*1_w^d1_z^d/3/(\beta+\gamma\sqrt{Z})^3$$

$$= 31_w^d/(\beta+\gamma\sqrt{Z})^3*(2/3*1_z^d + 1_w^d/2 - f1_w^d1_z^d/3) \qquad (D.25)$$

$$N_4^d= f1_w^d1_z^d1_{z+1}^d1_{z+2}^d/5/(\beta+\gamma\sqrt{Z})^4 + \gamma/2/\sqrt{Z}*(\beta+\gamma\sqrt{Z})*(F_4P_0+4F_3P_1+6F_2P_2$$

$$+4F_1P_3+P_4F_0)$$

$$=f1_w^d1_w^d1_{z+1}^d1_{z+2}^d/5/(\beta+\gamma\sqrt{Z})^4 + \gamma/2/\sqrt{Z}*(\beta+\gamma\sqrt{Z})*[1_w^d1_w^d1_{w+1}^d/(\beta+\gamma\sqrt{Z})^4*$$

$$(1-f1^{d}_{z+2}/5) + 4*2\sqrt{Z}/\gamma*1^{d}_{w}1^{d}_{z}/(\beta+\gamma\sqrt{Z})^{3}*(1-f1^{d}_{z+1}/4)*1^{d}_{w}/2/(\beta+\gamma\sqrt{Z})^{2}$$

$$+6*2\sqrt{Z}/\gamma*1^{d}_{w}(1-f1^{d}_{z}/3)/(\beta+\gamma\sqrt{Z})^{2}*1^{d}_{w}1^{d}_{z}/3/(\beta+\gamma\sqrt{Z})^{3} + 4(1-f1^{d}_{w}/2)*$$

$$1^{d}_{w}1^{d}_{z}1^{d}_{z+1}/4/(\beta+\gamma\sqrt{Z})^{4}]$$

$$=4f[(2-f1^{d}_{w}/2)1^{d}_{z+1}+1^{d}_{w}(1-1^{d}_{w}/2+1^{d}_{z})]/(2-f1^{d}_{w}+1^{d}_{w}/2) \qquad (D.26)$$

In deriving equations D.22-D.26, the relationships D.10-D.13 and D.17-D.21 were substituted with the definitions $f_1=f$ and $f_2=2-f_1 1^{d}_{w}/2$. These relationships are summarized in the right column of Table 2.2.

APPENDIX E

LIST OF COMPUTER PROGRAMS

AND

SAMPLE COMPUTER OUTPUT

The following table is a brief description of the computer programs used and mentioned in thid work. The printed programs have been edited by the RUNOFF text editing program. The sample output at the end of this Appendix is the simulation of Hamielec's methyl methacrylate data (3) at 90 deg. C and AIBN concentration of 0.05 wt. %.

Table E.1

COMPUTER PROGRAMS

Filename.Extension	Description
INT.FOR	Main program for producing the time-conv. and MWD data
DATA.FOR	Block data subroutine which supplies the physical and rate constants
MONOM.FOR	Initiation for the "True Gel Effect"
MONPCK.FOR	Same as MONOM except for the "Pseudo Gel Effect"
UPDATE.FOR	Calculates instantaneous rate and molecular weights for the "True Gel Effect"
UPDPCK.FOR	Same as UPDATE except for the "Pseudo Gel Effect"
MOLWT.FOR	Converts the instantaneous values from UPDATE or UPDPCK into the derivatives of the fractional conversion, the integration variable
COEFF.FOR	Calculates the cubic spline coefficients for the interpolation of master charts
SBRKPL.FOR	Calculates Z and Γ_i's with the given

Table E.1 con'd

	β, γ and W
CALCU.FOR	Interpolates the master charts
AUX.FOR	Interpolates the master charts
DIST.FOR	Calculates the moments of P(y) with the given values of β, γ, and Z
CONST.FOR	Produces the master charts data file CONST.DAT to be used by CALCU and AUX

```
C
C       Main Program:INT.FOR
C
C        This is the main program used for the computer
C       simulation .
C       of   Diffusion  Controlled Vinyl Polymerizations
C       where the monomer and the polymer are miscible.
C
C        This program is best suited for time-sharing.
C       The values of the adjustable constants of the model
C       should be typed in each time the program is run.
C       To run this program,the following command is issued
C       .EX INT,UPDATE,MCNCM,MOLWT,DATA,SERKPL,COEFF,
C        AUX,CALCU,APP:IMSL/SEARCH
C        It is recommended to make a MIC file which
C       contains the above command for convenience.
C        With the above command,the computer will respond
C                TYPE IN OUTPUT DEVICE NUMBER.
C        You have to type 1 if you want the results stored
C       in your disk area, 3 if you want the line printer
C       output.
C       For trial runs, it is better to type in 5 to see
C       if the result is worth to be printed.
C        If you have typed in 1, the computer will respond;
C                ENTER OUTPUT FILE NAME.
C        You should leave the first letter blank, and the
C       following five letters will be the name of the
C       output file with the extension .DAT.
```

```
C       If you type in ' STOP',
C       the program will not run. Otherwise, or if you
C       typed in a number not equal 1, the computer
C       response will be;
C                 ENTER TEMP,INCON.
C        You type in the reaction temperature in deg.C and
C       the initiator concentration in moles/liter.
C        The initiator decomposion constant
C       has to have been put in the DATA.FOR file already.
C       Example: 50.,0.0012
C        The computer will respond;
C                 ENTER FW,FX,VFXC,XK.
C        FW will multiply the molecular weight values
C       calculated by the factor FW.
C       FX will multiply the polymerization
C       rate calculated by the factor FX.
C       VFXC is the fractional
C       free volume from which the gel effect starts.
C       XK is the
C       residual termination reaction efficiency factor.
C        The values FW and FX will automatically change the
C       termination rate constant and the initiator
C       efficiency to fit the said requirements.
C       Example: 1.,1.,.13,1.
C        The next computer response will be;
C                 ENTER XFINAL,PRDEL,TIME SCALE,TOL.
C        XFINAL is the conversion level where the
```

```
C       integration will stop.
C       PRDEL is the print interval. TIME SCALE
C       is used to convert time into minutes,hours,etc..
C       TIME SCALE of 1 will give time in seconds,
C       60. in minutes,
C       3600. in hours,etc.. TOL is the error tolerence for
C       the IMSL DVERK. TOL of 0.001 will give approx.
C       0.1% relative error for each PRDEL interval.
C       If error criteria can not be met, the computer will
C       type a error message and stop.
C       It is reccmmended to use the
C       largest acceptable TOL value for fast result.
C       Example:.99,.05,60.,.002
C
C       The program calls the following subroutines;
C
C       UPDATE,FCNCN,PCIWT,SBRKPL,IATA,CALCU,AUX,COEFF,
C       DVERK,UERTST
C        The last two subrcutines are IMSL routines.
C        The data file CONST.DAT is read in COEFF routine.
C
C
C        COMMON blocks with other subroutines
C
        EXTERNAL UPDATE
        DIMENSION XDATA(25),X8(9)
        COMMON/DATA/XDATA
        COMMON/RATE/X8,PIO
```

```
      COMMON/VFDT/VFXC
      COMMON/DEV/JDEV
      COMMON/TCL/TCI
      COMMON/TF/TFACT
      REAL MAV(5),RATE(5),INCCN
      DIMENSION C(24),W(5,9)
      DATA N,NW/5,5/
C
C     Initial preparation to make the formulas for the
C     master charts
C
      CALL COEFF
C
C     Select Output Device
C
      TYPE 690
  690 FORMAT(10X,'TYPE IN OUTPUT DEVICE NUMBER.')
      ACCEPT 680,IDEV
  680 FORMAT(I3)
  700 IF(IDEV.EQ.1) TYPE 500
  500 FORMAT(10X,'ENTER OUTPUT FILENAME.')
      IF(IDEV.EQ.1)ACCEPT 900,FILE
  900 FORMAT(A6)
      IF(IDEV.EQ.1) TYPE 900,FILE
      IND=1
      IF(FILE.EQ.'STOP') STOP
      IF(IDEV.EQ.1) CALL OFILE(1,FILE)
```

```
C
C       Read the reaction temperature and the initiator
c       concentration
C
        TYPE 400
        IND=1
  400   FORMAT(10X,'ENTER TEMP,INCCN')
        ACCEPT *,TEMP,INCCN
C
C       Read the adjustable parameters
C
        TYPE 302
        IND=1
        ACCEPT *,XDATA(24),XDATA(25),VFXC,X8(9)
        JDEV=IDEV
C
C       Integration limit,print interval, time scale,
c       error criteria
C
        TYPE 148
  148   FORMAT(X,'ENTER XFINAL,PRDEL,TIME SCALE,TCI')
        ACCEPT *,XFINAL,PRDEL,TFACT,TCI
  302   FORMAT(10X,'ENTER FW,FX,VFXC,XK')
C
C       Initial setting of the variables
C
        X=0.
        DO 301 K=1,5
```

```
  301   MAV(K)=0.
        XC=0.
        CALL RCNCM(TEMP,INCON)
        CALL UPDATE(5,X,MAV,RATE)
C
C       Integration using the IMSL routine DVERK
C
  151   XC=XC+PRDEL
C
C       Test for the integration limit
C
        IF(XFINAL.LT.XC)STOP
C
C       Variable step integration without printout
C
        JDEV=0
        CALL DVERK(N,UPDATE,X,MAV,XC,TOL,IND,C,NW,W,IER)
C
C       Printout at conversion level integer multiple of
c       PRDEL
C
        JDEV=IDEV
        CALL UPDATE(N,X,MAV,RATE)
C
C       Discontinue integration when TOL limit can not be
C        met.
C
        IF(IND.LE.0.OR.IER.GE.129) GO TO 250
```

```
C
C       Continue integration
C
        GO TO 151
C
C       Error message
C
  250   TYPE 350,IND,IER
  350   FORMAT('0','IND=',I3,10X,'IER=',I4)
        STOP
        END



C       SUBROUTINE UPDATE
C
C       THIS SUBROUTINE CALCULATES THE DERIVATIVES
C       OF MAV'S WITH RESPECT TO CONVERSION X, RATE'S
C       WHEN CALLED BY THE MAIN PROGRAM INT OR THE IMSL
C       RUNGE-KUTA FOURTH ORDER INTEGRATION ROUTINE
C       DVERK.
C
C       N:NUMBER OF VARIABLES TO BE INTEGRATED.
C         6 WHEN MOL. WT. DEVELOPMENT UP TO MZ+1
C         ARE CALCULATED.
C       X:THE FRACTIONAL CONVERSION
C       MAV(1):TIME [SEC.]
C       MAV(2):MN, CUMULATIVE AVERAGE.
```

```
C       MAV(3):MW
C       MAV(4):MZ
C       MAV(5):MZ+1
C       RATE(I):THE CORRESPONDING DERIVATIVE WITH RESPECT
C               TO X OF MAV(I)
C       MINST(I):THE CORRESPONDING INSTANTANEOUS VALUE
C               FOR MAV(I)
C       Z:THE ENTANGLEMENT COUPLING FACTOR
C       KTVF:THE UNENTANGLED REFERENCE TERMINATION FACTOR
C       XC:MINIMUM D.P. FOR ENTANGLEMENT
C       L?:THE MOLECULAR WEIGHT INDEX FOR THE CORRESPONDING
C          MINST?.
C       MODE:THE MODE OF TERMINATION
C       XKTP:THE EFFECTIVE TERMINATION FACTOR
C       PHIM:VOL. FRACTION OF MONOMER
C       VF:FRACTIONAL FREE VOLUME
C       EPS:VOLUME SHRINKAGE FACTOR FOR POLYMN.
C       VFM:FRACTIONAL FREE VOLUME OF PURE MONOMER
C       VFP:FRACTIONAL FREE VOLUME OF PURE POLYMER
C       VFXC:VF AT THE START OF PHASE 2
C       XRDOT:RADICAL CONCENTRATION [MOL/L]
C       W:FRCTION OF REFERENCE TRANSLATIONAL CONTRIBUTION
C         FOR THE EFFECTIVE TERMINATION.
C       KFIM:MONOMER DIFFUSION CONTROLLED PROPAGATION
C            RATE CONSTANT.
C       KP:THE PROPAGATION RATE CONSTANT [L/MOL/SEC.]
C       XKP:RATIO OF KP TO KPO
C       KPO:KP AT INFINITE DILUTION
```

```
C       KTO:XKT AT INFINITE DILUTION
C       XS:XC AT PURE POLYMER
C       CM:CHAIN TRANSFER  RATE CONSTANT
C       BETA:DIMENSIONLESS CONSTANT
C       GAMMA:DIMENSIONLESS CONSTANT
C       MNO:INITIAL MINST(2)
C       KD:INITIATOR DECOMPOSITION RATE CONSTANT
C       P1:PROB. DISTRIBUTION FUNCTION P(Y) @Y=1
C       SIG:RADIUS OF EFFECTIVE TERMINATION SPHERE
C       BET:BETA VALUE OF GAUSSIAN CHAIN DISTRIBUTION
C       XKTP:RESIDUAL TERMINATION RATE CONSTANT
C       RDOT:RATIO OF XRDOT TO RDOTO
C       RDOTO:XRDOT @X=0
C       ALL OTHER SYMBOLS ARE EITHER DEFINED IN OTHER
C       SUBROUTINES ALREADY OR DUMMY VARIABLES.
C
C
      SUBROUTINE UPDATE(N,X,MAV,RATE)
      DIMENSION XD(4),X18(18)
      DIMENSION MAV(N),RATE(N)
      REAL MAV,MINST(5),KTVP,MNO,KD,KP,IW,IZ,
     1 LZP1,KT,KPDM,KPO,KTO
      COMMON/MODE/MODE,TERMINATION
      REAL MODE
      COMMON/RATE/RDOTO,RO,XKPDM,MNO,KD,CM,KPO,RIO,XK,RIO
      COMMON/TF/TFACT
      COMMON/KTVP/XKTVP
```

```
      COMMON/VF/VFM,VFP,EPS,CCNM,DSEG
      COMMON/DEV/IDEV
      COMMON/VFDT/VFXC
      COMMON/DATA/XL,ANGST,DS,XS,X18
C
C     DUMMY COMMON
C
      COMMON/OLD/XCLD,XKTCLD
      Z=1.;KTVF=XKTVF;XC=XS*1000.;LW=2.;LZ=3.;LZP1=4.
      IF(MODE.EQ.'RECOMB')LW=1.5
      IF(MODE.EQ.'RECOMB')LZ=2.
      IF(MODE.EQ.'RECOMB')LZP1=2.5
      IF(X.GT..001)GO TO 200
      IF(MODE.EQ.'DISERO')MINST(2)=MNO
      IF(MODE.EQ.'RECOMB')MINST(2)=2.*MNO
      XKTP=0.;XKTO=0.;MAV(3)=MINST(2)*LW;XEDOT=EDOTO;W=1.
  200 CONTINUE
      PHIM=(1.-X)/(1.-EPS*X)
      VF=VFM*PHIM+VFP*(1.-PHIM)
      IF(VF.LT.VFXC) KTVF=XKTVF*EXP(1./VFXC-1./VF)
      KPDM=XKPDM*EXP(1./XL(1)-1./VF)
      KE=KEO*KEDM/(KEDM+KPO)
      XKP=KE/KEO
      IF(XKP.GT.1.)XKP=1.
      IF(X.GT..001)   XC=XS/(1.-PHIM)
      BETA=XC*CM
      GAMMA=X18(7)*XC*SQRT(KTVF/(1.-EPS*X))/XKP/PHIM/MNO
     1  *EXP(-KD*MAV(1),2.)
```

```
      I=0 !PARAM TO BE USED TO PREVENT INFINITE LOOP
      IF(X.LE..5)XK=0.
  100 A1=BETA+GAMMA*SQRT(Z/W)/2.+GAMMA/2.*(1.-W)/SQRT(W*Z)
      A2=GAMMA/2.*SQRT(W/Z)
      P1=EXP(-1.*A1-A2)
      IF(X.EQ..5)PC=P1
      XKOLD=XK
      IF(X.GT..5)XK=(P1-PC)/(1.-PC)
      IF(XKOLD.GT.XK)XK=XKOLD
      IF(XK.LT.0.)XK=0.
  600 BET=SQRT(3./XC)/ANGST/1.E-8
      SIG=SQRT(ALOG(2.98E-22*BET**3/XRDOT))/BET
     1  XKTP=2.676E13*ANGST*KP*PHIM*CONM*SIG**2/SQRT(XC)*
        XK/KTO
      IF(XKTP.GT.1.)XKTP=1.
      IF(XKTP.EQ.1..AND.KTVF.EQ.1.) XKTP=0.
  300 CONTINUE
      W=KTVF/(KTVF+XKTP)
      IF(MAV(3)/XC/X1E(7).GT.1..AND.VF.LT.VFXC)
     1  CALL SBRKPL(MODE,BETA,GAMMA,W,Z,LW,LZ,LZP1)
      IF(Z.LT.1.-W)Z=1.-W
      XKT=Z*(KTVF+XKTP)
C
C     COMPARE XKT AND THE DUMMY COMMON OLD VALUES
C     TO PREVENT INCREASING XKT WITH CONVERSION
C
      IF(X.GT..5.AND.X.GT.XOLD.AND.XKT.GT.XKTOLD)
     1  XKT=XKTOLD
      IF(XKT.GT.1.)XKT=1.
```

```
      RDOT=SQRT(1./(1.-EPS*X)/XKT)*EXP(-KD*MAV(1)/2.)
      XRDOT=RDOTO*RDOT
      RATE(1)=1./RDOT/RO/PHIM/XKP*EXP(KD*MAV(1)/2.)
      XMIN=MNO*XKP*PHIM/RDOT/XKT*EXP(KD*MAV(1)/2.)
      IF(MODE.EQ.'DISPRC')XX=1.
      IF(MODE.EQ.'PROCMP')XX=.5
      MINST(2)=1./(XX/XMIN+CM/XKP/X18(7))
      MINST(3)=LW*MINST(2)
      MINST(4)=LZ*MINST(2)
      MINST(5)=LZP1*MINST(2)
      IF(X.LE..5)GO TO 400
      IF(XKTO.EQ.0..AND.XKTP.EQ.0.)GO TO 400
      IF(XKTO.EQ.0.) GO TO 500
      IF(ABS(XKTP/XKTO-1.).LE..001) GO TO 400
      I=I+1
      IF(I.GT.20) GO TO 400
  500 XKTO=XKTP
      GO TO 100
  400 CONTINUE
C
C     CHANGE THE DUMMY COMMON VALUES
C
      IF(X.LE..5)XKTOLD=XKT
      IF(XKTOLD.GT.XKT)XOLD=X
      IF(XKTOLD.GT.XKT) XKTOLD=XKT
      CALL MOLWT(X,MAV,RATE,MINST)
      IF(IDEV.NE.0)WRITE(IDEV,30)
     1 X,PHIM,VF,KTVP,XKP,W,BETA,GAMMA,
```

```
     1   MINST(2),KPDM,XKTP,SIG,Z,LW,LZP1,XKT
    30   FORMAT(1H0/1H0,5X,'X=',E5.3/1H0,10X,
     1   'PHIM =',E14.6,10X,'VF   =',E14.6/
     2   1H0,10X,'KTVF =',E14.6,10X,'KP   =',E14.6/
     3   1H0,10X,'W    =',E14.6,10X,'BETA =',E14.6/
     4   1H0,10X,'GAMMA=',E14.6,10X,'MINST=',E14.6/
     5   1H0,10X,'KPDM =',E14.6,10X,'KTP  =',E14.6/
     9   1H0,10X,'SIG  =',E14.6,10X,'Z    =',E14.6/
     1   1H0,10X,'LW   =',E14.6,
     1   10X,'IZ   =',E14.6/1H0,10X,'IZ+1 =',E14.6,10X,
     2   'KTEFF=',E14.6)
         TIME=MAV(1)/TFACT
         SAIT=X/MAV(2)*X18(7)
         IF(IDEV.NE.0) WRITE(IDEV,70) XRDCT,TIME,RATE(1),
     1   (MAV(I),I=2,5),P1,SAIT
    70   FORMAT(1H0,10X,'RDCT =',E14.6,10X,'TIME =',E14.6/
     1   1H0,10X,'DTDX =',E14.6,10X,
     2    'MNAVG=',E14.6/1H0,10X,'MWAVG=',
     2   E14.6,10X,'MZAVG=',E14.6/1H0,10X,'MZ+1A=',E14.6,
     3   10X,'P1   =',E14.6/1H0,10X,'X/MNA=',E14.6)
         RETURN
         END



C        SUBROUTINE UPDATE
C
C         THIS SUBROUTINE IS THE SAME AS UPDATE
C        EXCEPT THAT IT IS USED FOR THE
```

```
C       PSEUDO-CONVENTIONAL KINETICS.
C
        SUBROUTINE UPDATE(N,X,MAV,RATE)
        DIMENSION XD(4),X18(18)
        DIMENSION MAV(N),RATE(N)
        REAL MAV,MINST(5),KIVF,MNO,KD,KP,IW,LZ,IZP1,KT,
     1  KPDM,KPO,KTO
        COMMON/MODE/MODE,TERMINATION
        REAL MODE
        COMMON/RATE/RDOT0,RO,XKPDM,MNO,KD,CM,KPO,RIO,XK,RIO
        COMMON/IF/IFACT
        COMMON/KTVF/XKTVF
        COMMON/VF/VFM,VFP,EPS,CONM,DSEG
        COMMON/DEV/IDEV
        COMMON/VFDT/VFXC
        COMMON/DATA/XI,ANGST,DS,XS,X18
        DATA PHASE/.9/
        Z=1.;KTVF=XKTVF;XC=XS*1000.;LW=2.;LZ=3.;LZP1=4.
        IF(MODE.EQ.'RECOMB')LW=1.5
        IF(MODE.EQ.'RECOMB')LZ=2.
        IF(MODE.EQ.'RECOMB')LZP1=2.5
        IF(X.GT..001)GO TO 200
        IF(MODE.EQ.'DISPRO')MINST(2)=MNO
        IF(MODE.EQ.'RECOMB')MINST(2)=2.*MNO
        XKTP=0.;XKTO=0.;MAV(3)=MINST(2)*LW;XRDOT=RDOT0;W=1.
  200   CONTINUE
        PHIM=(1.-X)/(1.-EPS*X)
```

```
      VF=VFM*PHIM+VFP*(1.-PHIM)
      IF(VF.GT.VFXC) II=1
      IF(VF.GT.VFXC) ZC=1.
      IF(VF.LT.VFXC) KTVF=XKTVF*EXP(1./VFXC-1./VF)
      KPDM=XKPDM*EXP(1./XD(1)-1./VF)
      KP=KP0*KPDM/(PPDM+KP0)
      XKP=KP/KP0
      IF(XKP.GT.1.)XKP=1.
      IF(X.GT..001)  XC=XS/(1.-PHIM)
      BETA=XC*CM
      GAMMA=X18(7)*XC*SQRT(KTVF/(1.-EPS*X))/XKP/PHIM/ANO
     1  *EXP(-KD*MAV(1)/2.)
      I=0! PARAM TO BE USED TO PREVENT INFINITE LOOP
      IF(X.LE..5)XK=0.
100   A1=BETA+GAMMA*SQRT(Z/W)/2.+GAMMA/2.*(1.-W)/SQRT(W*Z)
      A2=GAMMA/2.*SQRT(W/Z)
      P1=EXP(-1.*A1-A2)
      IF(X.EQ..5)PC=P1
      XKOLD=XK
      IF(X.GT..5)XK=(P1-PC)/(1.-PC)
      IF(XKOLD.GT.XK)XK=XKOLD
      IF(XK.LT.0.)XK=0.
600   BET=SQRT(3./XC)/ANGST/1.E-8
      SIG=SQRT(ALOG(2.98E-22*BET**3/XRDOT))/BET
      XKTP=2.676E13*ANGST*KP*PHIM*CONM*SIG**2/SQRT(XC)*
     1  XK/KTO
      IF(XKTP.GT.1.)XKTP=1.
      IF(XKTP.EQ.1..AND.KTVF.EQ.1.)XKTP=0.
```

```
300   CONTINUE
      W=KTVF/(KTVF+XKTP*ZC)
      IF(MAV(3)/XC/X18(7).GT.1..AND.VF.LT.VFXC)
     1 CALL SBRKPL(MODE,BETA,GAMMA,W,Z,LW,LZ,LZP1)
      IF(Z.LT.1..AND.II.EQ.1) ZC=Z
      IF(Z.LT.1..AND.II.EQ.1) II=0
      IF(XKTP.EQ.0..AND.Z.LT.1..AND.Z.GT.ZC) ZC=Z
      IF(Z.LT.1.-W) Z=1.-W
      XKT=Z*(KTVF/ZC+XKTP)
      IF(XKT.GT.1.)XKT=1.
      RDOT=SQRT(1./(1.-EPS*X)/XKT)*EXP(-KD*MAV(1)/2.)
      XRDOT=RDOTO*RDOT
      RATE(1)=1./FDOT/RO/PHIM/XKP*EXP(KD*MAV(1)/2.)
      XMIN=ENO*XKP*PHIM/RDOT/XKT*EXP(KD*MAV(1)/2.)
      IF(MODE.EQ.'DISREC')XX=1.
      IF(MODE.EQ.'RECOMB')XX=.5
      MINST(2)=1./(XX/XMIN+CM/XKP/X18(7))
      MINST(3)=LW*MINST(2)
      MINST(4)=LZ*MINST(2)
      MINST(5)=LZP1*MINST(2)
      IF(X.LE..5)GO TO 400
      IF(XKTO.EQ.0..AND.XKTP.EQ.0.)GO TO 400
      IF(XKTO.EQ.0.) GO TO 500
      IF(ABS(XKTP/XKTO-1.).LE..001) GO TO 400
      I=I+1
      IF(I.GT.20) GO TO 400
500   XKTO=XKTP
```

```
      GO TO 100
400   CONTINUE
      CALL MOLWT(X,MAV,RATE,MINST)
      IF(IDEV.NE.0) WRITE(IDEV,30)  X,PHIM,VF,KTVF,XKP,
     9  W,BETA,GAMMA,
     1  MINST(2),KPDM,XKTP,SIG,Z,LW,LZ,LZP1,XKT
 30   FORMAT(1H0/1HC,5X,'X=',F5.3/1H0,10X,
     1  'PHIM =',E14.6,10X,'VF    =',E14.6/
     2  1H0,10X,'KTVF =',E14.6,10X,'KP    =',E14.6/
     3  1H0,10X,'W    =',E14.6,10X,'BETA =',E14.6/
     4  1H0,10X,'GAMMA=',E14.6,10X,'MINST=',E14.6/
     5  1H0,10X,'KPDM =',E14.6,10X,'KTP   =',E14.6/
     9  1H0,10X,'SIG  =',E14.6,10X,'Z     =',E14.6/
     1  1H0,10X,'LW   =',E14.6,
     1  10X,'LZ   =',E14.6/1H0,10X,'LZ+1 =',E14.6,10X,
     2  'KTEFF=',E14.6)
      TIME=MAV(1)/TFACT
      SAIT=X/MAV(3)*X18(7)
      IF(IDEV.NE.0) WRITE(IDEV,70) XRDCT,TIME,RATE(1),
     1  (MAV(I),I=2,5),E1,SAIT,ZC
 70   FORMAT(1H0,10X,'RDOT =',E14.6,10X,'TIME =',E14.6/
     1  1H0,10X,'DTDX =',E14.6,10X,
     1  'MNAVG=',E14.6/1HC,10X,'MWAVG=',
     2  E14.6,10X,'MZAVG=',E14.6/1H0,10X,'MZ+1A=',E14.6,
     3  10X,'P1   =',E14.6/1H0,10X,
     1  'X/MNA=',E14.6,10X,'ZC    =',E14.6)
      RETURN
      END
```

```
C
C       SUBROUTINE MCNCM
C
C        This subroutine recieves the reaction temperature
C       and the initiator concentration and calculates the
C       necessary reaction parameters using the data
C       stored in DATA.FOR BLOCK DATA subroutine and
C       transmits the results via the
C       COMMON blocks to UPDATE subroutine, and prints out
C       initial rate constants.
C
C       TEMP:reaction temperature in deg. C.
C       INCON:initial initiator concentration in MOLES/LITER
C       DM:density of monomer in GRAM/CC
C       EPS:volume shrinkage factor
C       VFM:fractional free volume of monomer
C       VFP:fractional free volume of polymer
C       CONM:concentration of pure monomer in MOLES/LITER
C       TABS:absolute temperature in deg. K
C       KP:propagation rate constant in LITER/MOLES/SEC
C       KT:termination rate constant in LITER/MOLES/SEC
C       KD:initiator decomposition rate constant in 1/SEC
C       CM:chain transfer rate constant to monomer
C       RIO:initial radical generation rate MOLES/LITER/SEC
C       RDOT:concentration of radical
C            @ time=0 in MOLES/LITER
C       MNO:the kinetic chain length*mol. wt. of monomer
C       RO:initial reaction rate dTIME/dX in SEC.
C       DSEG:diffusivity of monomeric unit for pure polymer
```

```
C            in CM**2/SEC.
C       KPDM: diffusion controlled propagation rate constant
C            multiplication constant
C       XI: used to calculate KPDM
C       BETA: the difference between fractional free volume
C            of polymer and monomer, or a dimensionless
C            parameter   @VF=VFXC
C       PHIM: volume fraction of monomer @VF=VFXC
C       XC: minimum degree of polymerization @VF=VFXC
C       GAMMA: dimensionless parameter @VF=VFXC
C       FJ: recalculated initiator efficiency
C       Z: entanglement factor @VF=VFXC
C       X1,X2,X3: dummy variables necessary to call SBRKPL
C       XKTVF: multiplication constant for phase II
C            termination rate constant
C       JDEV: output device number
C
C
      SUBROUTINE MONOM(TEMP,INCON)
      REAL INCON,LAMDA,M0,KPDM,KI,KD,MN0,KP
C
C       COMMON blocks
C
      COMMON/RATE/RDOT,R0,KPDM,MN0,KD,CM,KP,KT,XF,RIO
      COMMON/MODE/MODE,TERMINATION
      REAL MODE
      COMMON/KTVF/XKTVF
```

```
      COMMON/VEDT/VEXC
      COMMON/VF/VFM,VFP,EPS,CONM,DSEG
      COMMON/DATA/VFS,ALP,TS,LAMDA,ANGST,DS,XS,EPSO,EPST,
     1  ALMO,ALMT,DMO,DMT,MO,AKT,EKT,AKP,EKP,AKD,EKD,ACM,
     2  ECM,F,FW,FX
      COMMON/DEV/JDEV
C
C     Free volumes, density, and monomer concentration
C
      DM=DMO+DMT*TEMP
      EPS=EPSO+EPS*TEMP
      VFM=ALMO+ALMT*TEMP
      IF(TEMP.GE.TS) VFP=VFS+ALP*(TEMP-TS)
      IF(TEMP.LT.TS) VFP=VFS+ALP*LAMDA*(TEMP-TS)
      CONM=1000./MO*DM
C
C     Temperature, and rate constants from Arhenius
C     expression
C
      TABS=TEMP+273.15
      KP=AKP*EXP(-EKP/TABS)
      KT=AKT*EXP(-EKT/TABS)/FX/FW
      KD=AKD*EXP(-EKD/TABS)
      CM=ACM*EXP(-ECM/TABS)
C
C     Initial rate, kinetic chain length
C
      RIO=2.*F*KD*INCON*FX/FW
```

```
      RDOT=SQRT(RIO/KT)
      MNO=CONM*KP*MO/SQRT(RIO*KT)
      RO=KP*RDOT
C
C     Diffusion controlled propagation
C
      XI=(1000./CONM/6.023E23)**.333333
      DSEG=DS*TABS/(TS+273.15)
      KPDM=48.*DSEG/CONM/XL**2
C
C     Calculation of KTVF*
C
      BETA=VFM-VFP
      PHIM=(VFXC-VFP)/BETA
      XC=XS/(1.-PHIM)
      BETA=CM*XC
      GAMMA=XC*SQRT(RIO*KT)/KP/CONM/PHIM
      FJ=F*FX/FW
      Z=1.;X1=2.;X2=1.;X3=1.
      CALL SBRKPL(MODE,BETA,GAMMA,1.,Z,X1,X2,X3)
      XKTVF=1./Z
C
C     Printout of Constants
C
      IF(JDEV.NE.0) WRITE(JDEV,20) TEMP,INCON,FW,FX,VFXC,
     1 XK,DM,EPS,VFM,VFP,CONM,KP,
```

```
     2   KT,KD,CM,RIO,MNO,PO,RDOT,FJ,KPDM
    20   FORMAT(1H0,10X,'TEMP =',E14.6,10X,'INCON=',E14.6/
     9   1H0,10X,'FW   =',E14.6,10X,'FX   =',E14.6/
     8   1H0,10X,'VFXC =',E14.6,10X,'XK   =',E14.6/
     7   1H0,10X,'DM   =',E14.6,10X,'EPS  =',E14.6/
     1   1H0,10X,'VFM  =',E14.6,10X,'VFP  =',E14.6/
     2   1H0,10X,'CONM =',E14.6,10X,'KP   =',E14.6/
     3   1H0,10X,'KT   =',E14.6,10X,'KD   =',E14.6/
     4   1H0,10X,'CM   =',E14.6,10X,'RIO  =',E14.6/
     6   1H0,10X,'MNO  =',E14.6,10X,'DXDT0=',E14.6/
     7   1H0,10X,'RDOT =',E14.6,10X,'F    =',E14.6/
     8   1H0,10X,'KPDMS=',E14.6)
         RETURN
         END



C        SUBROUTINE MCNCM
C
C         THIS SUBROUTINE IS THE SAME AS MONOM
C        EXCEPT THAT IT IS APPLIED FOR THE
C        PSEUDO-CONVENTIONAL KINETICS.
C
C
         SUBROUTINE MCNCM(TEMP,INCON)
         REAL INCON,LAMI2,MO,KPDM,KT,KD,MNO,KP
C
C        COMMON blocks
```

```
C
      COMMON/RATE/RDCT,RO,KPDM,MNO,KD,CM,KP,KT,XK,RIO
      COMMON/MODE/MODE,TERMINATION
      REAL MODE
      COMMON/KTVF/XKTVF
      COMMON/VFDT/VFXC
      COMMON/VF/VFM,VFP,EPS,CONM,DSPG
      COMMON/DATA/VFS,ALP,TS,LAMDA,ANGST,DS,XS,EPSO,EPST,
     1  ALMO,ALMT,DMO,DMT,MO,AKI,EKT,AKP,EKP,AKD,EKD,ACM,
     2  FCM,F,FW,FX
      COMMON/DEV/JDEV
C
C     Free volumes, density, and monomer concentration
C
      DM=DMO+DMT*TEMP
      EPS=EPSO+EPS*TEMP
      VFM=ALMO+ALMT*TEMP
      IF(TEMP.GE.TS) VFP=VFS+ALP*(TEMP-TS)
      IF(TEMP.LT.TS) VFP=VFS+ALP*LAMDA*(TEMP-TS)
      CONM=1000./MO*DM
C
C     Temperature, and rate constants from Arhenius
C     expression
C
      TABS=TEMP+273.15
      KP=AKP*EXP(-EKP/TABS)
      KT=AKT*EXP(-EKT/TABS)/FX/FW
      KD=AKD*EXP(-EKD/TABS)
```

```
      CM=ACM*EXP(-ECM/TABS)
C
C     Initial rate, kinetic chain length
C
      RIO=2.*F*KD*INCON*FX/FW
      RDOT=SQRT(RIO/KT)
      MNO=CONM*KP*MC/SQRT(RIO*KT)
      RO=KP*RDOT
C
C     Diffusion controlled propagation
C
      XL=(1000./CONM/6.023E23)**.333333
      DSEG=DS*TABS/(TS+273.15)
      KPDM=48.*DSEG/CONM/XL**2
      FJ=F*FX/FW
      XKTVF=1.
C
C     Printout of Constants
C
      IF(JDEV.NE.0) WRITE(JDEV,20) TEMP,INCON,FW,FX,VFXC,
     1  XK,DM,EPS,VFM,VFP,CONM,KP,
     2  KT,KD,CM,RIO,MNO,RO,RDOT,FJ,KPDM
   20 FORMAT(1H0,10X,'TEMP =',E14.6,10X,'INCON=',E14.6/
     9 1H0,10X,'FW   =',E14.6,10X,'FX   =',E14.6/
     8 1H0,10X,'VFXC =',E14.6,10X,'XK   =',E14.6/
     7 1H0,10X,'DM   =',E14.6,10X,'EPS  =',E14.6/
     1 1H0,10X,'VFM  =',E14.6,10X,'VFP  =',E14.6/
```

```
     2   1HO,10X,'CONM =',E14.6,10X,'KP   =',E14.6/
     3   1HO,10X,'KT   =',E14.6,10X,'KD   =',E14.6/
     4   1HO,10X,'CM   =',E14.6,10X,'RIO  =',E14.6/
     6   1HO,10X,'MNO  =',E14.6,10X,'DXDTO=',E14.6/
     7   1HO,10X,'RDCT =',E14.6,10X,'F    =',E14.6/
     8   1HO,10X,'KPDMS=',E14.6)
         RETURN
         END



C
C        SUBROUTINE SBREEL
C
C         This subroutine recieves the MODE of termination,
C        and the dimensionless parameters BETA,GAMMA, and
C        W and computes the indices Z,LW,LZ,LZ+1.
C
C
C        MODE:either DISPROportionation or RECOMBination
C        BETA:dimensionless parameter
C        GAMMA:dimensionless parameter
C        W:dimensionless parameter
C        Z:entanglement factor which determines the
C          polymerization rate and the number average
C          instantaneous molecular weght
C        LW,LZ,LZP1:corresponding molecular weight indices
C        ZPNEW:new trial value of Z
```

```
C       WR:1/W-1
C       ZP:entanglement factcr fcr the hypothetical system
C       GAM:GAMMA value for the hypothetical system
C       BET:BETA value for the hypcthetical system
C       EPSCR:error criterion fcr the trial and error
C             calculaticn
C       GAMMPE:GAMMA value with residual terminaticn
C       XJW,FACTOR,XJW2,XZ,XZP1:intermediate results
C
C
        SUBROUTINE SBPREL(MODE,BETA,GAMMA,W,Z,LW,IZ,LZP1)
        REAL LW,LZ,LZP1
C
C       Error message fcr W>1
C
        IF(W.GT.1.) TYPE 111
  111   FORMAT(10X,'EPSCR:W>1')
C
C       Error message for W<0
C
        IF(W.LT.0.) TYPE 222
  222   FORMAT(10X,'EPSCR:W<0')
C
C       Master indices without residual terminaticn
C
        CALL CALCU(BETA,GAMMA,Z,LW,LZ,LZP1)
C
C       Shortcut for W>.999
```

```
C
      IF(W.GE.0.999) ZPNEW=Z
      IF(W.GE.0.999) GO TO 100
C
C     Equivalent state with rc residual termination
C
      WR=1./W-1.
  200 ZP=W*Z+1.-W
      GAM=GAMMA*SQRT(Z/(Z+WR))
      BET=BETA+GAMMA*WR/SQRT(Z+WR)
      CALL CALCU(BET,GAM,Z,IW,IZ,IZP1)
      ZPNEW=W*Z+1.-W
      ERROR=ABS(1.-ZP/ZPNEW)
      IF(ERROR.LT.0.001) GO TO 100
      GO TO 200
  100 Z=ZPNEW
C
C     Calculation for RECOMBination
C
      IF(MODE.EQ.'DISIBC')  GO TO 300
      GAMMAP=GAMMA/SQRT(W)
      FACTOR=(BETA+GAMMAP*SQRT(Z)/2.)/
     1 (BETA+GAMMAP*SQRT(Z))
      XJW=2.-FACTOR*LW/2.
      XJW2=2.-FACTOR*IW
      XZ=LZ*XJW2+IW/2.
      XZP1=LZ*(LZP1*XJW+IW*(1.-(LZ+LZP1)*FACTOR/2.))
```

```
      LW=FACTOR*LW*XJW
      LZ=3.*FACTOR*XZ/XJW
      LZP1=4.*FACTOR*XZP1/XZ
      IF(MODE.EQ.'RECOME') RETURN
C
C     Error message for the mode of termination
C
      TYPE 333
  333 FORMAT(10X,'ERROR:MODE OF TERMINATION')
      RETURN
C
C     Calculation for DISPROportionation
C
  300 LZ=3.*IZ;LZP1=4.*IZP1;RETURN
      END



C
C     SUBROUTINE CALCU
C
C      This subroutine calculates the indices Z,IW,IZ,
C     LZ+1 upon recieving BETA and GAMMA values.
C      The calculations are done by first calculating the
C     indices @ spline points calling the subroutine AUX
C     and then interpolating between the values.
C
C
```

```
      SUBROUTINE CALCU(BETA,GAMMA,Z,LW,LZ,LZP1)
C
C       COMMON blocks
C
      COMMON /J/ZDAT(10,3),LWDAT(10,3),LZDAT(10,3),
     2  LZ1DAT(10,3),
     1 CZ(9,3,3),CW(9,3,3),CZP(9,3,3),CZP1(9,3,3),GAM(10)
       REAL LW,LZ,LZP1,IW1,IZ1,IZP1I,LW2,LZ2,LZP1J
      REAL LWDAT,LZ1AT,IZ1DAT
C
C       Decide the necessary spline points
C
      IF(BETA.LT.0.) RETURN
        IF(BETA.GE.10..OR.GAMMA.GT.10.) GO TO 100
      IF(BETA.GT.0.1) GO TO 200
      IF(BETA.GE.0..AND.BETA.LT.0.001) I=1
      IF(BETA.GE.0..AND.BETA.LT.0.001) J=3
      IF(BETA.GE.0..AND.BETA.LT.0.001) SCALE=BETA*1000.
      IF(BETA.GE.0.001.AND.BETA.LE.0.1) I=3
      IF(BETA.GE.0.001.AND.BETA.LE.0.1) J=2
      IF(BETA.GE.0.001.AND.BETA.LE.0.1)
     1  SCALE=(BETA-0.001)/0.099
C
C       Calculate the indices @ spline points
C
        Z1=0.;Z2=0.;LW1=0.;LW2=0.;LZ1=0.
        LZ2=0.;IZP1I=0.;LZP1J=0.
      CALL AUX(I,GAMMA,Z1,LW1,LZ1,LZP1I)
```

```
      CALL AUX(J,GAMMA,Z2,LW2,LZ2,LZP1J)
C
C       Linear interpolation between spline points
C
      Z=(Z2-Z1)*SCALE+Z1
      LW=(LW2-LW1)*SCALE+LW1
      LZ=(LZ2-LZ1)*SCALE+LZ1
      LZP1=(LZP1J-LZP1I)*SCALE+LZP1I
        GO TO 330
C
C       Shortcut for GAMMA>10 or BETA>10
C
  100   Z=1.;LW=2.;LZ=1.;LZP1=1.;RETURN
C
C       Shortcut for 0.1<BETA<10
C
  200   CALL AUX(2,GAMMA,Z,LW,IZ,IZP1)
        SCALE=SQRT((BETA-0.1)/9.9)
        Z=Z+(1.-Z)*SCALE;LW=LW+(2.-LW)*SCALE
        LZ=IZ+(1.-IZ)*SCALE;LZP1=LZP1+(1.-LZP1)*SCALE
C
C       Minor adjustment if the estimated Z>1, etc.
C
  330   IF(Z.GT.1.) Z=1.
        IF(LW.LT.2.) LW=2.
        IF(LZ.LT.1.) LZ=1.
        IF(LZP1.LT.1.) LZP1=1.
```

```
      IF(Z.LT.0.)  Z=0.
      IF(LW.GT.4.)  LW=4.
      IF(LZ.GT.2.)  LZ=2.
      IF(LZP1.GT.2.)  IZP1=2.
      RETURN
      END


C
C       SUBROUTINE AUX
C
C        This subroutine calculates the indices Z,LW,LZ,
C       LZ+1 for GAMMA value given by calling routine with
C       BETA value @0,0.01, or 0.1 using the cubic spline
C       coefficients.
C
C
      SUBROUTINE AUX(I,GAMMA,Z,LW,LZP,LZP1)
C
C       COMMON blocks
C
      COMMON /J/ZDAT(10,3),LWDAT(10,3),IZDAT(10,3),
     2  LZ1DAT(10,3),
     1 CZ(9,3,3),CW(9,3,3),CZP(9,3,3),CZP1(9,3,3),GAM(10)
      REAL LWDAT,LZDAT,LZ1DAT
      REAL LW,LZP,LZP1
C
```

```
C       Starting point
C
      K=1
C
C       Bypass for GAMMA >10
C
      IF(GAMMA.GE.GAM(10)) GO TO 30
C
C       Selecting the right grid
C
      DO  10 J=1,9
      IF(GAMMA.GE.GAM(J)) K=J
      IF(GAMMA.LT.GAM(J)) GO TO 20
   10 CONTINUE
   20 CONTINUE
C
C       Interpolation formulas
C
        D1=GAMMA-GAM(K)
      Z    =  CZ(K,3,I)*D1**3+
     1   CZ(K,2,I)*D1**2+  CZ(K,1,I)*D1+ZDAT(K,I)
       LW=CW(K,3,I)*D1**3+CW(K,2,I)*D1**2
     1  +CW(K,1,I)*D1+LWDAT(K,I)
      LZP=CZP(K,3,I)*D1**3+CZP(K,2,I)*D1**2
     1  +CZP(K,1,I)*D1+IZDAT(K,I)
      LZP1=CZP1(K,3,I)*D1**3+CZP1(K,2,I)*D1**2
     1  +CZP1(K,1,I)*D1+LZ1DAT(K,I)
      RETURN
```

```
C
C       Shortcut for GAMMA >10
C
   30   Z=1.;LW=2.;LZ=1.;IZP1=1.
        RETURN
      END


C
C        SUBROUTINE MCIWT
C
C        This subroutine calculates the derivative with
C        respect to conversion X of polymerization rate DM(1)
C        and the cumulative molecular weight averages DM(i),
C        i=2,4 from the instantaneous polymerization rate
C        MINS(1) and the instantaneous molecular weight
C        averages MINS(i), i=2,5
C        calculated in the subroutine UPDATE.
C
C        X: the fractional conversion
C        MAV(1):TIME in seconds
C        MAV(2):cumulative number average molecular weight
C        MAV(3):cumulative weight average molecular weight
C        MAV(4):cumulative z-average molecular weight
C        MAV(5):cumulative z+1-average molecular weight
C        DM(1):d(TIME in seconds)/dX
C        DM(i),i=2,5:d/dX of the corresponding MAV(i)
```

```
C       MINS(1):equal to MAV(1)
C       MINS(i),i=2,5:instantaneous molecular weight
C       averages of the corresponding MAV(i)
C
C
      SUBROUTINE MOLWT(X,MAV,DM,MINS)
      REAL MAV(5),DM(5),MINS(5)
C
C       When X<1.E-9, DM(i)=MINS(i)
C
      IF(X.LT.1.E-9) GO TO 100
C
C       Error message when X>1.
C
      IF(X.GT.1.) TYPE 10
   10 FORMAT(10X,'ERROR:X GREATER THAN 1')
      IF(X.GT.1.) RETURN
C
C       Formulas for DM(i),i=2,5
C
      DM(2)=MAV(2)/X*(1.-MAV(2)/MINS(2)) !MN
      DM(3)=(MINS(3)-MAV(3))/X !MW
      DM(4)=MINS(3)/MAV(3)/X*(MINS(4)-MAV(4)) !MZ
      DM(5)=MINS(4)*MINS(3)/MAV(4)/MAV(3)*
     1 (MINS(5)-MAV(5))/X!MZ+1
      RETURN
C
```

```
C       Shotcut for X<1.E-9
C
  100   DC 200 I=2,5
        MAV(I)=MINS(I)
  200   DM(I)=0.
        MAV(1)=0.
        RETURN
        END
```

```
C
C
C       This is a BLOCK DATA subroutine which supplies
C      the necessary DATA.
C
C
C      MODE: the mode of termination.
C            either BECOME or DISPRO
C      VFS: fractional free volume of  pure polymer
C           at TS deg.C.
C      ALP: coefficient of thermal expansion OF free
C           volume
C      TS: reference temperature in deg.C at which VFS  is
C          obtained. the lowest temperature with the free
C          volume thermal  expansion coefficient is equal
C          to ALP.
C      LAMDA: ratio of the free volume thermal expansion
C             coefficient below TS to the value above TS.
C
C       VFP: The free volume of the pure polymer at temp. T
C            deg.C is calculated by the following
C            formula.
C      VFP=VFS+ALP*(T-TS)  at T>TS
C         =VFS+LAMDA*AIP*(T-TS) at T<TS
C
C      ANGST: the root-mean-square distance per monomeric
C             chain unit in ANGSTROM
C      DS:the diffusivity of monomeric chain unit for pure
```

```
C          polymer  at TS in CENTIMETER**2/SEC
C       XS: the minim decree of polymerization for
C          entanglement for pure polymer. It is assumed
C          XS is temperature insensitive.
C       EPS0,EPST: parameters to calculate the volume
C                  shrinkage factor by the EQN.
C                   EPS=EPS0+EPST*T
C       DM0,DMT: parameters to calculate the density of
C                  monomer by  the formula
C                 DM=DM0+DMT*T
C       ALM0,ALMT: parameters to calculate the fractional
C                  free volume of pure monomer
C
C                  by the formula
C                   VFM=ALM0+ALMT*T
C       M0: molecular weight of monomer
C
C        The subsequent reaction rate
C       constants have the dimension  LITER/MOLE/SEC.
C
C       AKT,EKT: Arhenius equation parameters
C                for termination
C                 KT=AKT*EXP(-EKT/(T+273.))
C       AKP,EKP: Arhenius equation parameters
C                for propagation
C                 KP=AKP*EXP(-EKP/(T+273.))
C       AKD,EKD: Arhenius equation parameters
```

```
C                for initiator decomposition
C                AKD=AKD*EXP(-EKD/(T+273.))
C        ACM,ECM:Arhenius equation parameters
C                for chain transfer to monomer
C                CM=ACM*EXP(-ECM/(T+273.))
C        F:initiator decomposition efficiency.
C
C         The values of KT and F can be adjusted during
C        running INT.FOR to fit the rate data and molecular
C        weight data simultaneously and will be PRINTED
C        out accordingly by the subroutine MONOM without
C        changing the DATA file.
C
C
C
C         THIS SUBROUTINE SUPPLIES DATA FOR MMA.
C
      BLOCK DATA
      COMMON/PCDE/DISPEC(2)
      COMMON/DATA/VFS,ALP,TS,LAMDA,ANGST,DS,XS,EPS0,EPST,
     1  ALM0,ALMT,DM0,DMT,M0,AKT,
     1   EPT,AEP,EKE,AKD,EKD,ACM,ECM,
     2  F,FW,FX
      COMMON/VFDT/VEXC
      REAL LAMDA,M0
      DATA DISPEC/'DISPEC'/
      DATA VFS,ALP,TS,LAMDA/.0175,3.E-4,98.,.416/
```

```
      DATA ANGST,DS,XS/7.9,1.575E-22,100./
      DATA EPSO,EPST,DMO,DMT/.183,9.E-4,.973,-1.164E-3/
      DATA AlMO,AlMT,MO/.149,2.9E-4,100./
      DATA AKT,EKT/1C.94E8,1245./,AKP,EKP/1.619E7,3500./
      DATA AKD,EKD/1.5E15,15450./,ACM,ECM/1.E-5,0./
      DATA F/.4/
      END
C
C       THIS SUBROUTINE SUPPLIES DATA FOR EMA.
C
      BICCK IATA
      COMMCN/MODE/DISERC(2)
      COMMON/DATA/VFS,ALP,TS,IAMDA,ANGST,DS,XS,EPSO,EPST,
     1  AlMO,AlMT,DMO,DMT,MO,AKT,
     !   EKT,AKP,EKP,AKD,EKD,ACM,ECM,
     2  F,FW,FX
      COMMON/VFDT/VFXC
      REAI IAMIA,MO
      DATA DISPRO/'DISPRC'/
      DATA VFS,ALP,TS,LAMIA/.C25,4.8E-4,62.,.416/
      DATA ANGST,DS,XS/5.9,1.,400./
      DATA EPSO,EPST,DMC,DMT/.18,.001,1.0811,-3.363E-3/
      DATA ALMO,AlMT,MO/.131,.001,114./
      DATA AKT,EKT/3.84E10,2590./
       DATA AKP,EKP/1.C11E7,3253./
      DATA
AKD,EKD/2.5946E15,15724./,ACM,ECM/8.119E-3,2144./
      DATA F/.4195/
      END
C
```

```
C         THIS SUBROUTINE SUPPLIES DATA FOR EAC.
C
          BLOCK DATA
          COMMON/MODE/DISPRC(2)
          COMMON/DATA/VFS,ALP,TS,LAMDA,ANGST,DS,XS,EPSO,EPST,
     1    ALMO,ALMT,DMO,DMT,MO,AKT,
     1     EPT,AKP,EKP,AKD,EKD,ACM,ECM,
     2    F,FW,FX
          COMMON/VFDT/VFXC
          REAL LAMDA,MO
          DATA DISPRC/'DISPRC'/
          DATA VFS,ALP,TS,LAMDA/.025,4.8E-4,-24.,.416/
          DATA ANGST,DS,XS/6.8,1.,200./
          DATA EPSO,EPST,DMO,DMT/.1626,0.E-4,.941,-.88E-3/
          DATA ALMO,ALMT,MO/.131,.001,100./
          DATA AKT,EKT/2.E6,0./,AKP,EKP/840.,0./
          DATA AKD,EKD/1.5E15,15450./,ACM,ECM/1.E-5,0./
          DATA F/.528/
          END
C
C         THIS SUBROUTINE SUPPLIES DATA FOR PAC.
C
          BLOCK DATA
          COMMON/MODE/DISPRC(2)
          COMMON/DATA/VFS,ALP,TS,LAMDA,ANGST,DS,XS,EPSO,EPST,
     1    ALMO,ALMT,DMO,DMT,MO,AKT,
     1     EKT,AKP,EKP,AKD,EKD,ACM,ECM,
     2    F,FW,FX
          COMMON/VFDT/VFXC
          REAL LAMDA,MO
```

```
      DATA DISPRO/'DISPEC'/
      DATA VFS,AIP,TS,LAMDA/.025,4.8E-4,-48.,.416/
      DATA ANGST,DS,XS/6.8,1.,200./
      DATA EPSO,EPST,DMO,DMI/.1565,0.E-4,.928,-.88E-3/
      DATA AIMO,AIMI,MO/.131,.001,114./
      DATA AKT,EKT/2.E6,0./,AKP,EKP/700.,0./
      DATA AKD,EKD/1.5E15,15450./,ACM,ECM/1.E-5,0./
      DATA F/.528/
      END
C
C       THIS SUBROUTINE SUPPLIES DATA FOR VAC.
C
      BLOCK DATA
      COMMON/MODE/FECCME(2)
      COMMON/DATA/VFS,ALP,TS,LAMDA,ANGST,DS,XS,EPSO,EPST,
     1  ALMO,ALMI,DMO,DMI,MO,AKT,
     1   EKT,AKP,EKP,AKD,EKD,ACM,ECM,
     2  F,FW,FX
      COMMON/VFDT/VFXC
      REAL LAMDA,MO
      DATA FECCME/'FECCME'/
      DATA VFS,AIP,TS,LAMDA/.0235,5.E-4,30.,.54/
      DATA ANGST,DS,XS/6.9,3.777E-19,256./
      DATA EPSO,EPST,DMO,DMI/.2074,8.02E-4,.96,-1.4E-3/
      DATA AIMO,ALMI,MO/.154,5.1E-4,86./
      DATA AKT,EKT/.9424E10,1245./,AKP,EKP/1.77E8,3500./
      DATA AKD,EKD/1.5E15,15450./,ACM,ECM/1.E-4,0./
      DATA F/.659/
```

```
      END
C
C       THIS SUBROUTINE SUPPLIES DATA FOR STY.
C
      COMMON/MODE/IFCOMP(2)
      COMMON/DATA/VFS,ALP,TS,LAMDA,ANGST,DS,XS,EPS0,EPST,
     1  ALM0,AIMT,DM0,DMT,M0,AKT,
     1    EKT,AKP,EKP,AKD,EKD,ACM,ECM,
     2  F,FW,FX
      COMMON/VEDT/VIXC
      REAL LAMDA,M0
      DATA IECOMB/'IECOMP'/
      DATA VFS,ALP,TS,LAMDA/.02445,4.5E-4,84.,.288/
      DATA ANGST,DS,XS/7.4,1.792E-13,385./
      DATA EPS0,EPST,DM0,DMT/.1369,4.429E-4,
     1   .9236,-.8873E-3/
      DATA ALM0,AIMT,M0/.1117,6.21E-4,104./
      DATA AKT,EKT/38.93E8,1670./,AKP,EKP/2.167E7,3905./
      DATA AKD,EKD/.8553E15,15220./,ACM,ECM/.8E-4,0./
      DATA F/.71/
      END
```

```
C       Main Program CONST.FOR
C
C        This program creates the CONST.DAT file to be used
C       in the model computations of Diffusion Controlled
C       Vinyl Polymerizations.
C        The interpolation constants are evaluated by
C       calling the IMSL subroutine IQHSCU.
C
C       GAM(i):GAMMA values read from GAMMA.DAT file
C       Zj(i):Z value for BETA=0.j and GAMMA=GAM(i)
C       LWj(i),IZj(i),I1j(i):the corresponding IW,IZ,IZ+1
C       CZj:cubic spline coefficients calculated by IQHSCU
C       CLWj:corresponding coefficients for LW
C       CLZj:corresponding coefficients for LZ
C       CI1j:corresponding coefficients for LZ+1
C
C
C
C       DIMENSION statements
C
      REAL GAM(10),Z0(10),Z1(10),Z001(10),LW0(10),
     2  LW1(10),LW001(10),
     1 IZ0(10),IZ1(10),IZ001(10),L10(10),L11(10),L1001(10)
      DIMENSION CZ0(10,3),CZ1(10,3),CZ001(10,3),
     3  CLW0(10,3),CLW1(10,3),
     1 CLW001(10,3),CIZ0(10,3),CIZ1(10,3),
     4  CIZ001(10,3),CL10(10,3),
     2  CI11(10,3),CL1001(10,3)
```

```
     3,DUMMY1(10),DUMMY2(10,3)
C
C       Constants used in IQHSCU
C
      IER=200
      N=10
  110 FORMAT(5F10.6,/ 10X,4F10.6,/ 10X,4F10.6)
  210 FORMAT(      10X,6(E14.6,5X),/ 10X,6(E14.6,5X))
      IC=N
C
C       Read GAMMA.DAT
C
      DO 100 I=1,N
      READ(02,110) GAM(I),Z0(I),LW0(I),LZ0(I),L10(I),
     1                    Z1(I),LW1(I),LZ1(I),L11(I),
     2 Z001(I),LW001(I),LZ001(I),L1001(I)
  100 CONTINUE
C
C       Call IMSL subroutine IQHSCU
C
      CALL IQHSCU(GAM,Z0,N,CZ0,IC,IER)
      CALL IQHSCU(GAM,Z1,N,CZ1,IC,IER)
      CALL IQHSCU(GAM,Z001,N,CZ001,IC,IER)
      CALL IQHSCU(GAM,IW0  ,N,CIW0  ,IC,IER)
      CALL IQHSCU(GAM,IW1  ,N,CLW1  ,IC,IER)
      CALL IQHSCU(GAM,LW001,N,CLW001,IC,IER)
      CALL IQHSCU(GAM,IZ0  ,N,CIZ0  ,IC,IER)
```

```
      CALL IQHSCU(GAM,LZ1,N,CIZ1,IC,IER)
      CALL IQHSCU(GAM,LZ001,N,CLZ001,IC,IER)
      CALL IQHSCU(GAM,L10  ,N,CL10  ,IC,IER)
      CALL IQHSCU(GAM,I11  ,N,CI11  ,IC,IER)
      CALL IQHSCU(GAM,I1001,N,CI1001,IC,IER)
C
C       Create CONST.DAT file
C
      CALL OFILE(01,'CONST.DAT')
      DO 200 J=1,N-1
      DO 200 K =1,3
      WRITE(01,210)CZC(J,K),CZ1(J,K),CZ001(J,K),CIW0(J,K),
     1 CLW1(J,K),CLWCC1(J,K),CIZ0(J,K),
     1   CIZ1(J,K),CIZ001(J,K),
     2  CL10(J,K),CI11(J,K),CI1001(J,K)
  200 CONTINUE
      STOP
      END
```

```
C
C       SUBROUTINE COEFF
C
C        This subroutine reads the data file GAMMA.DAT and
C       CONST.DAT which contains the cubic spline constants
C       necessary to interpolate the entanglement factor Z
C       and the molecular weight indices.
C
C       GAM(j):GAMMA value
C       ZDAT(j,1):entanglement factor Z @ GAMMA=GAM(j) and
C                 BETA=0
C       ZDAT(j,2):Z @ GAMMA=GAM(j) and BETA=0.01
C       ZDAT(j,3):Z @ GAMMA=GAM(j) and BETA=0.1
C       LWDAT(j,i):molecular weight index LW corresponding
C                  to ZDAT(j,i)
C       LZDAT(j,i):IZ corresponding to ZDAT(j,i)
C       LZ1DAT(j,i):LZ+1 corresponding to ZDAT(j,i)
C       CZ(j,k,i):cubic spline coefficients i=1~3
C                 for the corresponding ZDAT(j,k)
C       CW(j,k,i):spline coefficients for the corresponding
C                 to LWDAT(j,k)
C       CZP(j,k,i):corresponding to LZDAT(j,k)
C       CZP1(j,k,i):corresponding to LZ1DAT(j,k)
C
C
      SUBROUTINE COEFF
C
C       COMMON blocks with subroutine CALCU
```

```
C
      COMMON /J/ZDAT(10,3),LWDAT(10,3),LZDAT(10,3),
     2   LZIDAT(10,3),
     1 CZ(9,3,3),CW(9,3,3),CZP(9,3,3),CZP1(9,3,3),GAM(10)
      REAL LWDAT,LZDAT,IZIDAT
C
C        Read from the data file GAMMA.DAT
C
      CALL IFILE(1,'GAMMA.DAT[2000,31647]')
  100 FORMAT(5F10.6)
  110 FORMAT(10X,4F10.6)
      DO 1000 J=1,10
      READ(01,100) GAM(J),ZDAT(J,1),LWDAT(J,1),IZDAT(J,1),
     1   LZIDAT(J,1)
      READ(01,110) ZDAT(J,2),LWDAT(J,2),
     1    LZDAT(J,2),LZIDAT(J,2)
      READ(01,110) ZDAT(J,3),LWDAT(J,3),
     1    IZDAT(J,3),LZIDAT(J,3)
 1000 CONTINUE
  200 FORMAT(      10X,6(E14.6,5X),/ 10X,6(E14.6,5X))
C
C        Read the spline coefficients from CONST.DAT
C
      CALL IFILE(1,'CONST.DAT[2000,31647]')
      DO 2000 J=1,9
      DO 2000 K=1,3
      READ(01,200) CZ(J,K,1),CZ(J,K,2),CZ(J,K,3),
     1CW(J,K,1),CW(J,K,2),CW(J,K,3),
     2CZP(J,K,1),CZP(J,K,2),CZP(J,K,3),
```

```
     3CZP1(J,K,1),CZP1(J,K,2),CZP1(J,K,3)
2000 CONTINUE
     RETURN
     END
```

```
*
*       CSMP.DIS
*
*        This program calculates the moments of the
*       distribution function P(y) with the given values of
*       GAMMA, BETA, and Z.
*        These parameters are supplied by the PARAMETER
*       statement which can be altered easily without
*       changing the CSMP.SAV file.
*
*       GAMMA:dimensionless parameter
*       BETA: dimensionless parameter
*       Z:entanglement factor
*       TIME:dimensionless chain length y
*       PY: termination chain length dependence function
*       DPY: dP(y)/dy
*       DP1: d(first moment of P(y))/dy
*       DP2:d(second moment of P(y))/dy
*       DP3:d(third moment of P(y))/dy
*       P1: first moment of P(y)
*       P2:second moment of P(y)
```

```
*       P3:third moment of P(y)
*       FINTIM:integration limit
*       PRDEL:print interval
*
*
*
*       PARAMeter statement
*
PARAM GAMMA=.2  ,BETA=0.    ,Z=.055
DYNAMIC
*
*       Chain length dependent termination frequency
*       function
*
NOSORT
      IF(TIME.LE.1.) FY=TIME
      IF(TIME.GT.1.) FY=1.714286-TIME**(-1.4)/1.4
SORT
*
*       Evaluation of the derivatives of P(y)-ith moments
*
DPY=EXP(-(BETA+GAMMA*SQRT(Z)/2.)*TIME-GAMMA/2./SQRT(Z)*FY)
DP1=TIME*DPY
DP2=TIME**2*DPY
DP3=TIME*DP2
*
*       Integration
*
```

```
P1=INTGRL(0.,DP1)
P2=INTGRL(0.,DP2)
P3=INTGRL(0.,DP3)
*
*       Output
*
*       Output
*
PRINT P1,P2,P3
*
*       Integration limit and PRINT interval
*
TIMER FINTIM=2000.,PRDEL=50.
END
*
*       Examples of chainging PARAMETERS
*
PARAM GAMMA=.2  ,BETA=0.001,Z=.055
END
PARAM GAMMA=.1,BETA=.1,Z=.2
END
PARAM GAMMA=.2,BETA=.1,Z=.25
END
STOP
ENDJOB
```

Sample Output

MMA Polymerization at 90°C with 0.3% AIBN (3)

Corresponding to Fig. 5.2 and Fig. 5.4

TEMP =	0.900000E+02	INCON=	0.162200E-01
FW =	0.100000E+01	FA =	0.120000E+01
VFXC =	0.138000E+00	XK =	0.500000E+00
DM =	0.868240E+00	EPS =	0.183000E+00
VFM =	0.175100E+00	VFP =	0.165016E-01
CONM =	0.868240E+01	KP =	0.105576E+04
KT =	0.295753E+08	KD =	0.500371E-03
CM =	0.100000E-04	R10 =	0.779137E-05
MN0 =	0.603655E+05	DADT0=	0.541884E-03
ROOT =	0.513266E-06	F =	0.480000E+00
KPDMS=	0.256069E-06		

X= .000

PHIM =	0.100000E+01	VF =	0.175100E+00
KIVF =	0.177265E+01	KP =	0.100000E+01
W =	0.100000E+01	BETA =	0.100000E+01
GAMMA=	0.220485E+03	MINST=	0.600230E+05
KPDM =	0.557102E+16	KIP =	0.000000E+00
SIG =	0.184849E-04	Z =	0.100000E+01
LW =	0.200000E+01	LZ =	0.300000E+01
LZ+1 =	0.400000E+01	KIEFF=	0.100000E+01
ROOT =	0.513266E-06	TIME =	0.000000E+00
DIDA =	0.184541E+04	MNAVG=	0.600230E+05
MWAVG=	0.120046E+06	MZAVG=	0.180069E+06
MZ+1A=	0.240092E+06	P1 =	0.000000E+00

X= .100

PHIM =	0.916777E+00	VF =	0.161901E+00
KIVF =	0.177265E+01	KP =	0.100000E+01
W =	0.100000E+01	BETA =	0.120159E-01

GAMMA=	0.277321E+01	MINST=	0.603057E+05
KPDM =	0.349726E+16	KTP =	0.000000E+00
SIG =	0.354629E-05	Z =	0.100000E+01
LW =	0.200000E+01	LZ =	0.300000E+01
LZ+1 =	0.400000E+01	K1EFF=	0.100000E+01
ROOT =	0.492553E-06	TIME =	0.335929E+01
DIDX =	0.220607E+04	MNAVG=	0.601285E+05
MWAVG=	0.120258E+06	MZAVG=	0.160389E+06
MZ+1A=	0.240521E+06	P1 =	0.617151E-01

X= .200

PHIM =	0.830392E+00	VF =	0.148201E+00
KTVF =	0.177265E+01	KP =	0.100000E+01
W =	0.100000E+01	BETA =	0.589596E-02
GAMMA=	0.142637E+01	MINST=	0.611623E+05
KPDM =	0.197582E+16	KTP =	0.000000E+00
SIG =	0.274672E-05	Z =	0.100000E+01
LW =	0.200000E+01	LZ =	0.300000E+01
LZ+1 =	0.400000E+01	K1EFF=	0.100000E+01
ROOT =	0.467654E-06	TIME =	0.744173E+01
DIDX =	0.272736E+04	MNAVG=	0.603981E+05
MWAVG=	0.120800E+06	MZAVG=	0.181207E+06
MZ+1A=	0.241617E+06	P1 =	0.238767E+00

X= .300

PHIM =	0.740662E+00	VF =	0.133969E+00
KTVF =	0.142542E+01	KP =	0.100000E+01
W =	0.100000E+01	BETA =	0.585598E-02
GAMMA=	0.877071E+00	MINST=	0.717666E+05
KPDM =	0.964846E+15	KTP =	0.000000E+00

SIG =	0.232232E-05	Z =	0.538784E+00
LW =	0.311535E+01	LZ =	0.572547E+01
LZ+1 =	0.782729E+01	KIEFF=	0.767993E+00
RDOT =	0.499051E-06	TIME =	0.125444E+02
DTDX =	0.309350E+04	MNAVG=	0.611325E+05
MWAVG=	0.127106E+06	MZAVG=	0.203557E+06
MZ+1A=	0.299500E+06	PI =	0.414399E+00

X= .400

PHIM =	0.647389E+00	VF =	0.119170E+00
KTVF =	0.564358E+00	KP =	0.100000E+01
W =	0.100000E+01	BETA =	0.263599E-02
GAMMA=	0.441624E+00	MINST=	0.159270E+06
KPDM =	0.382006E+15	KIP =	0.000000E+00
SIG =	0.194370E-05	Z =	0.258081E+00
LW =	0.360754E+01	LZ =	0.600000E+01
LZ+1 =	0.793364E+01	KIEFF=	0.145989E+00
RDOT =	0.108850E-05	TIME =	0.105415E+02
DTDX =	0.172289E+04	MNAVG=	0.680419E+05
MWAVG=	0.188377E+06	MZAVG=	0.442674E+06
MZ+1A=	0.811954E+06	PI =	0.641171E+00

X= .500

PHIM =	0.550358E+00	VF =	0.103787E+00
KTVF =	0.162639E+00	KP =	0.100000E+01
W =	0.100000E+01	BETA =	0.222399E-02
GAMMA=	0.214885E+00	MINST=	0.500020E+06
KPDM =	0.110088E+15	KIP =	0.000000E+00
SIG =	0.159366E-05	Z =	0.671312E-01
LW =	0.368681E+01	LZ =	0.586516E+01

LZ+1 =	0.781145E+01	KIEFF=	0.109182E-01
RDOT =	0.391110E-05	TIME =	0.183763E+02
DTDX =	0.579809E+03	MWAVG=	0.798012E+05
MWAVG=	0.361914E+00	MZAVG=	0.129048E+07
MZ+1A=	0.247083E+07	P1 =	0.804842E+00

X= .000

PHTM =	0.449337E+00	VF =	0.877658E-01
KTVF =	0.280123E-01	KP =	0.100000E+01
W =	0.922255E+00	BETA =	0.161599E-02
GAMMA=	0.891020E-01	MINST=	0.706699E+00
KPDM =	0.189011E+14	KIP =	0.236142E-02
SIG =	0.140644E-05	Z =	0.117617E+00
LW =	0.277239E+01	LZ =	0.441885E+01
LZ+1 =	0.589063E+01	KIEFF=	0.357246E-02
RDOT =	0.683070E-05	TIME =	0.191203E+02
DTDX =	0.411195E+03	MWAVG=	0.934581E+05
MWAVG=	0.662267E+00	MZAVG=	0.247016E+07
MZ+1A=	0.412036E+07	P1 =	0.909738E+00

X= .700

PHTM =	0.344070E+00	VF =	0.710715E-01
KTVF =	0.192760E-02	KP =	0.100000E+01
W =	0.424977E+00	BETA =	0.152457E-02
GAMMA=	0.256145E-01	MINST=	0.634529E+00
KPDM =	0.130477E+13	KIP =	0.260818E-02
SIG =	0.130365E-05	Z =	0.595035E+00
LW =	0.207190E+01	LZ =	0.312914E+01
LZ+1 =	0.417340E+01	KIEFF=	0.209895E-02
RDOT =	0.785529E-05	TIME =	0.198411E+02

DTDX = 0.472028E+03 MNAVG= 0.106597E+06
MWAVG= 0.795091E+06 MZAVG= 0.248283E+07
MZ+1A= 0.391476E+07 P1 = 0.900005E+00

X= .800

PHIM = 0.234302E+00 VF = 0.536615E-01
KTVF = 0.200660E-04 KP = 0.100000E+01
W = 0.107134E-01 BETA = 0.130600E-02
GAMMA= 0.327990E-02 MINST= 0.535013E+06
KPDM = 0.135824E+11 KTP = 0.185291E-02
SIG = 0.121182E-05 Z = 0.989816E+00
LW = 0.200024E+01 LZ = 0.300043E+01
LZ+1 = 0.400058E+01 KTEFF= 0.185390E-02
RDOT = 0.945575E-05 TIME = 0.207042E+02
DTDX = 0.583365E+03 MNAVG= 0.118759E+06
MWAVG= 0.845089E+06 MZAVG= 0.236259E+07
MZ+1A= 0.371216E+07 P1 = 0.907544E+00

X= .900

PHIM = 0.119717E+00 VF = 0.354880E-01
KTVF = 0.143915E-08 KP = 0.998917E+00
W = 0.160949E-05 BETA = 0.113600E-02
GAMMA= 0.470520E-04 MINST= 0.407717E+06
KPDM = 0.974142E+06 KTP = 0.894160E-03
SIG = 0.111448E-05 Z = 0.999998E+00
LW = 0.200000E+01 LZ = 0.300000E+01
LZ+1 = 0.400000E+01 KTEFF= 0.894160E-03
RDOT = 0.135332E-04 TIME = 0.218290E+02
DTDX = 0.812198E+03 MNAVG= 0.129560E+06
MWAVG= 0.857513E+06 MZAVG= 0.224865E+07

APPENDIX F

EVALUATION OF $\bar{\ell}$

The effect of the excess chain end mobility was visualized as a sphere of effective reaction radius σ. Thus the jump distance $\bar{\ell}$ is identified as the distance the center of gravity of the reaction sphere moves with one propagation step. As it was assumed that chain from a node to the end of the chain is composed of j_c monomeric units on the average, the problem of finding $\bar{\ell}$ reduces to finding the change in the center of gravity of a chain where the one monomeric unit at one end (the node side) moves to the other end while the other units stay in the same position. Let us name the centers of mass of each monomeric units as $1,2,----,j_c$ starting from the node. The coordinate system can be set without loss of generality for the coordinate of the first monomeric unit to be the origin. Assuming the coordinate of the monomeric units as (x_1,y_1,z_1), (x_2,y_2,z_2),----, (x_{jc},y_{jc},z_{jc}), then $x_1=y_1=z_1=0$, as it is located at the origin.

The center of gravity is expressed by $(\bar{x},\bar{y},\bar{z})$, which are related as

$$\bar{x} = (x_1+x_2+---+x_{jc})/j_c \qquad (F.1)$$

$$\bar{y} = (y_1+y_2+---+y_{jc})/j_c \qquad (F.2)$$

$$\bar{z} = (z_1+z_2+---+z_{jc})/j_c \qquad (F.3)$$

Now we visualize the propagation step as moving the (x_1y_1,z_1) unit after the (x_{jc},y_{jc},z_{jc}) unit, essentially making a new unit $(x_{jc+1}$, $y_{jc+1},z_{jc+1})$. The node is now at unit (x_2,y_2,z_2). The new center of gravity $(\bar{x}',\bar{y}',\bar{z}')$ is related by

$$\bar{x}' = (x_2+x_3 + \ldots + x_{jc} + x_{jc+1})/j_c \qquad (F.4)$$

$$\bar{y}' = (y_2+y_3 + \ldots + y_{jc} + y_{jc+1})/j_c \qquad (F.5)$$

$$\bar{z}' = (z_2+z_3 + \ldots + z_{jc} + z_{jc+1})/j_c \qquad (F.6)$$

Thus the vector $\vec{\ell}$ is represented by the difference between the two centers of gravity.

$$\vec{\ell} = (\bar{x}'-\bar{x},\ \bar{y}'-\bar{y},\ \bar{z}'-\bar{z})$$

$$= \left(\frac{x_{jc+1}-x_1}{j_c},\ \frac{y_{jc+1}-y_1}{j_c},\ \frac{z_{jc+1}-z_1}{j_c}\right) \qquad (F.7)$$

By vector algebra, the magnitude of the vector $\vec{\ell}$ is given by

$$\bar{\ell} = \left\{\left(\frac{x_{jc+1}-x_1}{j_c}\right)^2 + \left(\frac{y_{jc+1}-y_1}{j_c}\right)^2 + \left(\frac{z_{jc+1}-z_1}{j_c}\right)^2\right\}^{1/2}$$

and since x_1, y_1 and z_1 = 0 (at the origin),

$$\bar{\ell} = \frac{1}{j_c^{1/2}}\left\{\frac{x_{jc+1}^2}{j_c} + \frac{y_{jc+1}^2}{j_c} + \frac{z_{jc+1}^2}{j}\right\}^{1/2} \qquad (F.8)$$

The term in the brackets is identically a, the average root-mean-square end-to-end distance per square root of the number of monomer units in the chain. Thus

$$\bar{\ell} = a/j_c^{1/2}$$

APPENDIX G

DESCRIPTION AND EVALUATION OF f_t

In order for the statistical averaging implied by using equation 3.32 to be meaningful, it is necessary that the movement of the chain end which leads to the continuously changing configurations is very fast within the time interval between propagation steps, $(k_p[M])^{-1}$ seconds. When the relaxation of the chain end is not complete within that time interval, the active chain end will not be able to sweep the whole space within the sphere of termination defined by σ and will lead to an effective radius less than that given by equation 3.36. If one assumes that σ is completely determined by the volume which the chain end can sweep within the time interval for propagation, the number of configurations required to sweep the entire volume will be proportional to σ^3. The number of jumps which lead to new configurations will be proportional to the diffusivity of the chain end (or a freely rotating segment of the dangling chain) and will be proportional to the exponential of the free volume as $\exp(-1/v_f)$, with units of jumps/time. The total number of new configurations possible in the propagation time interval will thus be proportional to $[k_p[M]\exp(1/v_f)]^{-1}$. When comparing the possible number of configurations to those required, one produces a ratio written as $C_1\sigma^3 k_p[M]\exp(1/v_f)$, where C_1 is some unknown constant. As long as this ratio is greater than or equal to unity, equation 3.36 will be an adequate description of σ. Otherwise σ should be proportional to $[\exp(-1/v_f)/(k_p[M])]^{1/3}$. However, since the diffusivity of the chain end will not be much different from that of the monomer itself, the sweeping efficiency

will not be impaired significantly during Phase III. It is a potential problem during Phase IV where the monomer diffusion becomes restricted, but there is an offsetting phenomenon there because the time interval between propagation steps increases as both k_p and [M] decrease. As shown in Chapter 4, k_p eventually becomes proportional to $\exp(-1/v_f)$ and it may be that this effectively renders f_t equal to unity even during Phase IV.

The other assumption which offers some difficulty in the real situation is that the diffusion of external macroradicals into the sphere of termination is negligible. At conversions where the translational motion of these radicals is significant, this assumption may not hold and the resultant radical concentration profile, [R·] vs r, will change as shown in Fig. 32 producing a smaller value of σ. This effect will become less significant with increasing conversion via the exponentially decreasing diffusivity of the macroradicals. This behavior suggests that $f_t = 0$ below a certain conversion level, especially during Phase II. f_t should increase rapidly from zero as the conversion increases due to the exponentially decreasing translational mobility of the polymer chain as a whole. Dealing in a quantitative fashion with this phenomenon will be difficult, but the translational diffusivity will surely be related to the molecular weight of the polymer radicals and to their entanglement with other polymer. In Chapter 2, the probability of a polymer radical growing beyond x_c, the degree of polymerization necessary for entanglement, was described by P(y) at y = 1, or P(1). In the absence of a better description of f_t during the conversion period under consideration, it was arbitrarily chosen that $f_t = 0$ at a conversion level of 0.5 and that f_t increases according to the relation

$$f_t = [P(1) - P(1)|_{X=0.5}]/[1.0-P(1)|_{X=0.5}] \qquad (G.1)$$

Although equation G.1 is artificial, it has the desired property of increasing rapidly from zero towards unity and can be continuously computed from the knowledge of β, γ and $f(y)$. Equation 3.39 will be used for the analysis of experimental data presented in Chapter 5.

APPENDIX H

SAMPLE CALCULATIONS FOR SUGDEN'S AND BILTZ' METHOD

For styrene, the occupied volume V_0 at 0 deg. K can be estimated by Sugden's method and Biltz' method.and shown here as an example.

SUGDEN'S METHOD

8	carbon atoms	8*1.1= 8.8
8	hydrogen atoms	8*6.7= 53.6
4	double bonds	4*8.0= 32.0
1	6-membered ring	1*0.6= 0.6
	total	95.0 [cm^3/mole]

BILTZ' METHOD

2	aliphatic carbon atoms	2*0.77= 1.54
6	aromatic carbon atoms	6*5.1 =30.6
8	hydrogen atoms	8*6.45=51.6
1	double bond	1*8.6 = 8.6
	total	92.3 [cm^3/mole]

APPENDIX I

RAW VISCOSITY DATA FOR MONOMER-POLYMER SYSTEMS

The viscometer used was Brookfield Model LVF, which was fitted with a cover lid to minimize evaporation. Four spindles were used and the readings of viscometer was converted into the unit of c.p. with the conversion chart supplied by the manufacturer.

VINYL ACETATE-POLYVINYL ACETATE DATA

wt.fraction of polymer / temp	0.5704	0.4484	0.3847	0.2780
32.2 deg.C	94600 c.p.	4640c.p.	1426c.p.	---
37.8	73800	4160	1266	294.5
43.3	63000	3520	1092	275.0
48.9	55200	2860	1006	246.5
54.4	47900	2600	932	220.0
60.0	41700	2260	816	187.5

STYRENE-POLYSTYRENE DATA

wt.fraction of polymer / temp	0.5163	0.4257	0.3095	0.2349
32.2	72850	9230	---	1920
37.8	68500	8750	---	1490
43.3	57450	8010	1075	964
48.9	46700	6730	954	829
54.4	38300	5980	836	726
60.0	33000	5220	744	640

METHYL METHACRYLATE-POLYMETHYL METHACRYLATE DATA

temp.°C / wt.fraction of polymer	32.2	37.8	40.0	43.3	48.9	54.4	60.0
0.4983	41400	8420	----	6545	4810	3470	4810
0.4274	-----	----	5300	----	3870	----	2270
0.3900	-----	----	2410	----	1550	----	1030
0.3856	1510	1295	----	1100	994	920	994
0.3438	----	----	610	----	610	---	300
0.3245	283	262	---	219	188	163	188
0.2870	---	---	135	---	135	---	95
0.2603	84	77	---	69	61	57	61
0.2210	--	--	50	--	50	--	32

APPENDIX J

MEASUREMENTS OF VISCOSITY AVERAGE MOLECULAR WEIGHT

The viscosity method of measuring molecular weight is based on the Mark-Houwink-Sakurada eq'n (49).

$$[\eta] = K \overline{M}_v^a \qquad (J.1)$$

where $[\eta]$ is the intrinsic viscosity defined by eq'n J.2.

$$[\eta] = \lim_{c \to 0} \frac{\ln \eta_r}{c} \qquad (J.2)$$

where the relative viscosity η_r is given by the ratio of the efflux time for the polymer solution to that of pure solvent.

Table J.1 shows the values of K used in this work. The details of experimental procedures are a routine one found in the textbooks (49).

Table J.2 shows the raw data obtained. These data are used to calculate the values of and are plotted in Fig. J.1. The intrinsic viscosity is found by the least-square fit of the data. Fig. J.1 also shows the straight line obtained by the least-aquare regression.

The viscosity average molecular weight calculated by eq'n J.1 are tabulated in Table 4.3.

Table J.1

VALUES OF K and a (ref.49)

polymer	solvent	temp.°C	$K*10^4$	a
PMMA	aceton	25	0.75	0.70
PSTY	cyclohexane	35	7.6	0.50
PVAC	aceton	25	2.1	0.68

Table J.2

DILUTE SOLUTION VISCOSITY DATA

polymer	c,gr/dl	efflux time*,sec	η_r	$\ln \eta_r/c$
PSTY	0	268.2	1.0	
	0.0293	270.6	1.00895	0.3041
	0.0585	273.6	1.02013	0.3408
	0.0878	276.4	1.03057	0.3430
	0.1171	280.2	1.04474	0.3738
PMMA	0	106.8	1.0	
	0.0280	107.3	1.00468	0.1668
	0.0560	108.0	1.01124	0.1996
	0.0840	108.5	1.01592	0.1880
	0.1120	109.4	1.02434	0.2147
	0.1400	110.5	1.03464	0.2432
PVAC	0	106.5	1.0	
	0.0861	112.4	1.05540	0.6262
	0.1148	114.5	1.07512	0.6309
	0.1436	116.6	1.09483	0.6309

* Cannon-Fenske viscometer, size 50

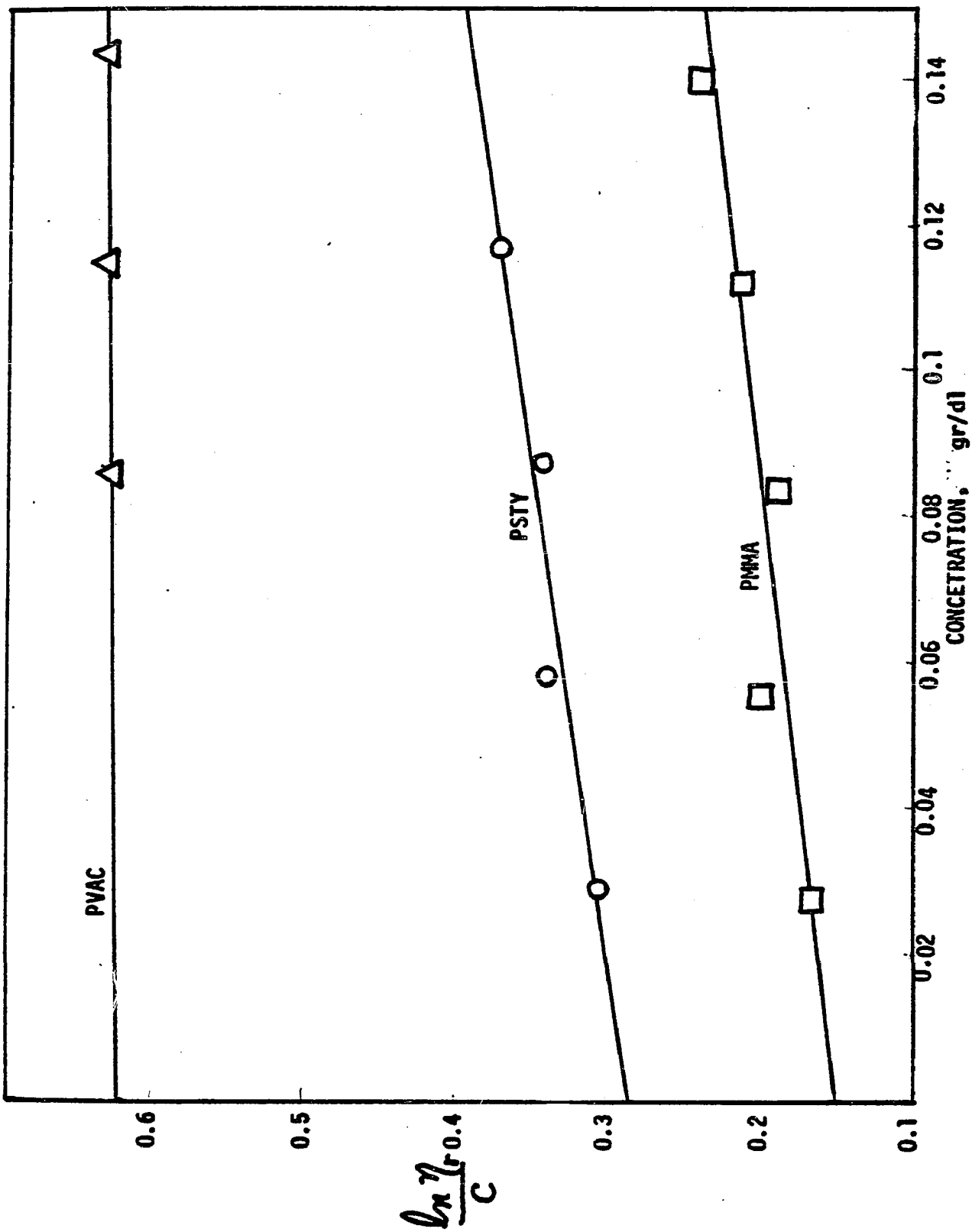

Fig. J-1 Determination of Intrinsic Viscosity

APPENDIX K

STYRENE POLYMERIZATION DATA

EXPERIMENTAL PROCEDURES

To obtain time-conversion data, flame-sealed glass tubes placed in an isothermal water bath were used as reactors. Caustic washed, vacuum distilled monomer was mixed with weighed initiator and injected into the glass tube by a hypodermic syringe. The amount of the reaction mixture put into each reactor was approximately 1.0 ml. These reactors were quenched and frozen in the dry-ice-isopropyl alcohol bath. Then the glass tube reactors were sealed with a smallpropane blow torch while vacuum was applied to the end being sealed. These reactors were put into the water bath which has been maintained in the predetermined reaction temperature. Due to the small diameter of the tubes used (5 mm O.D.), it was expected to reach the reaction temperature very quickly. No significant inhibition time was observed in the data, so it was assumed that the initial period of heating-inhibition was negligible. Samples were taken at regular time intervals, and the conversion was measured by gravimetric analysis, where the samples were dissolved in methylene chloride and the the polymer was precipitated by adding excess amount of methanol followed by drying in the forced air circulation oven until constant weight was obtained.

TEMPERATURE UNIFORMITY IN THE REACTOR

The proper diameter of the glass tube reactor can be estimated by consideration of the heat dissipation requirement to maintain the uniform reaction temperature at the predetermined level.

The thermal conductivity of reaction mixture is assumed to be 1.0 watt/m°C = 0.24 cal/sec,m°C. For the steady state heat conduction with constant heat generation, $\dot{q}$ in infinite cylinder (47) is

$$t_0 - t_w = \frac{\dot{q} R_i^2}{4k} \qquad (K.1)$$

By setting the maximum temperature difference between the center of the reactor, t_0, and the reactor wall, t_w, to be 1°C, and setting the heat dissipation rate $\dot{q}$ corresponding to 10%/min conversion rate with the heat of reaction 13.5 kcal/mole, the maximum value of $\dot{q}$ is estimated as 13.5 cal/cm^3,min for methyl methacrylate. As methyl methacrylate shows very strong gel effect, the value of 13.5 cal/cm^3,min can be considered to be the extreme case. In this case, R_i is equal to about 4 mm. With this 4mm I.D. and 1mm wall thickness and the heat transfer coefficient of 240 Btu/hr,ft^2,°F, 1°C temperature difference is more than enough to dissipate the 13.5 cal/cm^3,min. Thus 5mm O.D. glass tube with 1mm wall thickness is used in this work.

POLYSTYRENE MASS POLYMERIZATION DATA

Styrene monomer was supplied by Research Polymers, Inc., Ontario, New York. The initiator used was benzoyl peroxide (BPO) and supplied by Aldrich Chemicals, Milwaukee, Wisconsin.

Table K.1

POLYSTYRENE MASS POLYMERIZATION DATA

temp.,°C	wt.% BPO	time,min	% conversion
80	0.96	30	9.60
		60	17.63
		90	24.72
		120	31.59
		150	37.40
		180	46.26
		210	53.16
		240	61.40
		274	71.58
		300	87.79
		331	100.00
70	2.85	1.0 hrs.	13.34
		2.0	26.18
		3.0	37.37
		4.0	49.32
		5.0	65.22
		6.0	58.75
		7.0	96.52
80	0.96	240 min.	58.85
		270	66.43
		300	79.38
		330	95.60
		360	97.19

Appendix L

THE ENTANGLEMENT POINT

Equations 5.4 and 5.15 used to estimate the critical conversion where entanglement coupling begins are direct consequences of the entanglement theory, but there have been some doubts raised about its validity. Equation 5.14 stated that entanglement occurs when $\bar{M}_w$ equals or exceeds $M_o x_c$. Since x_c may be written as x_{co}/ϕ_{pe}, equation 5.14 may be written as

$$\phi_{pe}\bar{M}_w = M_o x_{co} \text{ or } \phi_{pe}\bar{M}_w = \text{constant} \qquad (L.1)$$

where ϕ_{pe} is the volume fraction of polymer at the entanglement point. Since ϕ_p is roughly proportional to fractional conversion,

$$X_e\bar{M}_w \cong \text{constant} \qquad (L.2)$$

Turner (7) has proposed an alternate form based upon macromolecular close packing which predicts that the critical conversion X_e is described by

$$X_e\rho_c\bar{M}_n^{1/2} = C(w)\left[\frac{\langle r_o \rangle}{M}\right]^{-3/2}p_f \qquad (L.3)$$

where C(w) is a constant depending upon the molecular weight distribution, and has the following values;

Distribution	$C(w)\times10^{21}$
Monodisperse	2.0
Most probable (recombination)	1.7
Most probable (disproportionation)	1.5

If the molecular weight distribution prior to the entanglement point can be approximated by the most probable distribution, $\bar{M}_w/\bar{M}_w = 1.5$ for

recombination and 2 for disproportionation, and eq'n L.3 becomes

$$X_e \bar{M}_w^{1/2} \cong \text{constant} \qquad \text{(L.4)}$$

It is seen that the difference between Turner's model and the one used in this paper rests in the power to which $\bar{M}_w$ is raised.

Recently, O'Driscoll (46) made an attempt to define the onset of the gel effect, which he described as the "explosive region", with the same type of model as Turner's, i.e. $X_e \bar{M}_n^{1/2}$ = constant. O'Driscoll applied this expression to the solution polymerization of MMA.

In order to look at the differences between the $\bar{M}^{1/2}$ model and the $\bar{M}$ model used in the present work, as it affects the outcome of the computed conversion profiles, it is instructive to discuss the bulk polymerization of styrene. In this case it has been demonstrated that there is a mild gel effect (pseudo gel effect) followed by a stronger gel effect after the entanglement point is reached. Recall that pseudo gel effect is simply caused by the reduction in free volume with increasing conversion, and that the entanglement point is reached fairly late in the reaction because of the short kinetic chain length of styrene (especially as compared with MMA). Using equation (L.1) to define the entanglement point yields the predicted conversion profiles shown in Figs. 5.18-5.20. It is seen here that the region of true gel effect has been predicted to be earlier in the reaction than actually happens. On the other hand, the use of Turner's criterion predicts X_e too high to obtain a good fit to the conversion data. At this point the author has been unable to resolve the issue between the two models. It should be mentioned once again that whatever the method of determining X_e, the results of the computations are sensitive to the value used.

For this reason it will be difficult to resolve the issues between the two models (or any others). New and more careful studies appear to be necessary for a variety of polymer systems in order to bring this issue to a conclusion.